Leukemogenic Mechanisms of MLL Fusion Proteins

by

Jiaying Tan

A dissertation submitted in partial fulfillment
of the requirements for the degree of
Doctor of Philosophy
(Molecular and Cellular Pathology)
in the University of Michigan
2012

Doctoral Committee:

Professor Jay L. Hess, Chair
Professor Gregory R. Dressler
Professor Tom K. W. Kerppola
Assistant Professor Yali Dou
Assistant Professor Ivan P. Maillard

To Mom and Dad

Acknowledgements

This thesis could not have been completed without the ones walking with me through the past four years. I would like to first thank my advisor, Dr. Jay Hess, for providing me the opportunity to learn and grow as a young scientist, for inspiring me to strive for my personal best in research, for encouraging me to think independently and creatively, and for guiding me to develop and pursue my scientific interests persistently. I would also like to thank my committee members, Drs. Yali Dou, Ivan Maillard, Tom Kerppola, and Gregory Dressler for generously offering their time and invaluable insights during the course.

I am grateful to all the current and previous Hess lab members. It has been such a pleasure to work with this group and to share the ups and downs along the way. I wish you all the best! In particular, I would like to thank Dr. Andrew Muntean, from whom I have learned so much through our productive collaboration and discussions, and Stephanie Jo, whose incredible diligence and determination has been a real inspiration. Additionally, a special thank you goes to the Dou lab next door for their moral and technical support and to the Maillard lab for the delightful collaboration. Many thanks to our program director Dr. Nicholas Lukacs and his amazingly enthusiastic assistant Laura Hessler, their strong support and

confidence on me has been tremendously encouraging the entire time. As every pathology graduate student would have said, Laura, you are beyond super!

I can never thank enough my dear friends for lightening up my life, both the ones in Michigan and those back in China. Everlasting gratitude goes to Hanyu, Jesse, Peng, and Haiyan, for hearing me out, for lifting me up, and for walking me through the rain, never giving up. The most special thank you goes to Jie for being you and for loving me. It has been an incredible journey for both of us, and I cannot wait to see where this leads. Finally, no words can adequately express how deeply grateful and indebted I am to my parents, Xiaoan and Feifei. Your unwavering support has been with me every step of the way. You encourage me to follow my heart and to explore my potential. I could have never accomplished this work without you two. I would never become who I am now without your unconditional love.

Table of Contents

List of Figures

List of Abbreviations

AEP, AF4 family/ENL family/P-TEFb;

ALL, acute lymphoblastic leukemia;

AML, acute myeloid leukemia;

ATM, ataxia telangiectasia mutated;

CBP, Creb-binding protein;

CBX, chromobox homolog;

CDK, cyclin-dependent kinase;

C/EBPα, CCAAT-enhancer-binding protein α

ChIP, chromatin immunoprecipitation;

CTD, carboxy-terminal domain;

DOT1L, disruptor of telomeric silencing 1-like;

EAP, Elongation Assisting Proteins or ENL-associated Proteins;

GM-CSF, granulocyte macrophage-colony stimulating factor;

HAT, histone acetyl transferase;

HDAC, histone deacetylase;

HMT, histone methyl transferase;

HOX, homeobox;

IL, interleukin;

LPS, lipopolysaccharide;

LT-HSC, long term-hematopoietic stem cell;

MLL, Mixed Lineage Leukemia;

MOF, males absent on the first;

MYST, Moz, Ybf2/Sas3, Sas2, Tip60;

NF-κB, nuclear factor kappa-light-chain-enhancer of activated B cells;

NuA4, nucleosome acetyltransferase of histone H4;

PAFc, polymerase associated factor complex;

Pc, polycomb;

PcG, polycomb group;

PCL, polycomblike;

PHD, plant homeodomain;

PMA, phorbol 12-myristate 13-acetate;

PRC, polycomb repressive complex;

PTD, partial tandem duplication;

RB, retinoblastoma;

RBBP, retinoblastoma-binding protein;

RNAP II, RNA polymerase II;

SCF, stem cell factor;

SET, Su(var), Enhancer of zeste, Trithorax;

STAT, signal transducers and activators of transcription

TEL, translocated ETS leukemia;

TIP60, HIV Tat-interacting protein of 60 kDa;

TrxG, trithorax group;

Abstract

Translocations that generate MLL fusion proteins are common causes of human acute leukemias. Aberrant target gene activation is the primary driver of *MLL*-rearranged leukemogenesis, but the underlying mechanisms remain poorly understood. In the present study, we identified two partners of the MLL fusion complex, PAFc and CBX8, which can interact with a common MLL fusion protein, MLL-AF9, through the N-terminal MLL part and the C-terminal AF9 part, respectively. Our data demonstrate that both PAFc and CBX8 are required for MLL-AF9-mediated transcriptional upregulation and leukemic transformation. The molecular mechanisms for their requirements in the leukemogenic process are different. By chromatin immunoprecipitation, we show that PAFc binds at the MLL target gene (*e.g., Hoxa9* and *Meis1*) loci in MLL-AF9 leukemic cells. Its binding contributes to the recruitment of MLL-AF9 and augments MLL-AF9-mediated transcriptional activation. In contrast, CBX8 promotes the transcriptional activation of MLL-AF9 target genes, not by regulating MLL-AF9 recruitment but may through interacting with other cofactors, such as the histone acetyltransferase TIP60, whose enzymatic activity could potentially facilitate gene transcription. Furthermore, although CBX8 is essential for MLL-AF9 transformation, it is not required for normal hematopoiesis, as shown by the

normal viability of hematopoiesis in Cbx8-deficient mice. This suggests targeting CBX8 may be of therapeutic value in treating *MLL*-rearranged leukemias. In conclusion, our findings demonstrate that both PAFc and CBX8 play essential roles in MLL-AF9-mediated transcriptional regulation and leukemogenesis.

Chapter 1

The Role of the PAF Complex in MLL Fusion Protein-Induced Leukemogenesis

Introduction

Mixed Lineage Leukemia

Mixed lineage leukemia is a highly aggressive hematopoietic malignancy that occurs predominantly in pediatric patients. In contrast to other types of acute leukemia, mixed lineage leukemia stands out as a particular clinical challenge because patients with this disease present with an extremely dismal prognosis, in part due to their poor responses to conventional therapeutic treatment, such as chemotherapy (Balgobind et al., 2011; Slany, 2009). Mixed lineage leukemia possesses unique clinical features, which were first described in the early 1980s. At the time, physicians realized that certain subsets of patients initially diagnosed with acute myeloid leukemia (AML) or acute lymphoblastic leukemia (ALL) fared far worse than others, especially some newborn and infant patients with similar clinical aspects. By fluorescent activated cell sorting (FACS) analysis, it was found that the leukemic blasts from these specific cases often expressed surface markers of both the myeloid and lymphoid lineages, although the immunophenotype may be more consistent with one or the other in a particular case (Krivtsov and Armstrong, 2007; Slany, 2009). In addition, a complete

lineage switch was even observed during treatment, meaning an ALL case could relapse as AML, therefore delivering the term of mixed lineage leukemia (Stass et al., 1984).

Although chromosomal translocations causing the rearrangements of the 11q23 locus were recognized as typical characteristics of mixed lineage leukemia soon after these genetic lesions had been observed, it was not until the early 1990s that the gene spanning this region was successfully cloned by four individual groups, which is now known as the mixed lineage leukemia (*MLL*) gene (Djabali et al., 1992; Gu et al., 1992; Tkachuk et al., 1992; Ziemin-van der Poel et al., 1991). *MLL* rearrangements generate a large variety of oncogenic MLL fusion proteins. To date, more than 60 different fusion partners have been identified, among which the most common ones are nuclear proteins with transcriptional activating activity (Krivtsov and Armstrong, 2007; Monroe et al., 2010; Yokoyama et al., 2010). In ALL, the most common translocations are t(11;19) and t(4;11), resulting in the fusion proteins MLL-ENL and MLL-AF4, respectively. In contrast, the t(9;11) translocation, resulting in the MLL-AF9 fusion protein, is more frequently found in AML. In addition to the nuclear translocation partners, another class of MLL fusion partners consists of cytoplasmic proteins that contain dimerization domains, such as AF6. Dimerization of these MLL fusion proteins leads to potent transcriptional activation and is essential for their leukemogenic capacity; however, the detailed leukemogenic mechanism remains elusive (Martin et al., 2003; So et al., 2003). *MLL*-related translocations are also commonly observed in secondary acute leukemias after topoisomerase inhibitor

treatment (Felix, 1998). In addition, around 8% of AML patients with normal cytogenetic features harbor internal tandem duplications of partial MLL N-terminal sequence, known as *MLL-PTD* (Figure 1.1). Overall, genetic lesions in the *MLL* gene are associated with more than 70% of infant leukemias and approximately 10% adult leukemias (Krivtsov and Armstrong, 2007).

Wild-Type MLL

The *MLL* gene encodes a histone methyltransferase containing a C-terminal SET domain that catalyzes the methylation of histone H3 lysine 4 (H3K4), a histone modification commonly associated with gene activation (Milne et al., 2002; Nakamura et al., 2002; Strahl et al., 1999). MLL was found to be part of a large chromatin-modifying complex that promotes transcription activation through histone methyltransferase and histone acetyltransferase activities (Nakamura et al., 2002). During the formation of this macromolecular complex, the MLL protein is cleaved by an aspartic protease named taspase into an N-terminal fragment (MLL^N) and a C-terminal subunit (MLL^C) (Hsieh et al., 2003a; Hsieh et al., 2003b; Takeda et al., 2006; Yokoyama et al., 2002). On the one hand, the MLL^N fragment contains several functional regions that are considered essential for correct localization of the MLL complex. On the other hand, the MLL^C subunit associates with at least four proteins, including MOF, WDR5, ASH2L and RBBP5, to modify chromatin structure, thereby facilitating transcription activation. Among these critical interacting partners, MOF neutralizes charges on histones by depositing a site-specific acetylation mark on histone H4 lysine 16, potentially decondensing chromatin for efficient transcription (Slany, 2009). WDR5, ASH2L

and RBBP5 form a common structural platform, which stabilizes the functionally active configuration of the catalytic MLL^C fragment. In particular, WDR5 mediates MLL^C interactions both with this platform and with the histone substrate, which in turn achieves the full H3K4 methyltransferase activity of the MLL complex (Dou et al., 2006; Ruthenburg et al., 2006; Schuetz et al., 2006; Southall et al., 2009). In summary, the MLL^N and MLL^C fragments, in coordination with the other MLL complex components, modulate the chromatin structure at MLL target loci, thereby mediating transcriptional regulation of downstream genes.

Major MLL Targets – *HOX* Genes

Based on the sequence similarity, MLL is a human homolog of the *Drosophila* trithorax (TrxG) protein originally identified in genetic screens as "anti-silencers" counteracting the action of Polycomb group (PcG) proteins that represses *Hox* gene expression (Mills, 2010). Consistent with the role of *Drosophila* TrxG proteins, in mice, Mll is required for normal embryonic development through maintaining the proper *Hox* gene expression pattern (Yu et al., 1995). Several studies demonstrated that it also plays a central role in regulating hematopoietic stem cell self-renewal and progenitor expansion (Jude et al., 2007; McMahon et al., 2007). Notably, *Hox* gene expression is dynamically regulated and functionally important in these processes (He et al., 2011).

Hox genes encode a large family of transcription factors that are evolutionarily conserved among metazoans. They play crucial roles during development by regulating a number of important physiological processes, including apoptosis, receptor signaling, cell motility, angiogenesis and hematopoiesis (Shah and

Sukumar, 2010). In human, a total of 39 *HOX* genes have been identified. They are linked in as four separate clusters, HOXA, HOXB, HOXC and HOXD, located on chromosomes 7, 17, 12 and 2, respectively (Ansari and Mandal, 2010). Based on sequence similarities and their positions within the clusters, they are further classified into 13 paralogue groups arranging from position 1 to 13 in a 3'-5' direction (He et al., 2011; Krumlauf, 1994).

This clustered organization is of particular interest because it correlates with the temporal and spatial expression patterns of *Hox* genes, meaning that the 3' *Hox* genes are expressed first and are more restricted to the anterior region of the embryo, whereas the 5' *Hox* genes are expressed sequentially later and more caudally (He et al., 2011). Mutation of single *Hox* genes does not cause dramatic alterations in morphogenesis in vertebrates, suggesting functional redundancy within the *Hox* family. Nevertheless, the expression of specific *Hox* genes and combinations of *Hox* gene products vary at different stages of development, indicating that proper regulation and maintenance of *Hox* gene expression are essential mechanisms governing developmental processes. For instance, *Hox*1-6 genes are maximally expressed in hematopoietic stem cells, whereas Hox7-13 genes are present in committed progenitors. During definitive hematopoiesis, *Hox* gene expression decreases as differentiation proceeds. In particular, previous studies have shown that 3' *HoxA* and *HoxB* cluster genes are preferentially expressed in primitive hematopoietic stem cells (HSCs), relative to their levels in the HSC-low or HSC-depleted subpopulations (Guo et al., 2003; Pineault et al., 2002). Moreover, in hematopoietic cells, *Hox* genes are

expressed in a lineage-specific manner, with most *HoxB* and certain *HoxC* genes selectively expressed in cell lines showing erythroid characteristics and certain *HoxA* genes predominantly expressed in myeloid-lineage cell lines (Lawrence et al., 1996). More specifically, populations enriched for myeloid progenitors preferentially express 5' *Hox* genes, such as *HoxA9*, *HoxB9* and *HoxA10*, and these genes are coordinately activated in myeloid leukemia cells (Celetti et al., 1993).

Leukemogenic MLL Fusion Proteins

The most striking property of leukemogenic MLL fusion proteins is the significant diversity of this family. While the oncogenic mechanisms are likely to differ in detail, all rearranged forms of MLL upregulate expression of certain *HOX* genes and their cofactors, including *HOXA9* and *MEIS1*, which is critical for leukemogenic transformation (Armstrong et al., 2002; Ayton and Cleary, 2003; Kumar et al., 2004). Although it is well established that constitutive activation of these downstream targets, particularly *HOXA9*, is a key feature of MLL leukemia pathogenesis, the molecular mechanisms governing the aberrant *HOX* gene activation have not been defined (Sitwala et al., 2008; Yokoyama and Cleary, 2008).

Within multiple domains that are present in the wild-type MLL protein, only the N-terminus containing the Menin interaction domain, AT-hooks and CxxC-RD2 domain (up to the break point region) are invariably retained in all *MLL*-rearranged oncoproteins, whereas the Plant Homeodomain (PHD) and the SET

domain, which is required for the histone methyltransferase activity, are consistently deleted (Figure 1.1) (Caslini et al., 2007). Extensive studies have

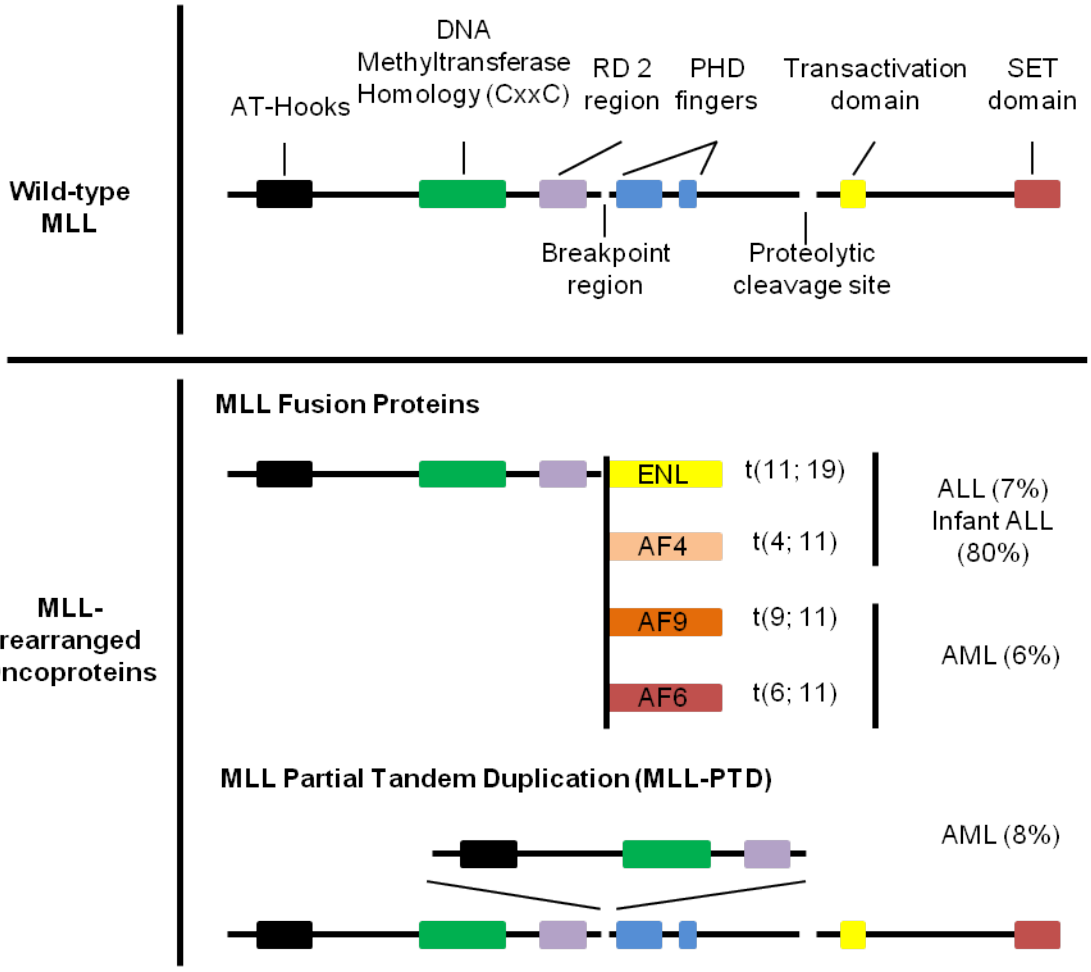

Figure 1.1 Schematic of Wild-Type MLL and MLL-Rearranged Oncoproteins. Major functional domains and the proteolytic cleavage site of wild-type MLL are indicated. MLL fusion proteins consist of the N-terminus of wild-type MLL (up to the breakpoint region) fused in frame with a translocation partner (either a nuclear protein, such as ENL, AF4 and AF9, or a cytoplasmic protein, such as AF6). MLL-PTD is generated by exon duplication of the sequences encoding the N-terminus of wild-type MLL at the breakpoint region.

been conducted to explore the functional significance of the retained portion of MLL in MLL fusion proteins in transcriptional activation and leukemogenesis. For example, Menin, a tumor suppressor encoded by the *MEN1* gene, directly interacts with the extreme N-terminus of MLL, and this interaction is essential for MLL-rearranged leukemogenesis (Caslini et al., 2007; Chen et al., 2006). This interaction also involves a chromatin-associated protein, LEDGF (lens epithelium-derived growth factor) (Yokoyama and Cleary, 2008). Moreover, the CxxC domain selectively binds unmethylated CpG DNA and contributes to the binding of MLL fusion proteins to the target loci, protecting the corresponding regions against DNA methylation (Ayton et al., 2004). However, the role of the CxxC-RD2 region, particularly the RD2 region that is immediately adjacent to the CxxC domain and proceeds to the breakpoint region, in the cellular activities of wild-type MLL or MLL fusion proteins remains elusive. The importance of this region is highlighted by recent work by Bach et al. who demonstrated that the DNA-binding affinity alone does not fully account for the indispensible role of this region in leukemogenesis, indicating the presence of uncharacterized activities or interactions critical for MLL-rearranged leukemogenesis (Bach et al., 2009).

On the other hand, during MLL rearrangements, the SET domain at the C-terminus of wild-type MLL is replaced by translocation partners. The mechanisms, by which the major fusion partners contribute to MLL-rearranged leukemogenesis, are beginning to be defined (Monroe et al., 2010). It has been reported that a complex of proteins termed ENL-associated proteins (EAPs), or a closely related complex named AEP for AF4 family/ENL family/P-TEFb complex, interacts with

the major MLL fusion partners AF9, ENL and AF4 (Lin et al., 2010; Muntean et al., 2010; Yokoyama et al., 2010). The EAP complex includes both the common MLL fusion partners, such as AF9 and ENL, and also the histone methyltransferase DOT1L and the P-TEFb complex (consisting of CDK9 and cyclin T1), both of which positively regulate transcription elongation (Krivtsov et al., 2008; Mueller et al., 2007). Meanwhile, other investigators have described an H3K79 methyltransferase complex, DotCom, which contains several common MLL fusion partners, including AF9, ENL and AF10, that play a positive role in leukemogenesis (Mohan et al., 2010a). The components of these complexes partially overlap, suggesting that they may share certain mechanisms that contribute to MLL-rearranged leukemogenesis (Mohan et al., 2010b; Mueller et al., 2007). Notably, the interaction partners of MLL fusion proteins are distinctive from the components of the wild-type MLL complex, suggesting that they may activate transcription through differential mechanisms.

PAFc

The Polymerase Associated Factor complex (PAFc) is a multi-protein complex, with the core components of PAF1, LEO1, CDC73, CTR9, WDR61 (also known as hSki8), and, in some cases, Rtf1 (Jaehning, 2010a; Kim et al., 2010; Rozenblatt-Rosen et al., 2005; Zhu et al., 2005a). Increasing evidence has revealed that PAFc plays important roles in a wide range of biological processes, including H2B monoubiquitination, the initiation, elongation and termination of gene transcription, cell cycle regulation, and mRNA processing (Figure 1.2) (Chaudhary et al., 2007; Kim et al., 2009; Kim and Roeder, 2009).

In addition, several components of PAFc are known to play important roles in carcinogenesis. For instance, in a study to identify genes involved in pancreatic tumor progression, PAF1 was found to be overexpressed as a result of a double minute amplification involving chromosome 19q13 (Batra et al., 1991). Along this line, overexpression of PAF1 results in transformation of NIH3T3 cells (Moniaux et al., 2006). These findings suggest that PAF1 may function as an oncogene promoting tumorigenesis. In contrast, CDC73 has been implicated to serve as both a tumor suppressor and an “aider and abettor” of an oncoprotein in a context-dependent manner. One the one hand, most notably mutations in CDC73, encoded by *HRPT-2* (hereditary hyperparathyroidism type 2), are responsible for the familial hyperparathyroidism-jaw tumor (HPT-JT) syndrome (Szabo et al., 1995). HPT-JT is an autosomal dominant disorder associated with hyperparathyroidism (HPT) and a high incidence of parathyroid adenomas, hyperplasias and carcinomas as well as renal abnormalities and uterine tumors (Newey et al., 2009). Some mutations in *HRPT-2* are predicted to lead to loss of function due to premature termination. The chromosome 1q25-q31 region spanning *HRPT-2* frequently undergoes loss of heterozygosity in tumors arising in HPT-JT patients, suggesting that CDC73 functions as a tumor suppressor (Newey et al., 2009). Consistent with this role, overexpression of wild-type CDC73, but not a mutant form found in HPT, blocks cell proliferation and inhibits the cell cycle regulator cyclin D1 (Woodard et al., 2005). On the other hand, CDC73 overexpression in 293T and COS7 cells increases S-phase entry and promotes cellular proliferation. This induction of CDC73-mediated cell-dependent

proliferation requires the SV40 large T-antigen, which is directly bound by CDC73 (Iwata et al., 2007), suggesting the potential role of CDC73 as an oncogene cofactor. In addition, the *CTR9* gene has been localized to chromosome 11p15, which contains chromosomal aberrations associated with the pathogenesis of different tumor types including lung cancer and leukemia (Chaudhary et al., 2007), suggesting a possible role of CTR9 in tumorigenesis.

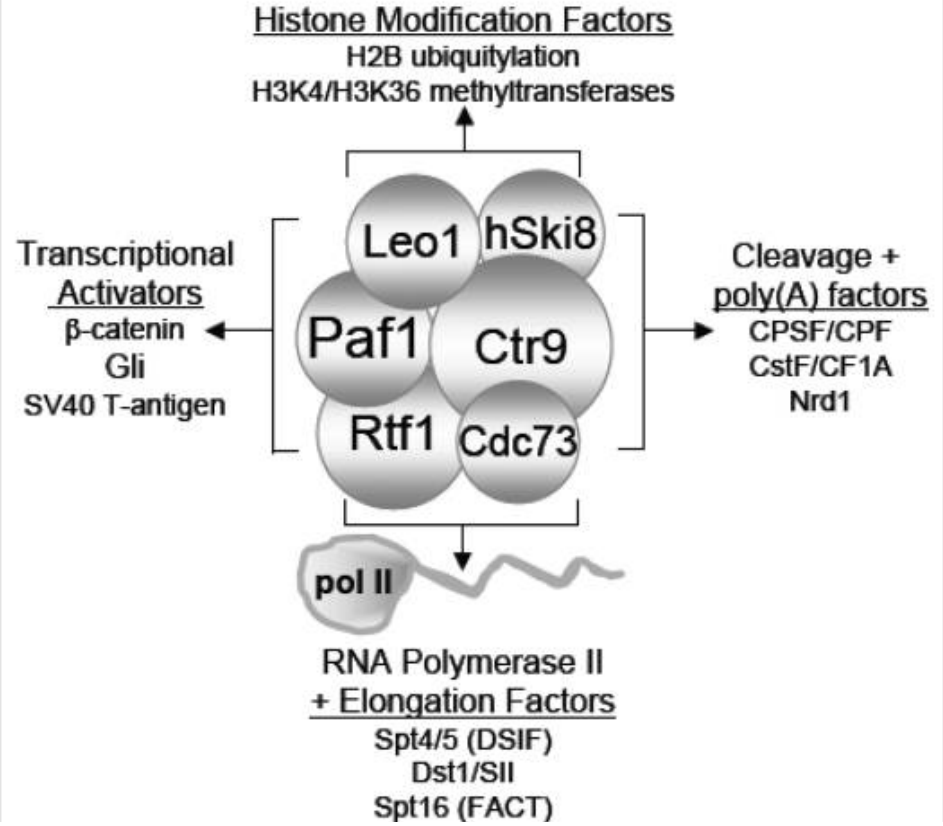

Figure 1.2 Overview of Paf1C Interactions with Transcriptional Activation, Histone Modification, Elongation and 3' End Formation Factors. Adapted from (Jaehning, 2010b)

Previous studies have demonstrated that the yeast PAF complex is required for the recruitment of the yeast Set1 methyltransferase complex, termed COMPASS, to RNA polymerase II. It is also indispensable for both COMPASS-mediated histone H3K4 and Dot1L-mediated H3K79 methylation (Krogan et al., 2003; Rozenblatt-Rosen et al., 2005). Given that the MLL complex is a human homolog of COMPASS, and that the only H3K79 methyltransferase in human, hDOT1L, is recruited by MLL fusion proteins, it is both mechanistically important and therapeutically intriguing to investigate whether PAFc is physically and functionally associated with the MLL complex, as well as the leukemogenic MLL fusion protein complexes.

Materials and Methods

Cell Culture

293 and HeLa cells were cultured in Dulbecco's modified Eagle's medium (DMEM) supplemented with 10%FBS and 1X non-essential amino acids. MLL-ENL and E2A-HLF cells were cultured in Iscove's modified Dulbecco's medium (IMDM) supplemented with 15% fetal calf serum (FBS) (Stem Cell Technologies). Hoxa9-ER cells were cultured in IMDM supplemented with 15% FBS and 0.1% IL3. Plat-E cells were cultured in DMEM supplemented with 10% FBS. HL-60, THP-1, KOPN8 and K562 cells were cultured in RPMI-1640 medium supplemented with 10% FBS. Differentiation of HL-60 and THP-1 cells was induced by 10 nM PMA treatment.

Luciferase Assay

293 cells were transiently transfected with MSCV MLL-AF9 (and derivatives), CMV-Renilla, and Hoxa9-LUC (or Myc-E box-LUC) constructs using FuGene 6 (Roche) according to manufacturer's instructions. Cells were then serum starved in 0.5% FBS in OPTI-MEM media for 48 hours. Luciferase assays were performed using the Dual Luciferase assay kit (Promega) according to manufacturer's instructions. Emission was detected using a Monolight 3010 (BD Biosciences).

Vector Construction

The pFMLL-AF9 vector and pMSCV-neo constructs encoding MLL-AF9 have been described previously (Muntean et al., 2008). The expression vectors for various MLL-AF9 deletions and CxxC-RD2-AF9 deletions tagged with FLAG/Myc

were generated by restriction enzyme digestion and PCR-based mutagenesis. Expression vectors for CDC73, CTR9, PAF1, LEO1 and WDR61 were purchased from Origene. pSM2c scrambled, pSM2c shCdc73 (clone ID V2MM_49292) and pSM2c shCtr9 (clone ID V2MM_46348) retroviral vectors were purchased from Open Biosystems.

Retrovirus Packaging

pMSCV (for FLAG-MLL-AF9 and deletions) and pSM2c (for shScram, shCdc73 and shCtr9) were transfected using FuGene 6 reagent (Roche) into Plat-E cells and selected using puromycin (1 μg/ml) and blasticidin (10 μg/ml). Media containing the recombinant retrovirus was collected for transduction at 48 and 72 hours post transfection.

Bone Marrow transformation assays

Bone marrow transformation assays were performed as described (Muntean et al., 2008) with the addition of p-iodonitro tetrazolium violet (INT) staining of tertiary colonies. Briefly, bone marrow was isolated from 6-8 week old C57B6 mice injected with 5-fluorouracil. Cells were collected from the tibia and femur and cultured in pre-stimulation cocktail that includes SCF, IL3 and IL6. Cells were transduced by spinoculation twice with MLL-AF9 or MLL-AF9 deletion retroviruses and plated in MethoCult® M3234 (Stem Cell Technologies) with IL3, IL6, SCF, GM-CSF and 1mg/ml G418. After three rounds of replating colonies were stained with 0.1% INT for 30 minutes and scored. Cells harvested from bone marrow transformation assays were cytospun and stained with Hema 3 Stain Kit (Thermo Fisher Scientific). Images were acquired using a 100× lens and

Olympus BX-51 microscope with Olympus DP controller software (Olympus). For knock down experiments, MLL-AF9 transduced cells were collected after the second round of plating and transduced twice with either scrambled control retrovirus, shCdc73 retrovirus or shCtr9 retrovirus by spinoculation and replated in the MethoCult® medium described above and selected in 2 μg/ml puromycin at 5 x 10^4 cells per plate. Colonies of greater than 50 cells were scored after the final replating. All animal studies were approved by the University of Michigan Committee on Use and Care of Animals and Unit for Laboratory Medicine.

Immunoprecipitation and Immunoblotting

Preparation of cell lysates, immunoprecipitation, and immunoblotting were performed as described previously (Muntean et al., 2008). 293 cells were transiently transfected with FuGene 6 (Roche) according to manufacturer's instructions. Cells were lysed in BC-300 buffer (20mM Tris-HCl (pH 7.4), 10% glycerol, 300 mM KCl, 0.1% NP-40), and immunoprecipitations were performed overnight with resins described below. IPs were washed 4 times with BC-300 buffer and proteins were eluted by boiling in SDS-loading buffer. Proteins were visualized by SDS-PAGE and western blotting. Primary antibodies included rabbit anti-Paf1, anti-Leo1, anti-Parafibromin, anti-Ctr9 (Bethyl Laboratories, Inc.) and mouse anti-WDR61 (Abcam). Rabbit anti-MLL C was generously provided by Dr. Yali Dou. Additional primary antibodies included rabbit anti-Hoxa9 (Millipore), goat anti-Myc (Abcam), mouse anti-beta-actin (Sigma), rabbit anti-cyclin-T1 (H-245) (Santa Cruz) and rabbit anti-HA tag (Abcam). Rabbit anti-FLAG antibody and agarose affinity beads coupled to mouse anti-FLAG M2 monoclonal

antibody were purchased from Sigma. Agarose affinity beads coupled to mouse anti-Myc monoclonal antibody were purchased from Clontech.

In Vitro Binding

Equal amounts of MLL and individual PAF proteins (1-2 µg) along with 15 µl of Protein G affinity agarose beads (Roche) were incubated with MLL antibodies (Bethyl) in Binding Buffer (50 mM Tris-HCl pH7.9, 100 mM KCl, 0.05% NP40, 0.1% BSA) overnight at 4 degrees. Bound material was washed with Wash Buffer (50 mM Tris-HCl pH 7.9, 500 mM KCl, 0.3% NP40) 4 times and eluted from beads by boiling in SDS loading buffer. Eluted material was visualized by western blot or Coomasie staining. Reciprocal IPs were performed by incubating individual PAF proteins and MLL fragments with Amylose resin (New England Biolabs) in Binding Buffer overnight at 4 ℃. Bound material was washed with Wash Buffer 4 times and eluted by boiling in SDS loading buffer. Proteins were visualized as described above.

Protein Identification by LC-Tandem Mass Spectroscopy

293 cells were transiently transfected with control or FLAG/HA CxxC-RD2 vectors as described above. Cells were lysed and immunoprecipitations were performed as described above. Bound material was eluted with 40 µg FLAG peptide followed by 15 rocking at 4 ℃ (Sigma). FLAG elutions were repeated and protein was concentrated with a Micron YM-30 centrifugal filter column (Millipore). Proteins were separated by SDS-PAGE on a 4-20% gradient tris-glycine gel and visualized by silver staining (Sigma). Silver stained (PROTSIL-2, Sigma) gel lanes corresponding to control and CxxC-RD2 IP were cut into 16 slices each

and destained following manufacturer's protocol. Upon reduction (10 mM DTT) and alkylation (50 mM iodoacetamide) of the cysteines, proteins were digested overnight with sequencing grade, modified trypsin (Promega). Resulting peptides were resolved on a nano-capillary reverse phase column (Picofrit column, New Objective) using a 1% acetic acid/acetonitrile gradient at 300 nl/min and directly introduced in to an ion-trap mass spectrometer (LTQ XL, ThermoFisher). Data-dependent MS/MS spectra on the 5 most intense ion from each full MS scan were collected (relative CE ~35%). Proteins were identified by searching the data against Human IPI database (v 3.41, 72,254 entries) appended with decoy (reverse) sequences using X!Tandem/Trans-Proteomic Pipeline (TPP) software suite (Keller et al., 2002) (Nesvizhskii et al., 2003). All proteins with a ProteinProphet probability score of >0.9 (error rate <2%) were considered positive identifications and manually verified.

Bacterial Expression

CxxC-RD2, RD2, PAF1 and LEO1 were cloned into the pMocr (DelProposto et al., 2009) bacterial expression vector, which contains a His-MOCR tag. CDC73, CTR9-N and CTR9-C were generated by cloning into the pMCSG9 (Donnelly et al., 2006) vector with a His-MBP tag. Expression plasmids were transformed into BL21(DE3) bacteria containing pRARE-CDF (for additional tRNA expression) and screened at the University of Michigan High-Throughput Protein Lab. Bacteria was grown at 37 degrees Celsius in TB at 250 rpms with 50ug/ml spectinomycin and 100 µg/ml ampicillin to an OD600 of approximately 1 followed by temperature reduction to 20 degrees Celsius for 1 hour. Protein expression

was induced with 200 μM IPTG and continued growth overnight. Proteins were purified by lysis in CelLytic B buffer (Sigma) supplemented with 0.15 M NaCl, 1 mM PMSF, 1 mM DTT, 0.4 mg/ml lysozyme, 2 mM $MgCl_2$, and 100 units/ml Benzonase. Proteins were purified over a Ni column (GE Pharmacia) using an AKTA Purifier liquid chromatography system (GE Pharmacia) and eluted with 20 CV of elution buffer (20 mM Tris-HCl, pH 7.5, 10% glycerol, 1 mM DTT, 0.15 M NaCl, 20-500 mM imidazole). Secondary purifications were performed using a Mono-Q column (GE Pharmacia) or amylose column (GE Pharmacia) and identical elution buffers except 0.15 M-1 M NaCl gradient. Purified proteins were visualized by Coomasie staining.

Real Time PCR

RNA was extracted from cells using TRIzol reagent (Invitrogen). cDNA was generated using Superscript III Reverse Transcriptase (Invitrogen) according to manufacturer's instructions. Relative quantitation of real time PCR product was performed using comparative ΔΔCt method (described in ABI Prism 7700 Sequence Detection System User Bulletin No. 2) and TaqMan or SYBR green fluorescent labeling and ABI 7500 PCR Detection System. FLAG-MLL-AF9 was detected using the following primers for SYBR green detection: FLAG-F-5'-ggactacaaggacgacgatga-3' and MLL-R-5'-acagctgtgcgccatgtt-3'. TaqMan primer probe sets were purchased from Applied Biosystems for mouse *Hoxa9*, *Meis1, Paf1, Leo1, Cdc73, Ctr9, Wdr61,* and human *PAF1, LEO1, CDC73, CTR9, WDR61* and *HOXA9*.

THP-1 Electroporation and FACS

THP-1 cells were transfected with pTurbo-GFP and either empty MSCV or a mixture of the five PAFc expression plasmids at a ratio of 1:5. A total of 600 ng of DNA was transfected into THP-1 cells using the Amaxa Nucleofector II device (Lonza) using Amaxa Cell Line Nucleofector Kit V for THP-1 cells according to manufacturer's instructions. Briefly, $1X10^6$ cells were transfected using either program U-001 or V-001. Cells were allowed to recover overnight. Cells were split in half with one half being treated with 10 nM PMA to induce differentiation. Cells were incubated an additional 24 hours and then washed twice with PBS followed by staining with PE-mouse anti-human CD11b or isotype control (BD Pharmingen). After 30-minute incubation cells were washed with Standard Buffer (1X PBS, 0.1% sodium azide, 1% heat inactivated FBS) twice and resuspended in 250 µl Standard Buffer. FACS data was collected on an LSRII (BD). CD11b expression was monitored on both the GFP positive and GFP negative populations as an internal control.

Chromatin Immunoprecipitation

ChIP was performed as described previously (Milne et al., 2005a) using primary antibodies specific for MLL^C (gift from Dr. Yali Dou), ENL (gift from Dr. Robert Slany), histone H3, H3K4 dimethylation, H3K4 trimethylation and H3K79 tri-methylation (Abcam) and Paf1, Leo1, Parafibromin and Ctr9 (Bethyl Laboratories Inc,. as described above). Quantitative real-time PCR was performed on the precipitated DNAs with TaqMan fluorescent labeling using the following primers and qPCR probes:

Human HOXA9 TaqMan primer probe sets

Promoter

Forward Primer – TCTAACCTTTCCAAGTCCTCGTAAA

Reverse Primer – GCGGGAAGTCGGAAACG

Probe – FAM-CCACGGCGAGGCAAACGAATCT-TAMRA

Coding

Forward Primer – GGCCCAGGACCGAGATACTT

Reverse Primer – CGCTCACGGACAATCTAGTTGT

Probe – FAM-CGTTCTTCGAAAGCAGTGCAGCCC-TAMRA

Mouse *Hoxa9* TaqMan primer probe sets have been described earlier (Milne et al., 2005a).

Binding was quantitated as follows: $\Delta C_T = C_T(\text{input}) - C_T(\text{Chromatin IP})$, % total = $2^{\Delta CT}$.

siRNA Knockdown of PAFc

siRNA smart pools were obtained from Dharmacon for CTR9, CDC73, PAF1 and LEO1. siRNA transfection of HeLa cells was achieved using Lipofectamine 2000 (Invitrogen) according to manufacturer's instructions for analysis in luciferase assays. Oligofectamine (Invitrogen) was used according to manufacturer's instructions for siRNA transfection of HeLa cells and PAFc knock down for ChIP assays.

Accession Numbers

Microarray data has been deposited in the Gene Expression Omnibus (GEO) repository from the National Center for Biotechnology Information (NCBI) with accession code GSE21299.

Results

PAFc Interacts with the CxxC-RD2 Domain of MLL

To identify proteins that associate with MLL CxxC-RD2, we transiently expressed epitope tagged portions of this region in human embryonic kidney 293 cells (Figure 1.3A). FLAG-tagged CxxC-RD2 including a nuclear localization signal (NLS) was immunoprecipitated from transiently transfected 293 cells using M2 anti-FLAG agarose beads. An "empty" expression vector with FLAG epitope tag and NLS was also subjected to immunoprecipitation as a non-specific immunoprecipitation control. Coeluted proteins were resolved by SDS-PAGE (Figure 1.3B) and analyzed by mass spectroscopy. Multiple peptides corresponding to subunits of PAFc were identified with high probability including CTR9, LEO1, PAF1, CDC73 and WDR61 that correlated with silver stained bands at 133 kDa, 105 kDa, 75 kDa, 64 kDa and 34 kDa, respectively (Figures 1.3B and 1.3C). Each of the five PAFc subunits identified by mass spectrometry (PAF1, CDC73, CTR9, LEO1 and WDR61) was confirmed to co-immunoprecipitate with Myc-tagged CxxC-RD2 by western blotting in 293 cells (Figure 1.4A).

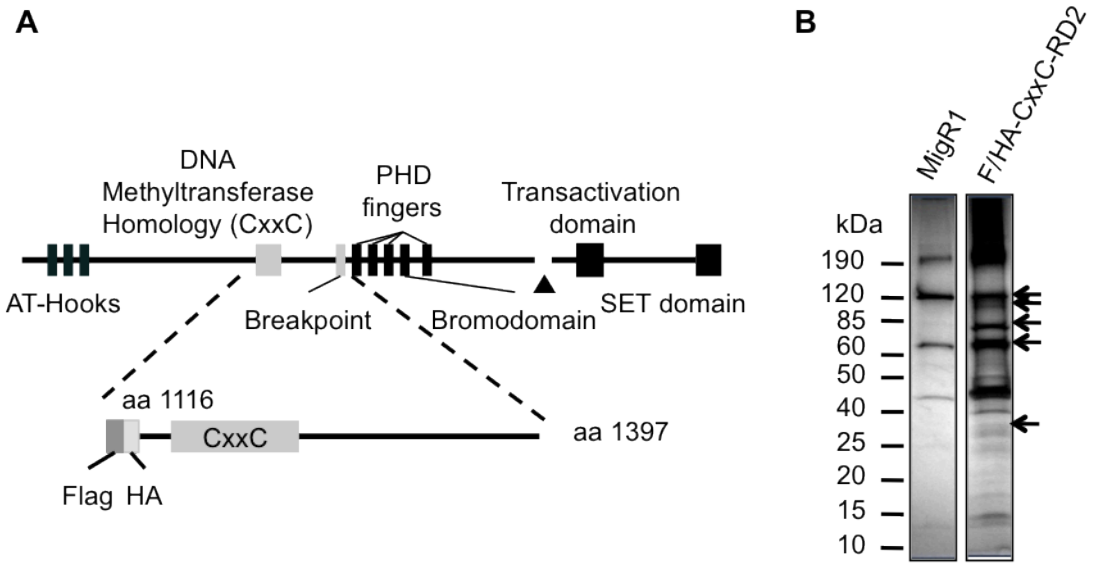

C

Protein	# Specs	# Peptides	Coverage
PAF1	8	5	13.2%
CDC73	17	9	17.5%
WDR61	4	4	18.0%
LEO1	1	1	4.6%
CTR9	3	2	3.2%

Figure 1.3 MLL Fragment Interacts with the PAF Complex (PAFc) (A) Schematic diagram of the full-length MLL protein with key domains indicated. The FLAG/HA tagged CxxC-RD2 MLL fragment used for immunoprecipitation is shown below. The first and last amino acids of the protein fragments are indicated. (B) MigR1 and FLAG/HA-tagged CxxC-RD2 was expressed in 293 cells and immunoprecipitated. Immunoprecipitates were analyzed by SDS-PAGE and visualized by silver staining. Arrows indicate bands at the predicted molecular weights of the PAF complex components. (C) PAFc identification by mass spectroscopy analysis of the immunoprecipitates obtained in (B).

To exclude the possibility of a DNA-mediated MLL-PAFc interaction and confirm that the PAFc interaction is preserved in the context of a fusion protein, immunoprecipitations were repeated with Myc-tagged CxxC-RD2-AF9 in 293 cells following Benzonase treatment. Immunoprecipitation was preserved in the presence of Benzonase suggesting the interaction is not DNA dependent (Figure 1.4B). Furthermore, PAFc co-immunoprecipitated with Myc-CxxC-RD2-AF9, as well as with CxxC-RD2 (Figures 1.4B-1.4D).

These experiments were repeated with transfection of an expression vector for FLAG-tagged full-length MLL-AF9 or wild-type MLL into 293 cells followed by immunoprecipitation and western blotting (Figures 1.5A and 1.5B). We also confirmed the PAFc interaction by co-immunoprecipitation of CDC73 with MLL-ENL in the KOPN8 cell line (Figure 1.5C). Together, these experiments show the MLL-PAFc interaction is maintained both in the context of full-length (MLL^N) and in the context of leukemogenic MLL fusion proteins (Figure 1.5).

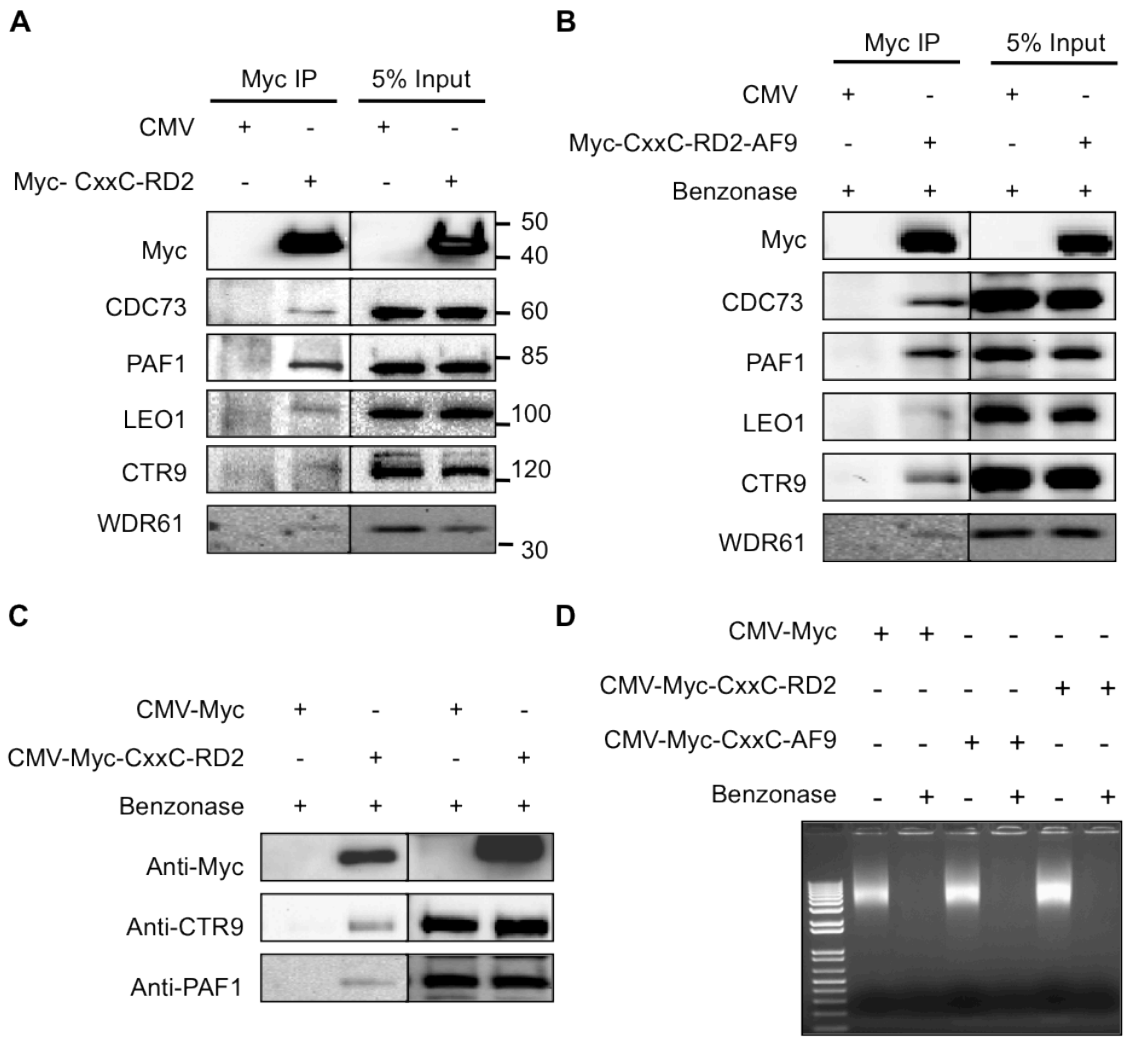

Figure 1.4 MLL and MLL-AF9 Fragments Interact with PAFc in a DNA-Independent Manner (A) Immunoprecipitation and western blot of the PAF complex following immunoprecipitation of Myc tagged CxxC-RD2 or Myc tag control. (B) The experiment described in A was repeated in the presence of Benzonase, using CxxC-RD2-AF9 fragment. Myc tagged CxxC-RD2-AF9 but not the Myc tag alone interacts with PAFc subunits. (C) Immunoprecipitation of Myc tagged CxxC-RD2 and western blot showing interaction with the PAF components CTR9 and PAF1 in the presence of Benzonase. (D) Lysates from the experiment shown in B and C were treated with Benzonase. Ethidium bromide staining of an agarose gel before and after Benzonase treatment shows complete DNA digestion after the treatment.

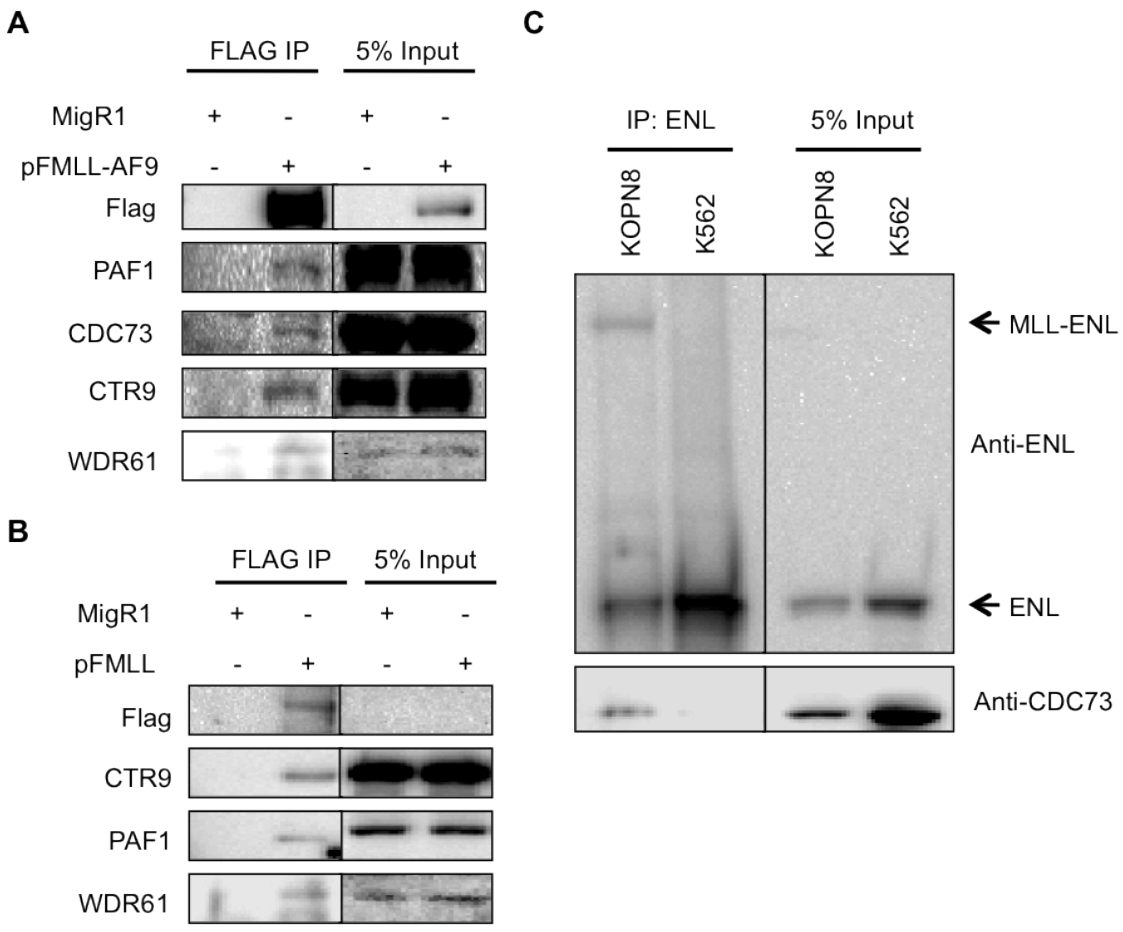

Figure 1.5 MLL and MLL Fusion Proteins Interact with PAFc in a DNA-Independent Manner (A and B) A full-length FLAG-tagged MLL-AF9 fusion protein (A) or wild-type MLL (B) was expressed in 293 cells and immunoprecipitated. PAFc stably associated with full-length MLL-AF9 and wild-type MLL as indicated by western blot. (C) Immunoprecipitation of endogenous MLL-ENL from KOPN8 cells and western blotting for the PAF component CDC73 shows interaction of endogenous MLL-ENL with endogenous PAFc. IP of wild-type ENL in K562 cells serves as a negative control.

To determine if the interaction between MLL and PAFc is direct and to identify the PAFc subunit(s) involved, we bacterially expressed and purified the MLL CxxC-RD2 region (amino acids 1115 - 1396) and the RD2 region alone (amino acids 1202 - 1396) for *in vitro* pull-down experiments with bacterially expressed PAF1, LEO1, CDC73 and CTR9 (expressed as N and C terminus proteins termed CTR9-N and CTR9-C) (Figure 1.6). These *in vitro* immunoprecipitations

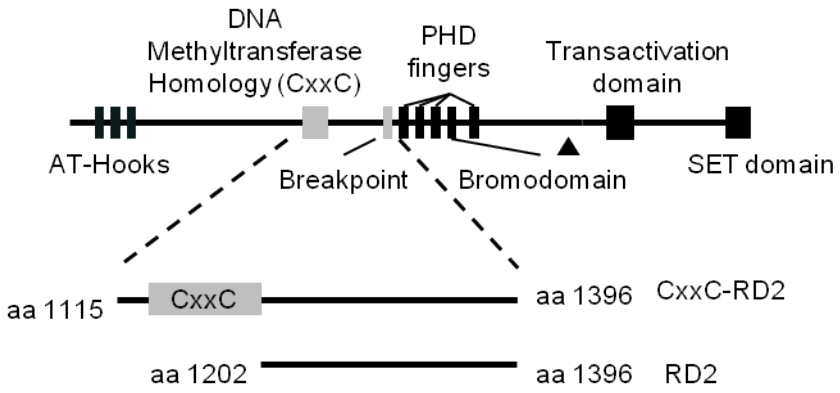

Figure 1.6 Schematic Diagram of MLL and Bacterially Purified CxxC-RD2 and RD2 Regions. Starting and ending amino acids are indicated.

were performed with either CxxC-RD2 or RD2 with MLL antibodies after incubation with individual components of PAFc. Strong interaction of PAF1 with CxxC-RD2 but not the RD2 region was detected indicating an interaction between PAF1 and amino acids 1115 and 1201 of MLL (Figure 1.7). These findings are consistent with our *in vivo* immunoprecipitation experiments in which PAFc co-immunoprecipitated with a small fragment of MLL N-terminal to the CxxC domain (amino acids 1115 - 1154) (Figure 1.8, see below). We also

detected a second interaction between CTR9-C and both the MLL CxxC-RD2 and RD2 regions (Figure 1.7).

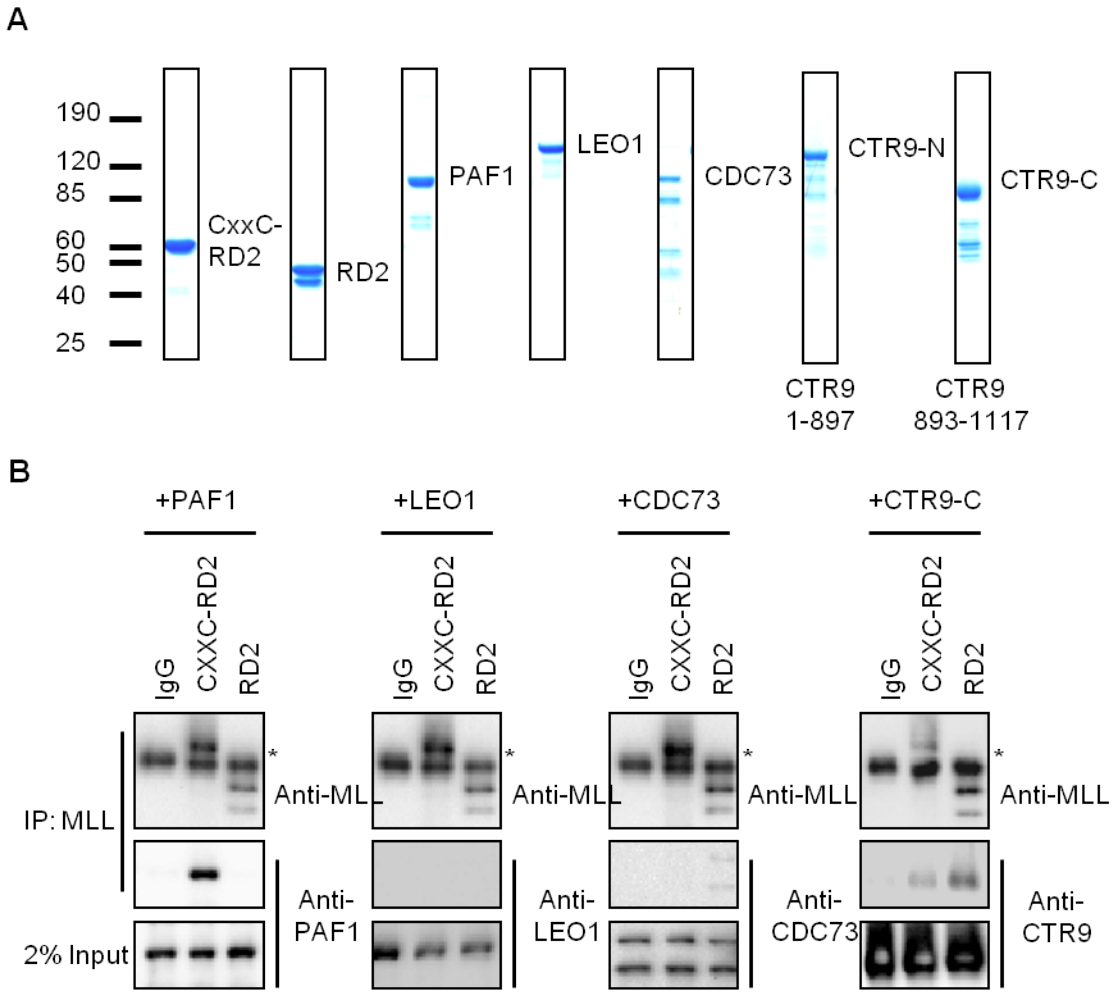

Figure 1.7 PAF1 and CTR9 Bind Directly to the CxxC-RD2 Region of MLL (A) Coomassie blue staining of bacterially purified His-MOCR tagged CxxC-RD2, RD2, PAF1, LEO1, and His-MBP tagged CDC73, CTR9-N and CTR9-C. The amino acids of CTR9-N and CTR9-C are indicated. (C) Immunoprecipitations performed with bacterially purified recombinant CxxC-RD2 or RD2 and PAF complex components. Individual PAF components were incubated with either CxxC-RD2 or RD2 and immunoprecipitated with MLL antibodies. PAF components and immunoprecipitated MLL fragments were detected with the indicated antibodies by western blot. Asterisk denotes detection of the IgG heavy chain.

We then performed a series of deletion experiments to further map the MLL residues that participate in the MLL-PAFc interaction. Expression vectors for Myc-tagged CxxC-RD2-AF9 deletion mutants spanning the RD2 region of MLL (Figure 1.8A, Cx-1154-AF9 through Cx-1357-AF9) were transiently transfected into 293 cells and tested for PAFc interaction. These experiments reveal a sharp decrease in the MLL-PAFc interaction when C terminal deletions were made past amino acid 1299 (Figure 1.8B, compare lanes 6 and 7). To overcome the residual low level binding of PAFc with proteins deleted at amino acids 1209 or amino acids 1258, presumably due to the multiple binding sites between PAFc and MLL, which were only partially affected by these deletions (Figure 1.7), we repeated this experiment with a set of deletion constructs that begin with MLL amino acid 1180 thereby deleting the proximal site of PAFc interaction (Figure 1.9A, Cx-del-1209-AF9 through Cx-del-1357-AF9). These experiments showed PAFc interaction with MLL is completely eliminated with deletions beyond amino acid 1299 (Figure 1.9B, compare lanes 4 and 5). Together, our data suggest the MLL-PAFc interaction is multivalent involving residues of MLL in both the pre-CxxC domain and the RD2 region. Furthermore, the binding of PAFc by both pre and post CxxC domains is consistent with the structure of the MLL CxxC domain determined by multidimensional NMR spectroscopy (Protein Database structure, 2J2S) (Allen et al., 2006), which shows the DNA binding CxxC domain coordinates two zinc atoms thereby bringing the pre and post CxxC regions into close opposition (Figure 1.28).

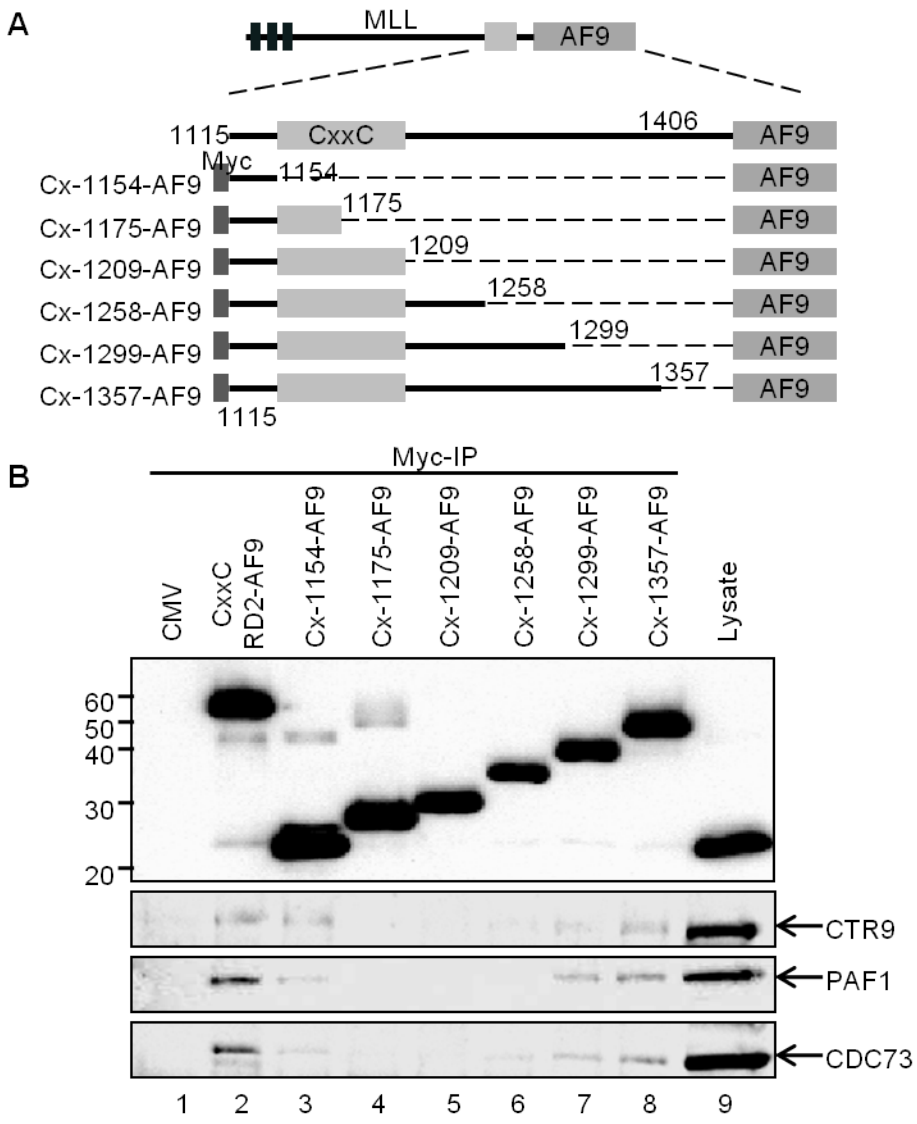

Figure 1.8 Amino Acids within the RD2 Region are Necessary for MLL-PAFc Interaction (A) Schematic of Myc-tagged CxxC-RD2-AF9 constructs made with serial deletions of the RD2 region. The first and last MLL amino acid retained in the expression constructs are indicated. All constructs include the AF9 fusion partner at the C-terminus and Myc tag at the N-terminus. The Cx-1154-AF9 through Cx-1357-AF9 constructs are named according to the last MLL residue retained in the fusion protein. (B) Myc-tagged RD2 deletion constructs described in A were expressed in 293 cells followed by immunoprecipitation. The Myc-tagged MLL deletion proteins and associated PAF complex components were detected by western blot with the indicated antibodies.

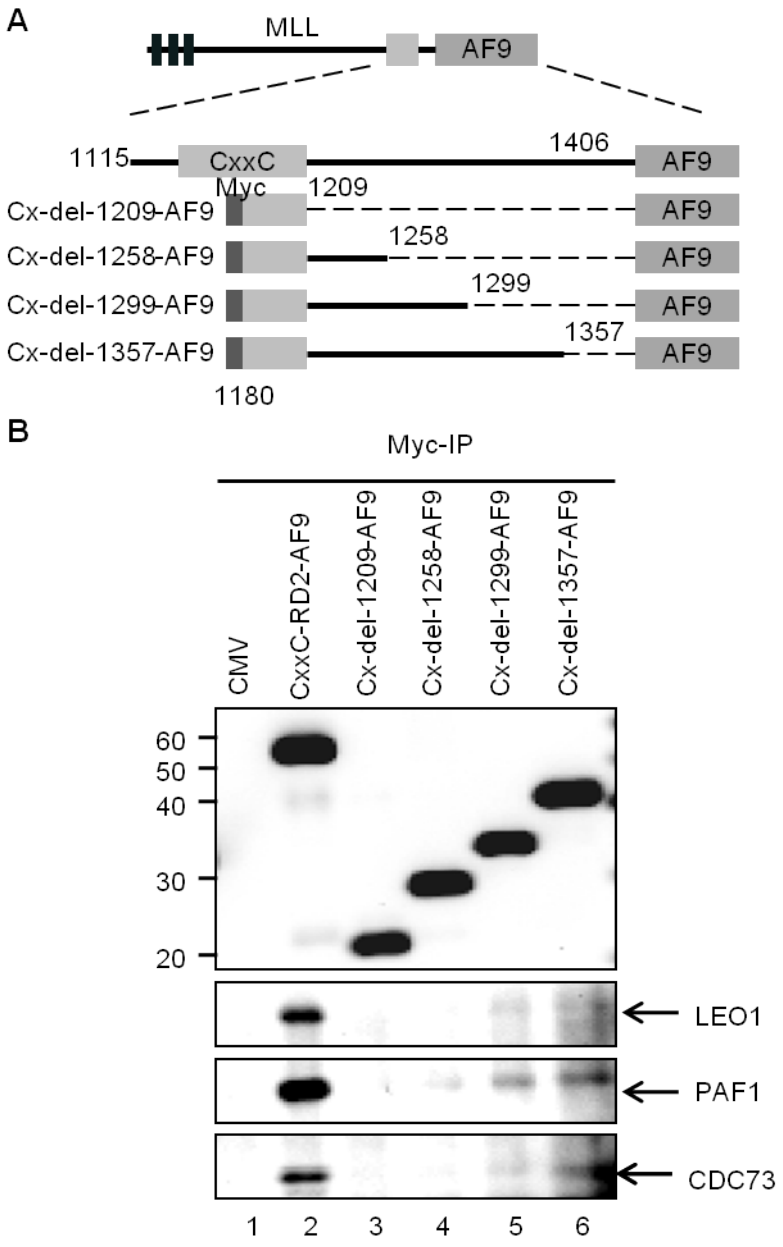

Figure 1.9 Pre-CxxC and RD2 Regions are Both Involved in MLL-PAFc Interaction
(A) Schematic of a second set of deletion constructs made through the RD2 region that also delete the pre-CxxC domain. Cx-del-1209-AF9 through Cx-del-1357-AF9 were made by deleting amino acids 1115 through 1179 of MLL. The amino acids included in each construct are indicated. (B) Myc tagged constructs described in C were expressed in 293 cells, immunoprecipitated and detected as described in Figure 1.8.

PAFc Stimulates Transcriptional Activation Induced by MLL and MLL Fusion Proteins

We then tested whether PAFc affects the transcriptional output mediated by MLL and the MLL-AF9 fusion protein. Dual luciferase assays were performed in 293 cells transfected with a luciferase reporter construct under the transcriptional control of the murine *Hoxa9* promoter (*Hoxa9-LUC*). These experiments showed that transcriptional activation by wild type MLL is enhanced by co-expression of the five PAFc subunits (Figure 1.10A). Consistent with our earlier finding (Milne et al., 2002), we observed a dose dependent transcriptional activation of the reporter gene driven by the *Hoxa9* promoter by expression of increasing amounts of MLL-AF9 (Figure 1.10B). Furthermore, we observed a dose-dependent augmentation of MLL-AF9 dependent transcription when increasing amounts of PAFc were expressed. Notably, expression of PAFc alone had little effect in our assay (Figures 1.10A and 1.10B). A similar trend was observed when using an MLL-AF9 responsive luciferase construct containing a thymidine kinase promoter and multimerized Myc E-boxes (Figure 1.11). Furthermore, we did not observe augmented transcription when single PAF components were introduced (Figure 1.10C). Together, these findings show that MLL and MLL-AF9 synergize with PAFc to augment transcriptional activation on MLL-responsive elements.

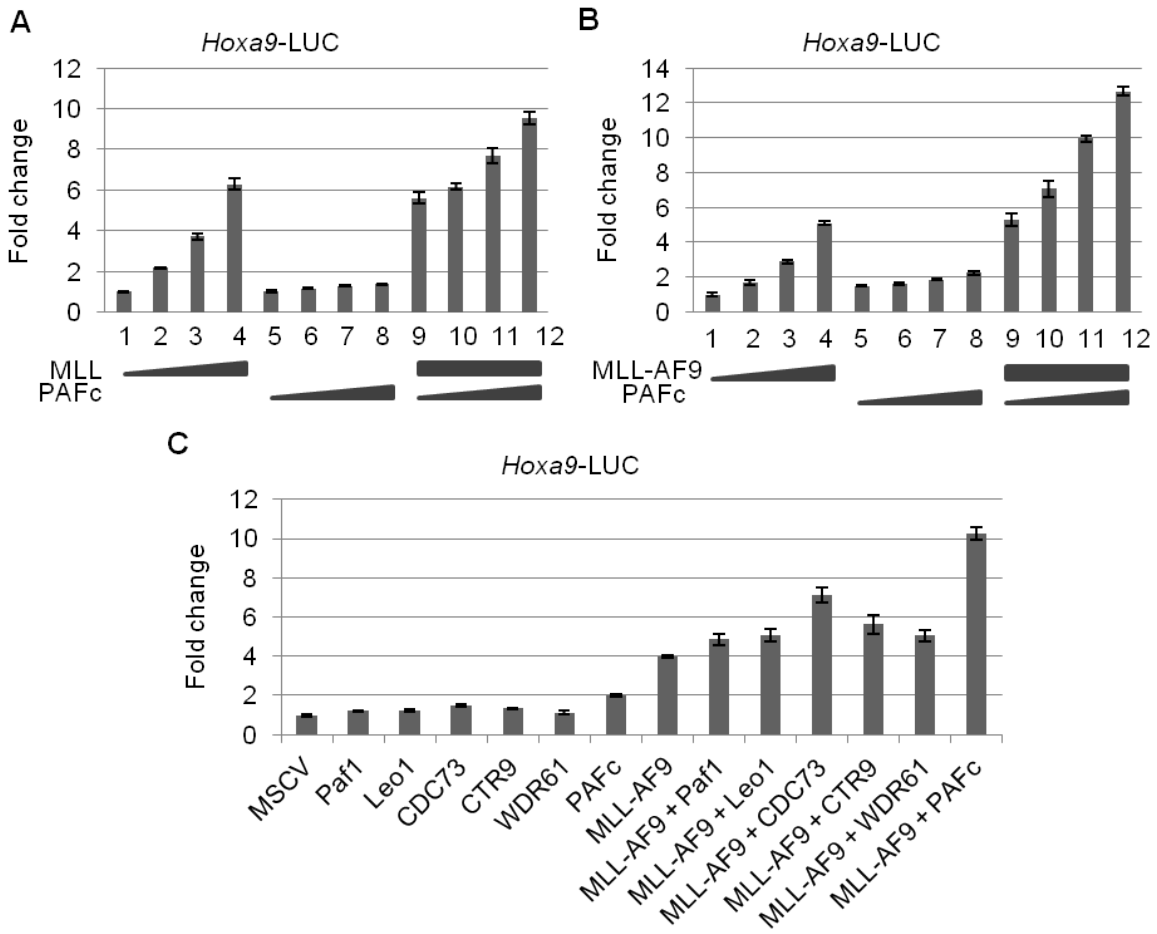

Figure 1.10 PAFc Synergizes with MLL and MLL-AF9 to Augment Transcriptional Activity (A) Luciferase assays were performed with the *Hoxa9-LUC* reporter construct and increasing doses of full length MLL (lanes 1-4) (0-0.6 µg) or PAFc (lanes 5-8) (0 – 0.6 µg). PAFc includes equal amounts of PAF1, LEO1, CDC73, CTR9 and WDR61. Lanes 9-12 show constant MLL (0.6 µg) with increasing doses of PAFc (0-0.6 µg). All changes are shown relative to lane 1. Error bars indicate +/- SD. Results of one of three representative experiments performed are shown. (B) Experiment was performed as described in A, except for using MLL-AF9 instead of MLL. Error bars indicate +/- SD. One of three representative experiments is shown. (C) Luciferase assay performed in transfected 293 cells using the *Hoxa9-LUC* reporter construct and individual PAFc components in lanes 1-6, PAFc (lane 7), MLL-AF9 alone (lane 8), MLL-AF9 plus individual PAF components (lanes 9-13) and MLL-AF9 with PAFc (lane 14). Error bars indicate +/- SD. Results of one of three representative experiments are shown.

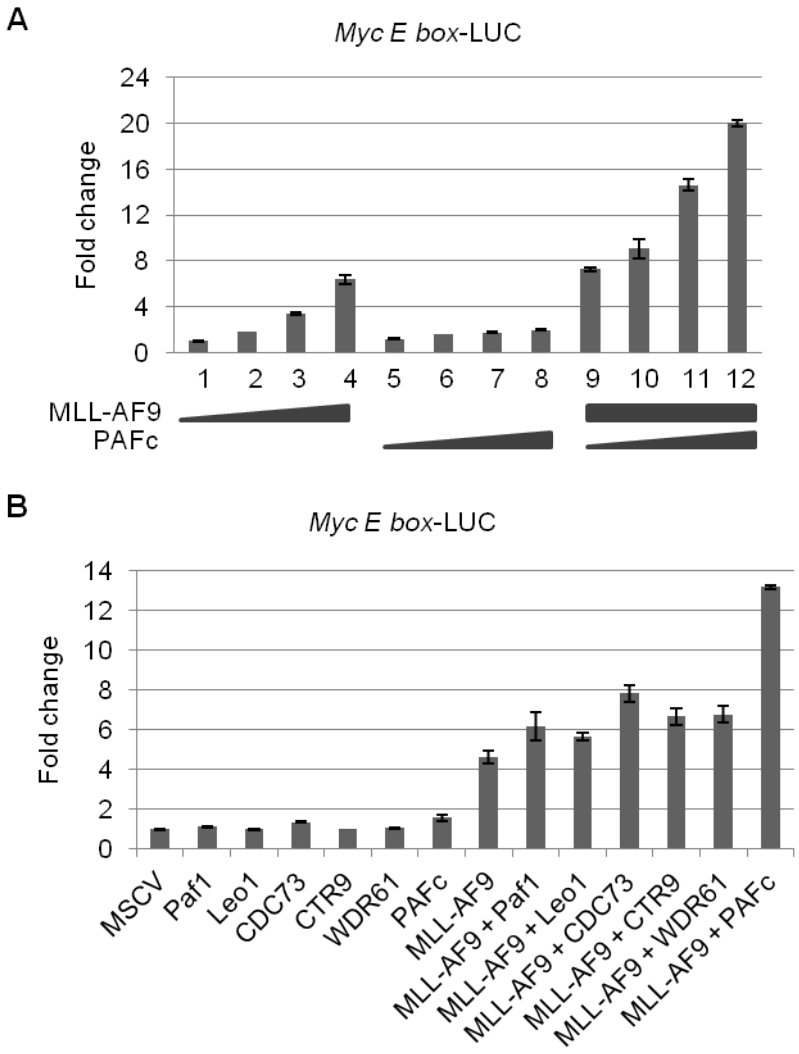

Figure 1.11 PAFc Synergizes with MLL-AF9 to Promote Transcription (A) Luciferase assays were performed in transiently transfected 293 cells with a *Myc-E-box-LUC* reporter construct and increasing doses of MLL-AF9 (lanes 1-4) (0-0.6 μg). Increasing doses of PAFc were transfected in lanes 5-8 (0-0.6 μg). Increasing doses of PAFc (0 – 0.6 μg) were transfected with constant MLL-AF9 (0.6 μg) in lanes 9-12. Error bars indicate the standard deviation of experiment performed in triplicate. One of more than three representative experiments is shown. B) Luciferase assays were performed as described in A except individual PAF components were transfected (lanes 1-6), PAFc (lanes 7), MLL-AF9 (lane 8), MLL-AF9 plus individual PAF components (lanes 9-13) and MLL-AF9 plus PAFc (lane 14). Error bars indicate the standard deviation of experiment performed in triplicate. One of three representative experiments is shown.

MLL Fusion Protein-Mediated Transformation Is Dependent upon Interaction with PAFc

We then tested whether the transforming potential of MLL fusion proteins is dependent on the MLL-PAFc interaction. The deletions in the MLL RD2 region tested in immunoprecipitations described above (Figure 1.8A) or the pre-CxxC region were cloned into full-length MLL-AF9 in MSCV-based retroviral vectors (Figure 1.12B). These were packaged in Plat-E cells and transduced into 5-FU primed bone marrow and analyzed in methylcellulose replating assays as previously described (Morita et al., 2000). Briefly, transduced cells were cultured under G418 selection in the presence of IL3, IL6, GM-CSF and SCF and colonies quantitated after the first, second and third rounds of replating (Figure 1.12A). Western blotting confirmed proteins of the predicted molecular weights were expressed following transient transfection of Plat-E cells (Figure 1.12C). In addition Real Time PCR confirmed expression of fusion gene mRNA in retrovirally transduced bone marrow (Figure 1.12D).

As shown in Figures 1.12E, similar numbers of tertiary colonies were observed when cells were transduced with MLL-AF9, MLL-1357-AF9 or MLL-1299-AF9. Further deletions of RD2 that extended more proximally than amino acid 1299, which markedly reduced PAFc interaction in our immunoprecipitation experiments (Figure 1.8), resulted in marked decreases in colony numbers (Figures 1.12E and 1.13). Importantly, the morphology of these colonies was also dramatically different. Tertiary colonies from MLL-AF9, MLL-1357-AF9 and MLL-1299-AF9 all displayed a dense, compact morphology indicative of

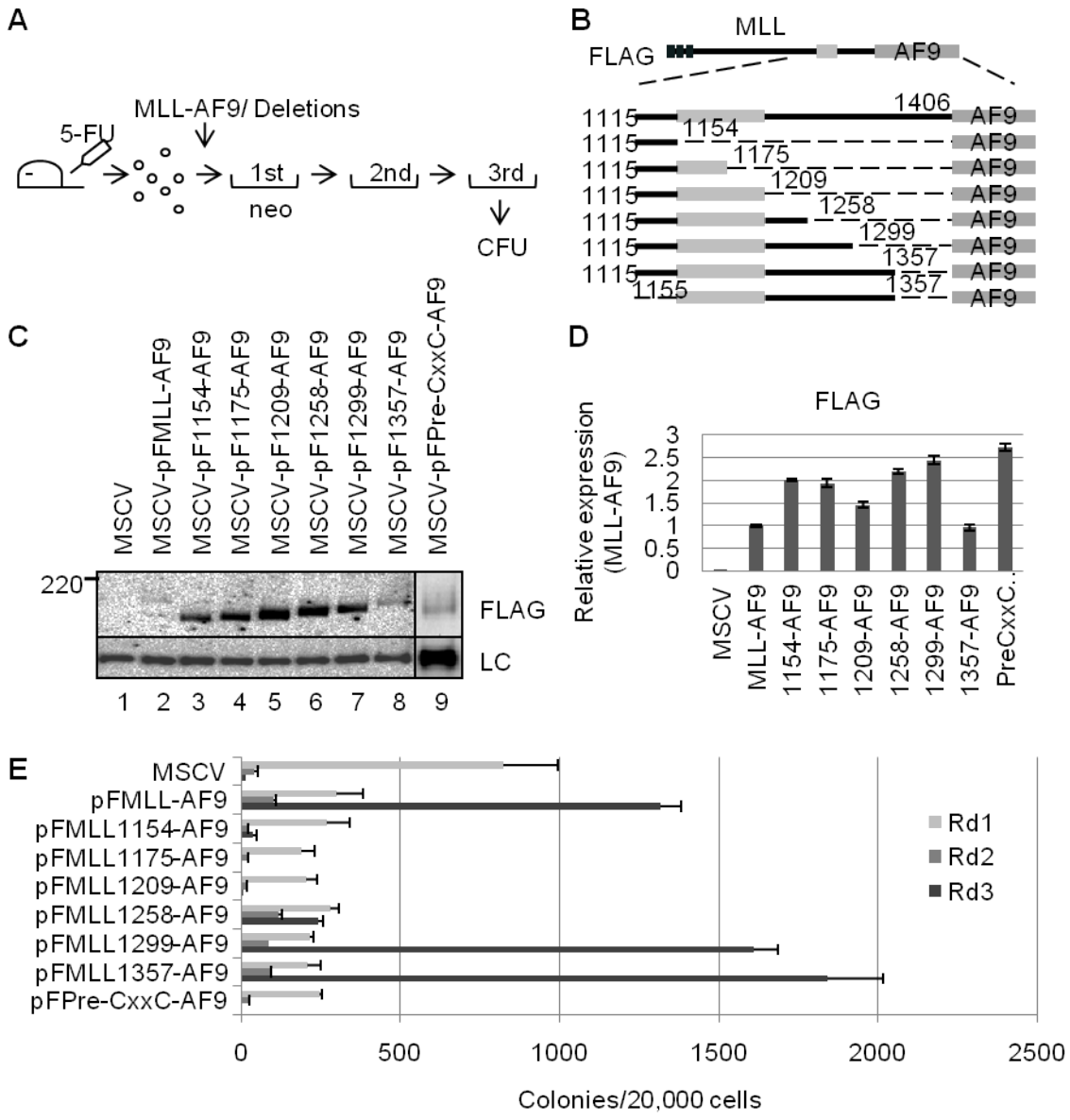

Figure 1.12 PAFc Interaction Region on RD2 Is Necessary for Bone Marrow Transformation (BMT) by MLL-AF9 (A) Schematic diagram for MLL-AF9 and MLL-AF9 deletion BMT assay. (B) Constructs used for the BMT assay. Final amino acids of the MLL deletions are shown. (C) Protein levels of the FLAG-tagged MLL-AF9 deletions shown in B. LC: loading control. (D) Relative mRNA levels of the FLAG-tagged MLL-AF9 deletions shown in B. Error bars indicate +/- SD. (E) Primary, secondary and tertiary colony counts are shown for BMT assays performed with the indicated MLL-AF9 fusion proteins. Error bars indicate SD from duplicate experiments. One of more than three representative experiments is shown.

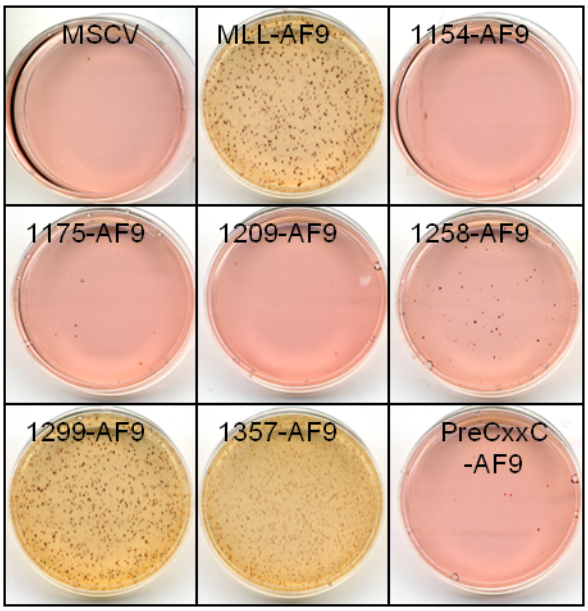

Figure 1.13 p-Iodonitro Tetrazolium Violet (INT)-Stained Colonies after Three Rounds of Colony Replating. Dense red colonies are visible from MLL-AF9, MLL-1299-AF9 and MLL-1357-AF9 transduced bone marrow.

transformation (Lavau et al., 1997) (Figure 1.14A). Wright Giemsa-stained cytospins showed these compact colonies were composed of myeloblasts (Figure 1.14B). In contrast, transductions of constructs with more extensive deletions resulted in diffuse colonies composed of differentiating myeloid cells including monocytes and macrophages (Figures 1.13 and 1.14). Of note, MLL-1258-AF9 retained a limited capacity to produce dense colonies after tertiary replating, but colony numbers were significantly reduced compared to MLL-AF9, MLL-1357-AF9 and MLL-1299-AF9 (Figures 1.13 and 1.14). In keeping with this, minimal binding of PAFc was observed with the Cx-1258-AF9 construct (Figure 1.8).

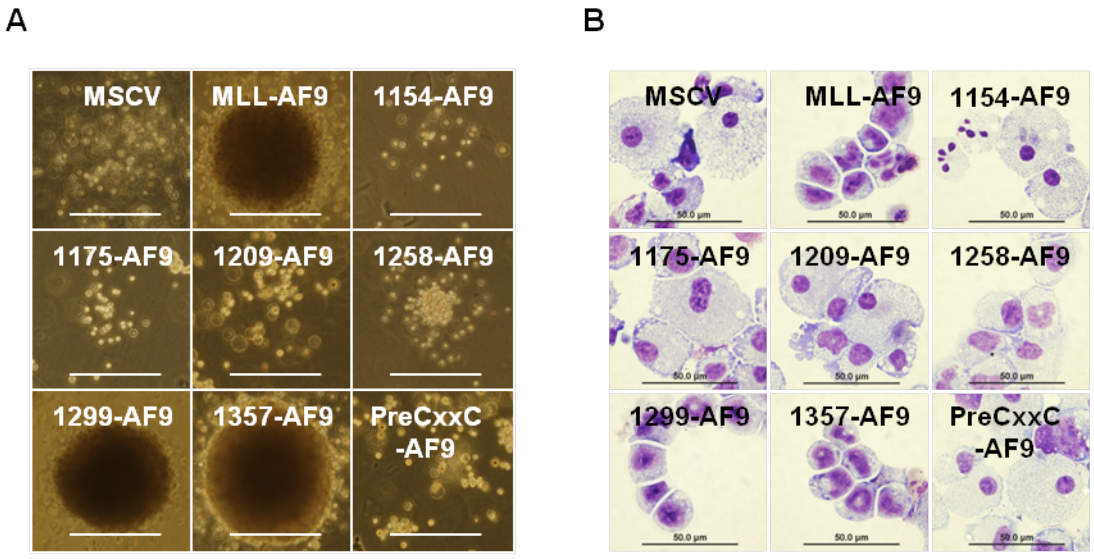

Figure 1.14 Morphology of Primary Bone Marrow Transduced by MLL-AF9 Fusion Proteins (A) Representative colony morphology is shown for each transduced MLL-AF9 fusion protein. Dense colonies are indicative of transformation while diffuse colonies indicate differentiation. Scale bar = 500 μm (B) Wright-Giemsa stained cytospins on cells isolated after the third round of methylcellulose plating. Scale bars indicate 50 μm.

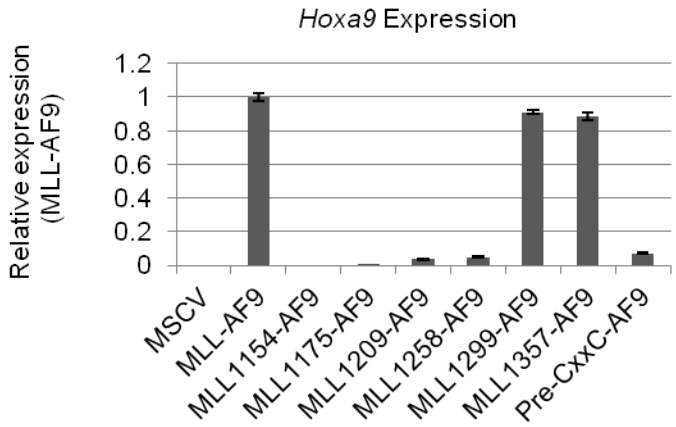

Figure 1.15 *Hoxa9* Expression in Cells Collected after the Third Round of BMT Assays. Error bars indicate SD for experiments performed in triplicate.

We then used compared the *Hoxa9* expression in cells transduced by wild-type MLL-AF9 and different deletion constructs. As expected, MLL-AF9, as well as 1357 and 1299 deletions, markedly upregulated *Hoxa9* expression, while forms incapable of PAFc interaction did not (Figure 1.15).

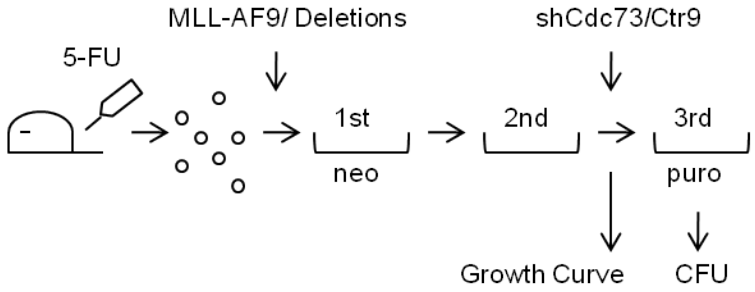

Figure 1.16 Schematic Diagram for MLL-AF9 BMT Assay with shRNA-Mediated Knockdown of Cdc73 and Ctr9. BMT assays were performed as described in Figure 1.12A, except for an additional transduction after the second replating with shScram, shCdc73 or shCtr9 retroviruses followed by plating in methylcellulose with puromycin selection. Colonies were scored after the third plating.

To confirm PAFc is necessary for MLL-AF9 mediated transformation we performed colony assays by transducing primary bone marrow cells with MLL-AF9 followed by a second round of transduction with shRNA retroviruses directed against Cdc73 or Ctr9 (Figure 1.16). Both shCdc73 and shCtr9 were confirmed to knock down Cdc73 and Ctr9, respectively, at both mRNA level and protein level (Figures 1.17A and 1.17B). Knockdown of either Cdc73 or Ctr9 resulted in significantly reduced colony formation compared to a scrambled control shRNA (Figure 1.17C). We also observed a moderate reduce in proliferation rate when

either Cdc73 or Ctr9 was knocked down in primary cells grown in liquid culture in the presence of IL3 and SCF (Figure 1.17D). Together, these data suggest the PAFc interaction with MLL is crucially important for both MLL fusion protein-mediated *Hox* deregulation and transformation.

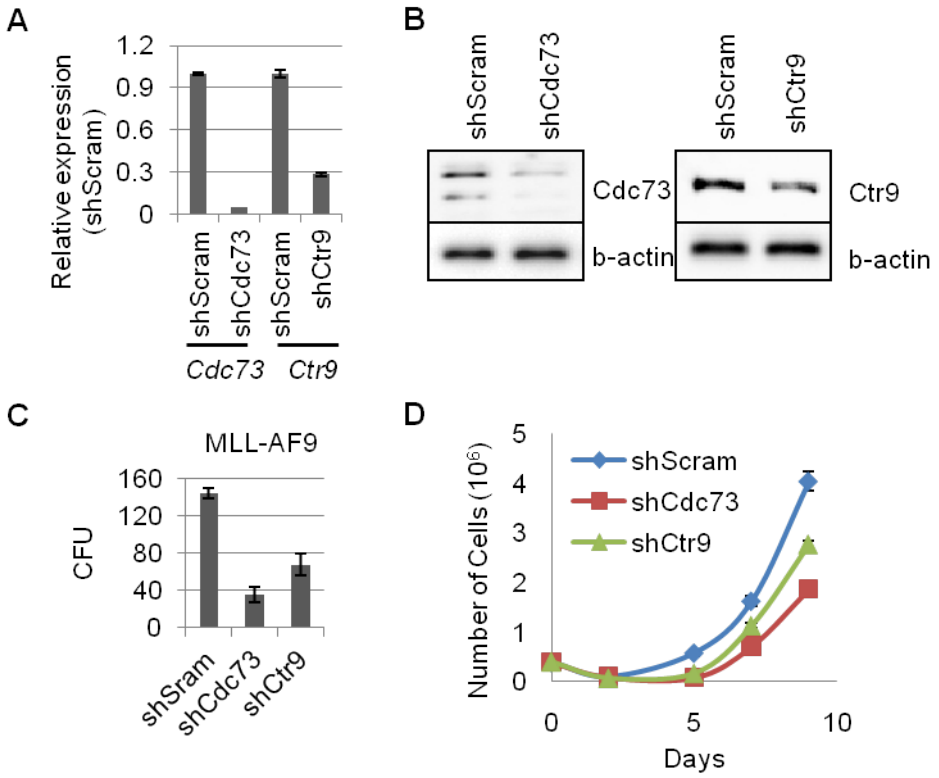

Figure 1.17 Knockdown of Cdc73 or Ctr9 Impairs MLL-AF9-Induced Bone Marrow Transformation (A) RT-qPCR confirming knockdown of *Cdc73* and *Ctr9* mRNA, compared to the control, in 3T3 cells. Error bars indicate +/- SD. (B) Western blot confirming knockdown of Cdc73 and Ctr9 protein, compare to the control, in 3T3 cells. β-actin serves as a loading control. (C) Third round colony counts following transduction with shScram, shCdc73 or shCtr9. Error bars indicate +/- SD. (D) Growth curve analysis of MLL-AF9-transduced primary bone marrow with knockdown by shCdc73 or shCtr9.

PAFc Promotes MLL and MLL Fusion Protein Recruitment to Target Loci

We then examined the localization of PAFc to a leukemogenic target gene of MLL such as *Hoxa9*. For these experiments we generated cell lines by transducing mouse bone marrow with either MLL-ENL or E2A-HLF. MLL-ENL cells express much higher levels of both *Hoxa9* and *Meis1* compared to E2A-HLF cells, which are not dependent on *Hoxa9* expression for transformation (Ayton and Cleary, 2003) (Figure 1.18).

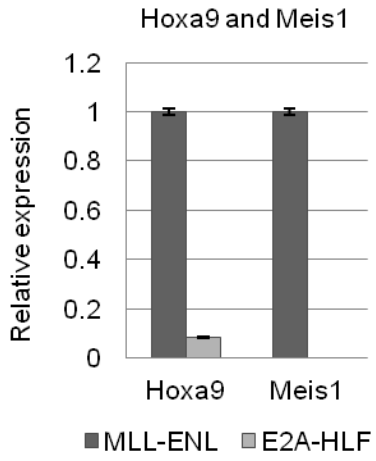

Figure 1.18 RT-PCR for *Hoxa9* and *Meis1* Expression in MLL-ENL and E2A-HLF Cell lines. Error bars indicate +/- SD.

We performed chromatin immunoprecipitation (ChIP) experiments for PAF components, PAF1, LEO1, CDC73 and CTR9 at the *Hoxa9* locus in both cell lines (Figure 1.19). These experiments showed robust binding of MLL-ENL as detected by the ENL antibody in MLL-ENL cells compared to E2A-HLF cells (Figure 1.19). Furthermore, levels of histone H3K79 di- and tri-methylation are

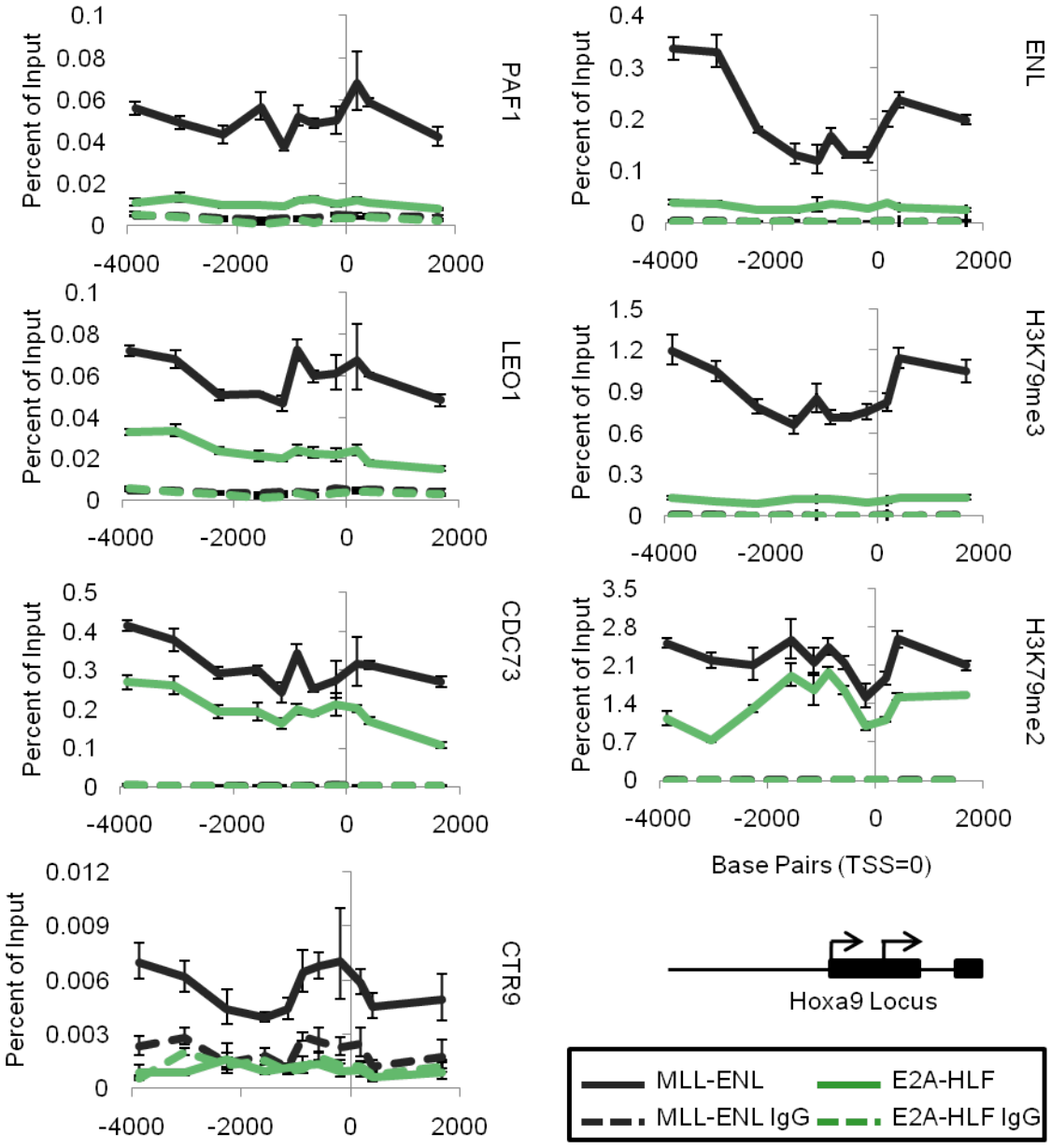

Figure 1.19 PAFc and MLL-ENL Bind across the *Hoxa9* Locus. ChIP experiment performed in mouse bone marrow cell lines established with the MLL-ENL or E2A-HLF fusion protein. MLL-ENL IPs are shown in black and H2A-HLF IPs are shown in green. Solid lines indicate the binding pattern of the component or histone modification listed to the right. The dotted lines indicate control IgG IPs for each cell line. The *Hoxa9* locus is shown schematically at the bottom.

markedly elevated in MLL-ENL cells consistent with ENL mediated recruitment of DOT1L (Mueller et al., 2007). Similarly, we also observed binding of MLL-ENL and PAFc at the *Meis1* locus in MLL-ENL cells, with minimal binding seen in E2A-HLF cells (Figure 1.20). Together, these data suggest that PAFc binds to the target loci of MLL fusion proteins to augment gene transcription.

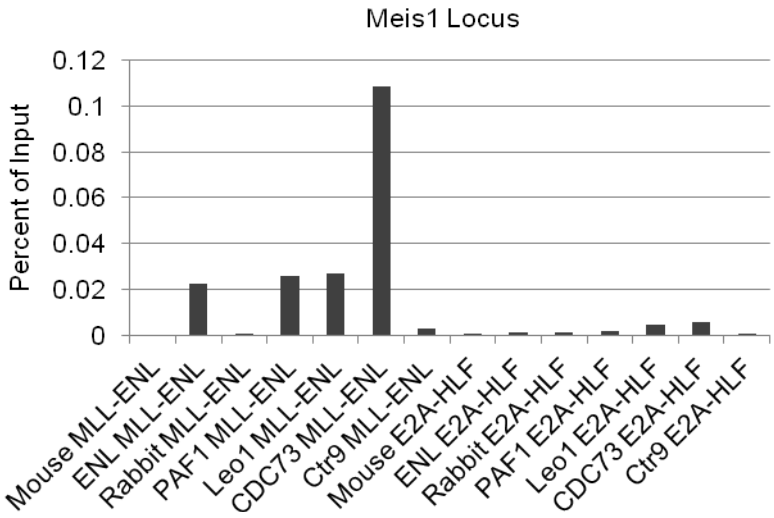

Figure 1.20 PAFc and MLL-ENL Bind at the *Meis1* Locus. ChIP experiment was performed as described in Figure 1.19, except that the binding on the *Meis1* locus, instead of the *Hoxa9* locus, was determined.

To further evaluate the role of PAFc in transcriptional activation we measured the effect of PAFc subunit knockdown on MLL-AF9 mediated transcriptional activation. Knockdown of PAF1, LEO1, CDC73 and CTR9 was successfully achieved in HeLa cells using siRNA transfection (Figure 1.21A). As previously reported, PAFc knockdown decreases *HOXA9* expression in HeLa cells (Figure 1.21B) (Zhu et al., 2005b). Consistently, MLL-AF9 transcriptional activation of

Hoxa9-LUC is also impaired by PAF1, LEO1, CDC73 or CTR9 knockdown (Figure 1.21). Furthermore, we saw an additive effect by knocking down both CTR9 and LEO1 suggesting MLL fusion proteins require PAFc for efficient transcriptional activation (Figure 1.21B).

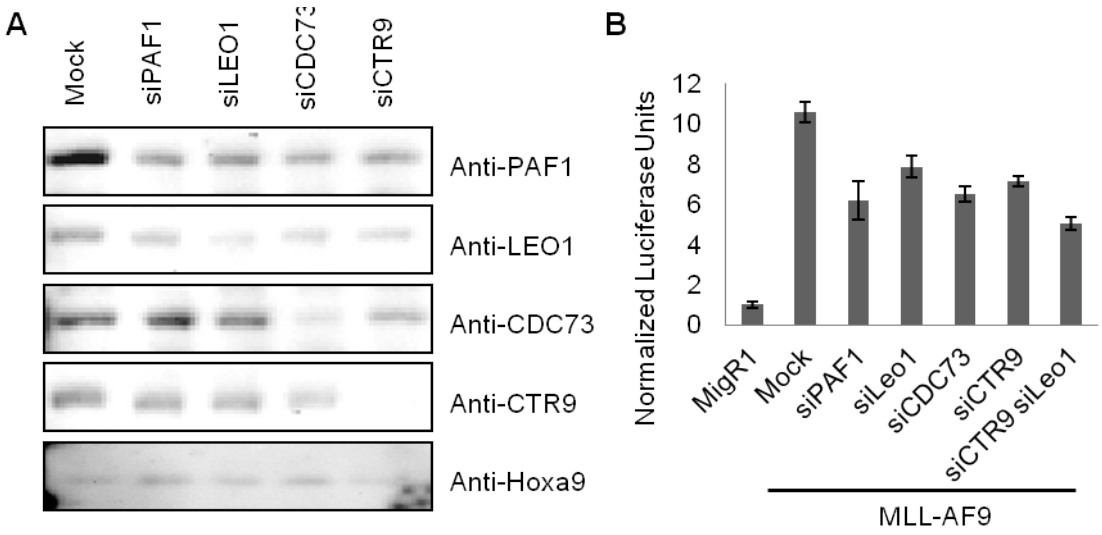

Figure 1.21 Knockdown of PAFc Reduces MLL-AF9-Induced Transactivation (A) siRNA-mediated knockdown of individual PAF components was verified by western blotting. (B) Luciferase assays were performed with the *Hoxa9-LUC* reporter construct and MLL-AF9 in HeLa cells after transfection with the indicated siRNA. Luciferase units are shown relative to the MigR1 control transfected cells.

We then determined the effect of knock down of the PAF complex on MLL recruitment to the *HOXA9* locus by performing ChIP assays on HeLa cells after simultaneous knock down of CTR9, PAF1, CDC73 and LEO1 (Figure 1.22). We observed a significant decrease in binding of CDC73, PAF1 and LEO1 in both the promoter and coding region of the *HOXA9* locus following knockdown, as expected, while histone H3 levels remain unchanged or elevated in siPAFc-treated cells (Figure 1.23). PAFc knock down resulted in a marked decrease in wild-type MLL binding compared to mock treated cells (Figure 1.23), without affecting MLL protein levels (Figure 1.22), suggesting PAFc enhances MLL recruitment to *HOXA9*. Consistent with reduced binding of MLL, knock down of the PAF complex also resulted in a decrease in H3K4 tri-methylation at the *HOXA9* locus (Figure 1.23). We also observed a decrease in histone H3K79 tri-methylation (Figure 1.23).

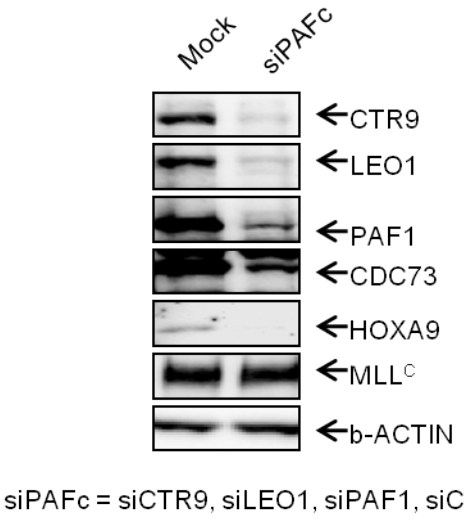

Figure 1.22 Simultaneous siRNA-Mediated Knockdown of PAFc (siCTR9, siLEO1, siPAF1 and siCDC73). β-ACTIN serves as the loading control.

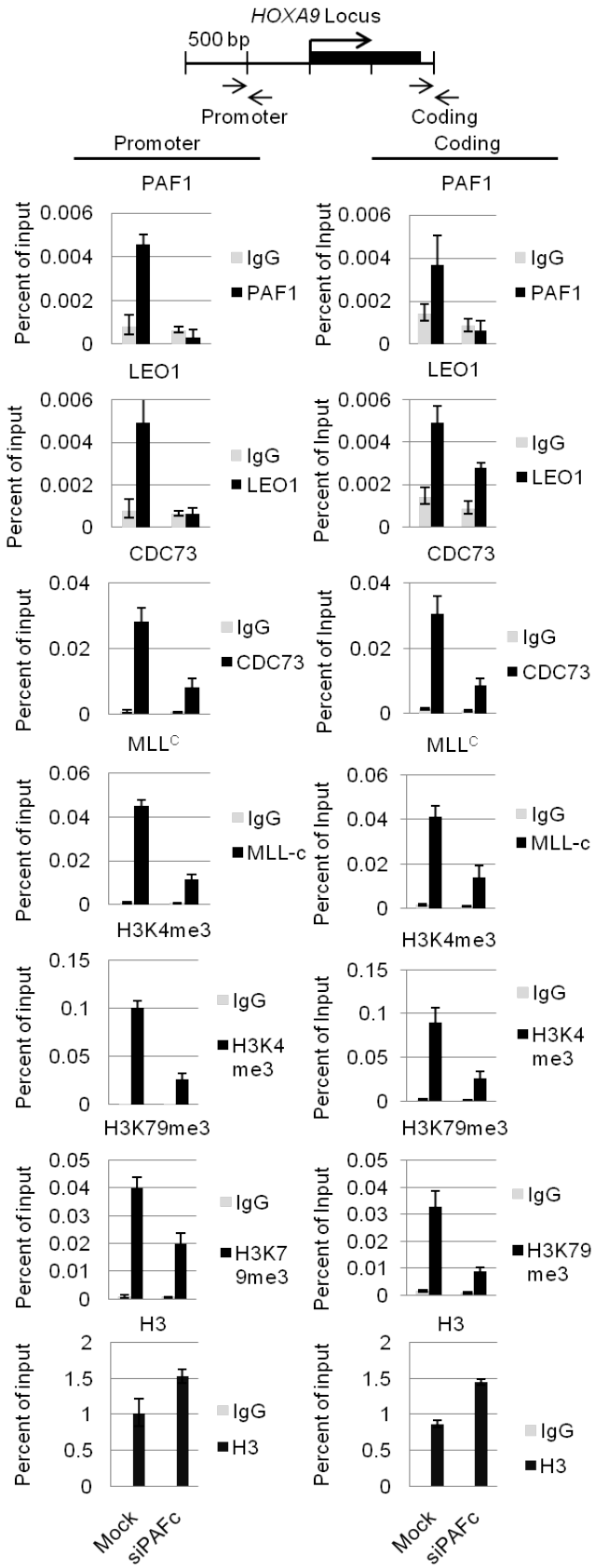

Figure 1.23 Knockdown of PAFc Reduces MLL Binding to the *HOXA9* Locus. ChIP experiments were performed in HeLa cells following simultaneous knockdown of PAFc shown in Figure 2.22. PAF1, LEO1, CDC73, MLL^C, H3K4me3, H3K79me3 and H3 were immunoprecipitated from HeLa cells treated with siPAFc or non-targeting siRNA (Mock). Binding was assessed in both the promoter and coding region as indicated. A schematic of the *HOXA9* locus and location of the primer-probe sets used for qPCR are shown. Error bars indicate +/- SD. One of more than three representative experiments is shown.

PAFc expression is coordinately downregulated during myeloid differentiation

The above results suggest that the PAF complex enhances MLL recruitment to the *HOXA9* locus and that modulating PAFc levels may be an important mechanism for modulating MLL activity. It is noteworthy in this regard that a recent unbiased genome-wide siRNA screen identified PAFc subunits Ctr9, Wdr61 and Rtf1 amongst the 30 top genes regulating Oct4 expression and stem cell renewal (Ding et al., 2009). In this study PAFc was found to bind to key pluripotency genes, which is remarkable because MLL fusion protein transformed cells show, in addition to *HOX* gene over expression, a distinctive embryonic stem cell (ESC)-like pluripotency signature (Somervaille et al., 2009). Furthermore, expression of PAFc subunits is strongly regulated upon differentiation of ESCs into embryoid bodies (Ding et al., 2009). Collectively, these findings suggested that PAFc might be positively involved in maintaining the relatively undifferentiated stage of hematopoietic progenitors.

We established two differentiation models to explore the potential role of PAFc in regulation during hematopoietic differentiation. First, we created a conditional AML cell line by immortalizing murine bone marrow by transduction with Hoxa9-ER in the presence of tamoxifen (4-OHT). Upon 4-OHT withdrawal, these cells undergo differentiation and cell cycle arrest, which is largely complete by 120 hours (Figure 1.24). Microarray expression profiling was performed in triplicate at 24, 48, 72, 96 and 120 hours following 4-OHT withdrawal (only results for 72, 96 and 120 hours are shown in Figure 1.25A. These experiments showed a marked

down regulation of all PAFc subunits and MLL target genes after induction of differentiation accompanied by up regulation of genes associated with myeloid differentiation (Figure 1.25A). The down regulation of PAFc expression was confirmed by qPCR in independently differentiated Hoxa9-ER cells (Figure 1.25B).

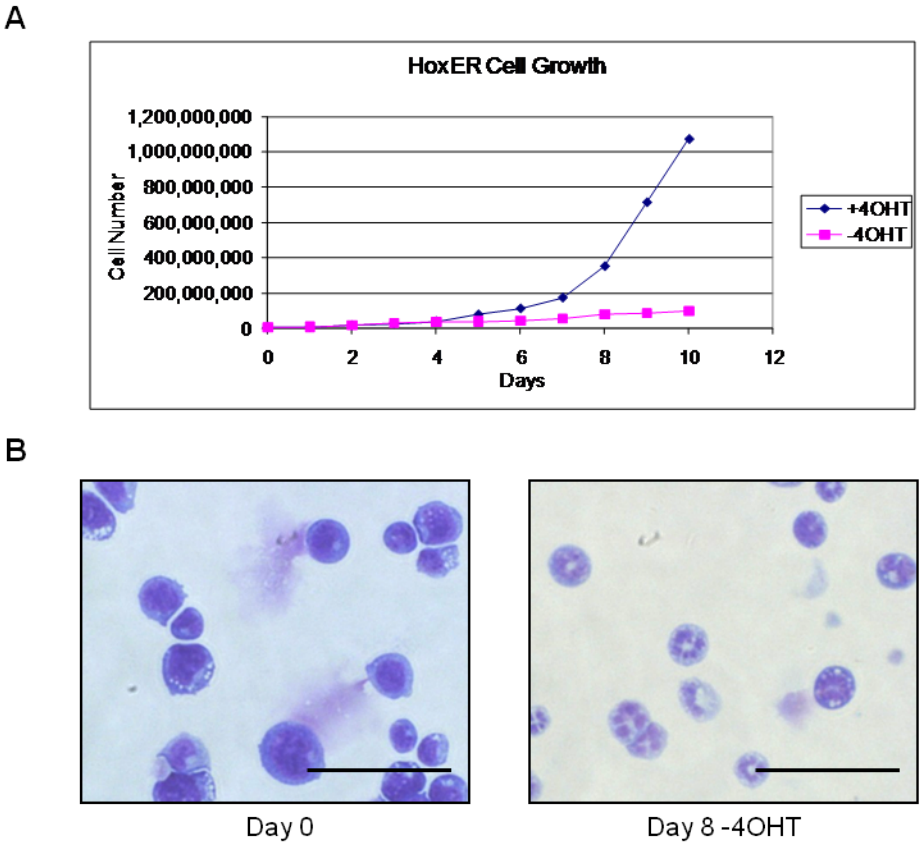

Figure 1.24 Differentiation of Hoxa9ER Cell Line Induced by 4-OHT Withdrawal (A) Growth curves for the Hoxa9ER cell line was determined in the presence and absence of tamoxifen (4OHT). B) Wright-Giemsa stained cytospins demonstrate the morphology of the Hoxa9ER cells in the presence of tamoxifen and 8 days post tamoxifen withdrawal. Scale bars = 50 μm.

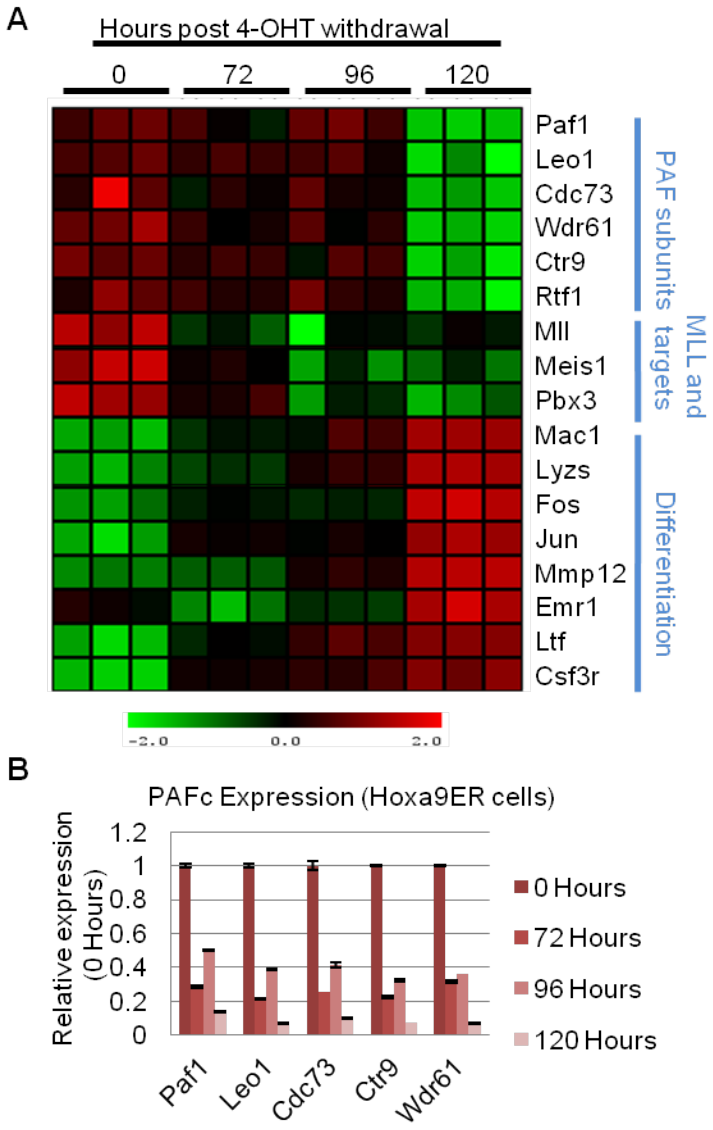

Figure 1.25 PAFc Is Downregulated during Differentiation of Hoxa9ER Cells Induced by 4-OHT Withdrawal (A) Heat map generated from expression array data collected from differentiation of the Hoxa9ER cell line. Data is shown in triplicate for each time point following tamoxifen withdrawal. Labels indicate components of the PAF complex, MLL and MLL targets, and genes associated with myeloid cell differentiation. B) Expression of PAF components were verified using qPCR by separately differentiating the Hoxa9ER cell line by tamoxifen withdrawal. Time points indicate hours post tamoxifen withdrawal that RNA was collected. Expression for each component is shown relative to 0 hours. Error bars indicate +/- SD.

We also analyzed the human HL-60 cell line, which rapidly differentiate into macrophages after exposure to phorbol 12-myristate 13-acetate (PMA) (Figure 1.26A). PMA treatment also led to a dramatic down regulation of PAFc in HL-60 cells (Figure 1.26B).

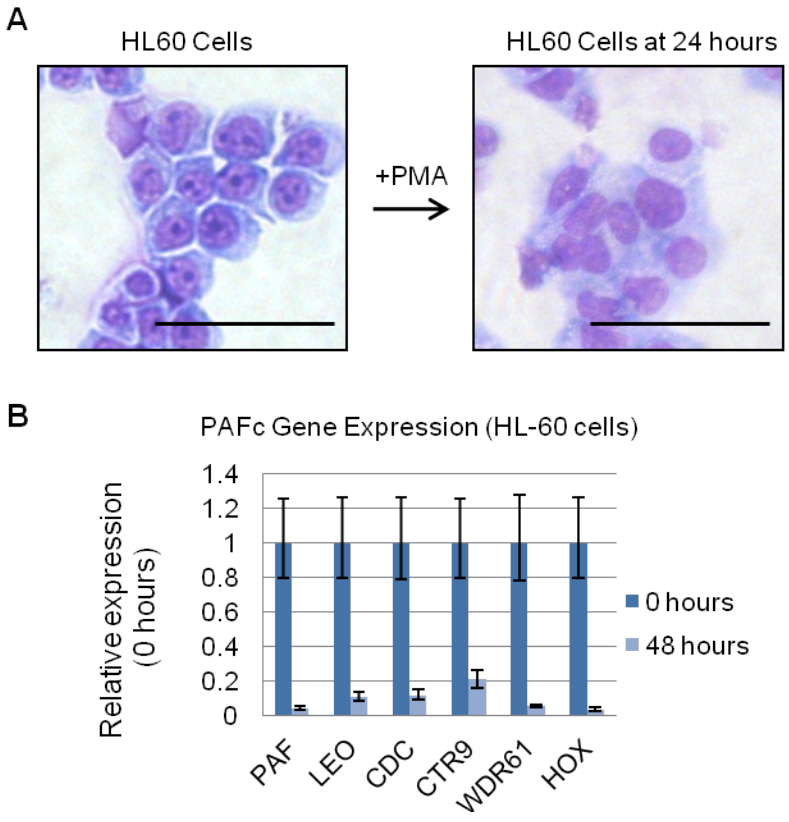

Figure 1.26 PAFc Is Downregulated during Differentiation of HL-60 Cells Induced by PMA Treatment (A) Differentiation of the HL-60 cell line induced by PMA treatment was confirmed by Wright-Giemsa staining of cytospin preparations. Scale bars = 50 μm. (B) PAFc expression levels were determined by RT-PCR before and after PMA treatment for 48 hours. Error bars indicate SD of experiment performed in triplicate.

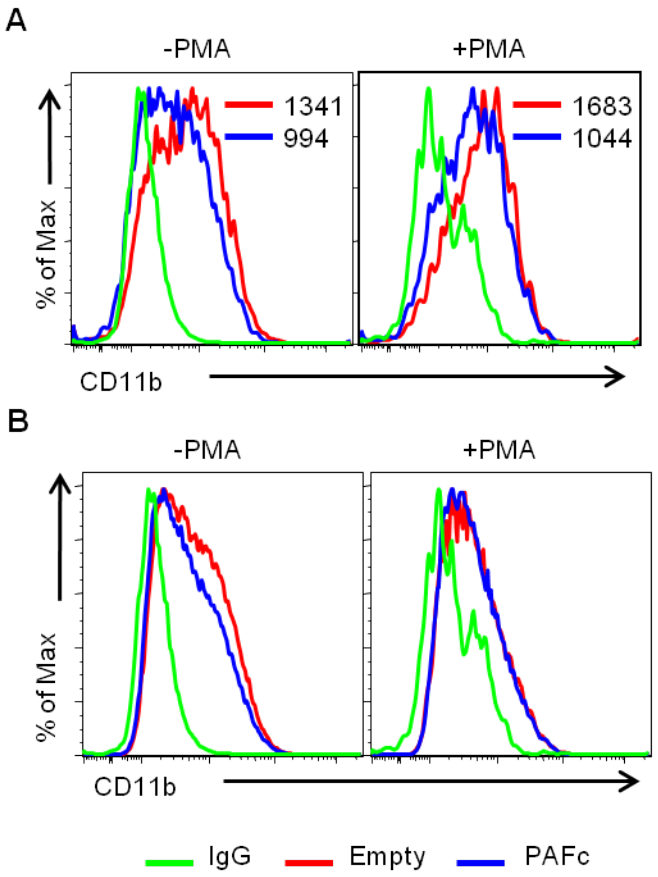

Figure 1.27 PAFc Overexpression in THP-1 Cells Leads to Resistance to Differentiation Induction by PMA Treatment (A) THP-1 cells were transfected with an equal mixture of PAFc expression vectors or empty vectors along with a GFP vector at a 5:1 ratio (PAFc/Empty:GFP). Half were treated with PMA to induce differentiation. Surface expression of CD11b was monitored by FACS in the GFP positive gated cell population to track differentiation. Mean fluorescence values are shown for each sample. (B) THP-1 cells were transfected with empty vectors or PAFc together with a GFP expression vector. In contrast to the GFP positive population, CD11b expression was monitored on the GFP negative population which showed little to no change in expression with or without PMA treatment.

To test the role of PAFc in hematopoietic differentiation, we enforced expression of PAFc in THP-1 cells with or without PMA induced differentiation. THP-1 cells

were more resistant to differentiation, as determined by CD11b surface expression, when PAFc was over expressed (Figure 1.27A). Importantly, GFP negative cells showed no significant difference in CD11b expression (Figure 1.27B). Together, these data show PAFc expression is specifically down regulated during myeloid differentiation and that high level PAFc expression inhibits differentiation. Thus, PAFc may play an important role in regulating MLL binding to target genes during differentiation.

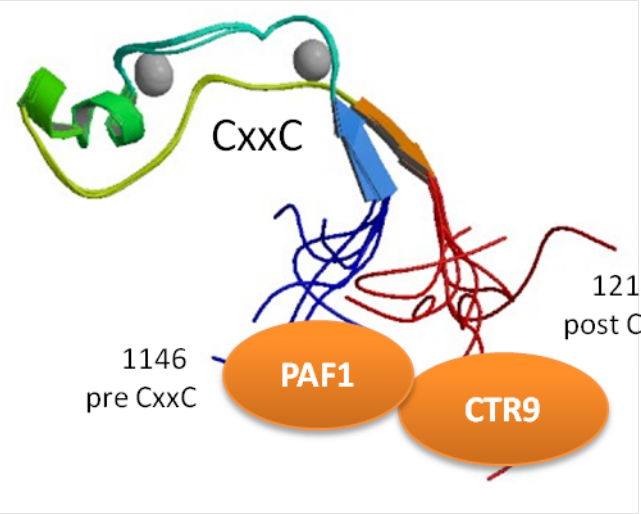

Figure 1.28 Structure of the CxxC Domain and Flanking Sequences (PDB code: 2JYI)**.** Solution structure of MLL CxxC region shows the flanking sequences of the CxxC domain brought into close juxtaposition creating a binding surface for both PAF1 and CTR9 of the PAF complex.

Discussion

The work presented here establishes PAFc as an important cofactor for both transcriptional regulation by MLL and for leukemogenesis mediated by MLL fusion proteins (Figure 1.29). By mass spectrum analysis, we demonstrated that PAFc interacts with the CxxC-RD2 region of MLL, a region that is always retained in MLL-rearranged oncoproteins. Detailed mapping revealed two interaction sites flanking the CxxC domain with two individual components of PAFc (Figure 1.28). Most importantly, we were able to show that the PAFc-MLL interaction enhances the transcriptional activation by MLL-AF9 and plays an indispensible role in MLL-AF9-induced leukemogenic transformation. Characterization of the PAFc-MLL interaction provides valuable insight into the mechanisms of *MLL*-rearranged leukemogenesis. The best-defined target genes of MLL are the clustered homeobox (*Hox*) genes, a transcription factor family important in cell fate determination during development. Among these targets, Hoxa9 and its cofactor Meis1 have been shown to be crucial for MLL-rearranged leukemogenesis. Normally, *Hoxa9* and *Meis1* are only briefly expressed in hematopoietic stem cell and progenitor cell populations and are then rapidly down regulated during hematopoietic differentiation (Lawrence et al., 1996; Magli et al., 1997; Zeisig et al., 2004). However, in the presence of MLL-rearranged oncoproteins, both remain expressed at high levels, which accounts for their leukemogenic capacity. Although many interaction partners of MLL-rearranged proteins have been identified and shown to be important in leukemogenesis, it

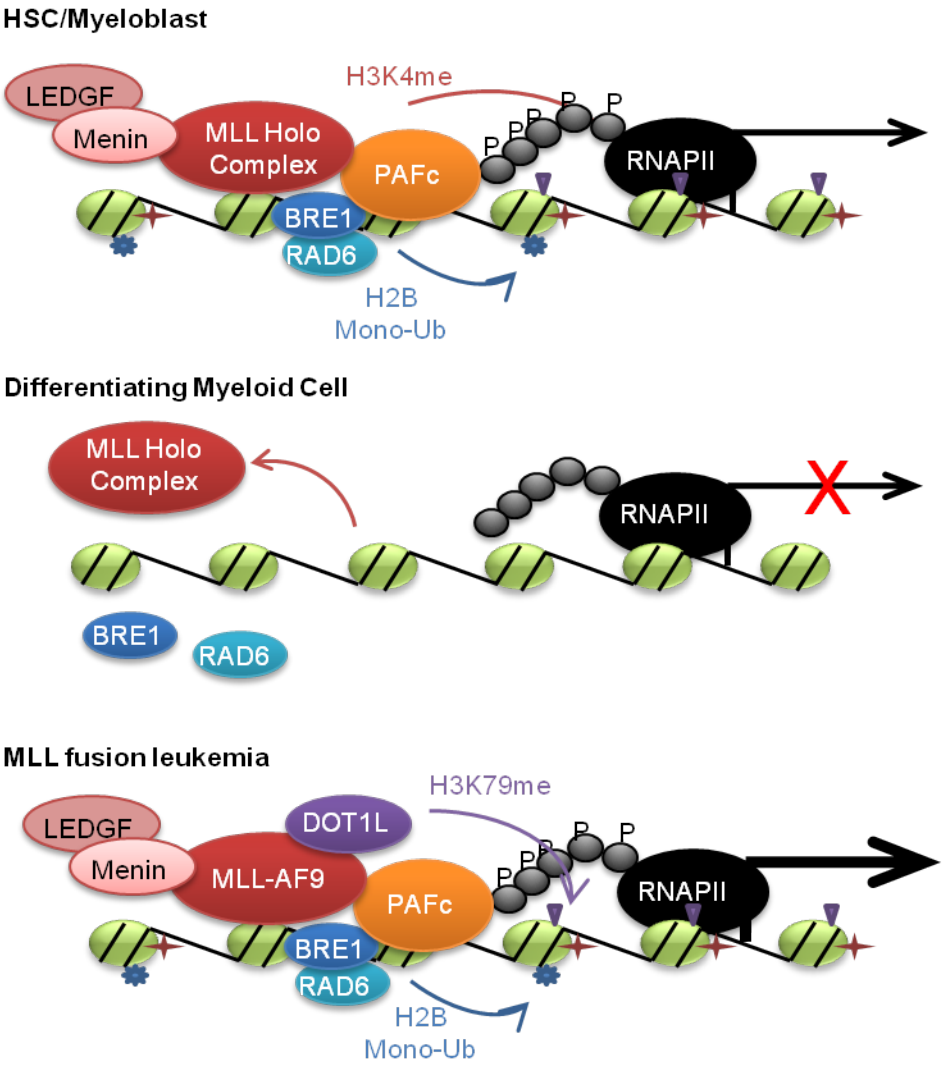

Figure 1.29 Functional Implication of the MLL-PAFc Interaction. (Top) PAFc-dependent recruitment of MLL to target genes in hematopoietic progenitors (HSC/myeloblasts). PAFc and MLL recruitment promotes H2B mono-ubiquitination and H3K4 and H3K79 methylation resulting in transcriptional activation. (Middle) More differentiated myeloid cells down regulate PAFc expression resulting in decreased recruitment and transactivation by MLL. (Bottom) In leukemic cells harboring MLL fusion proteins the fusion protein synergizes with PAFc resulting in robust transcriptional activation of target genes. This is associated with increased H2B mono-ubiquitination and histone H3K79 methylation by DOT1L recruited through the MLL fusion partner.

remains unclear what are the exact molecular mechanisms responsible for the dysregulation of the expression of these target genes.

Aside from our identification of the PAFc-MLL interaction, several lines of evidence also indicate the direct role of PAFc in *Hox* gene dysregulation in MLL-rearranged leukemias. First, increasing evidence suggests that a significant mechanism for *Hox* gene expression is mediated through regulating transcriptional elongation (Chopra et al., 2009), a process in which PAFc has been known to play a key regulatory role (Jaehning, 2010b). Second, we observed a significant dose-dependent transcriptional activation of the *Hoxa9* promoter induced by MLL-AF9 overexpression, whereas wild-type MLL overexpression only delivered a somewhat more muted response, suggesting the differential roles of PAFc in cellular activities of MLL-rearranged oncoproteins vs. wild-type MLL. Third, a previous study by Chen et al. has demonstrated that the susceptibility of hematopoietic progenitors to MLL-AF9-induced transformation decreases along differentiation (Chen et al., 2008), consistent with the decreasing PAFc expression along hematopoietic differentiation shown by our work and others (Ding et al., 2009). Based on these findings, a potential mechanism for MLL-rearranged leukemogenesis is that by interacting with PAFc, MLL-rearranged oncoproteins are able to stably engage the basic transcription elongation machinery at target loci, such as *Hoxa9* and *Meis1*, to constitutively activate transcription, leading to leukemogenesis. Therefore, PAFc may be a crucial component mediating the dysregulation of normal transcription elongation of MLL target genes by MLL-rearranged oncoproteins (Figure 1.30).

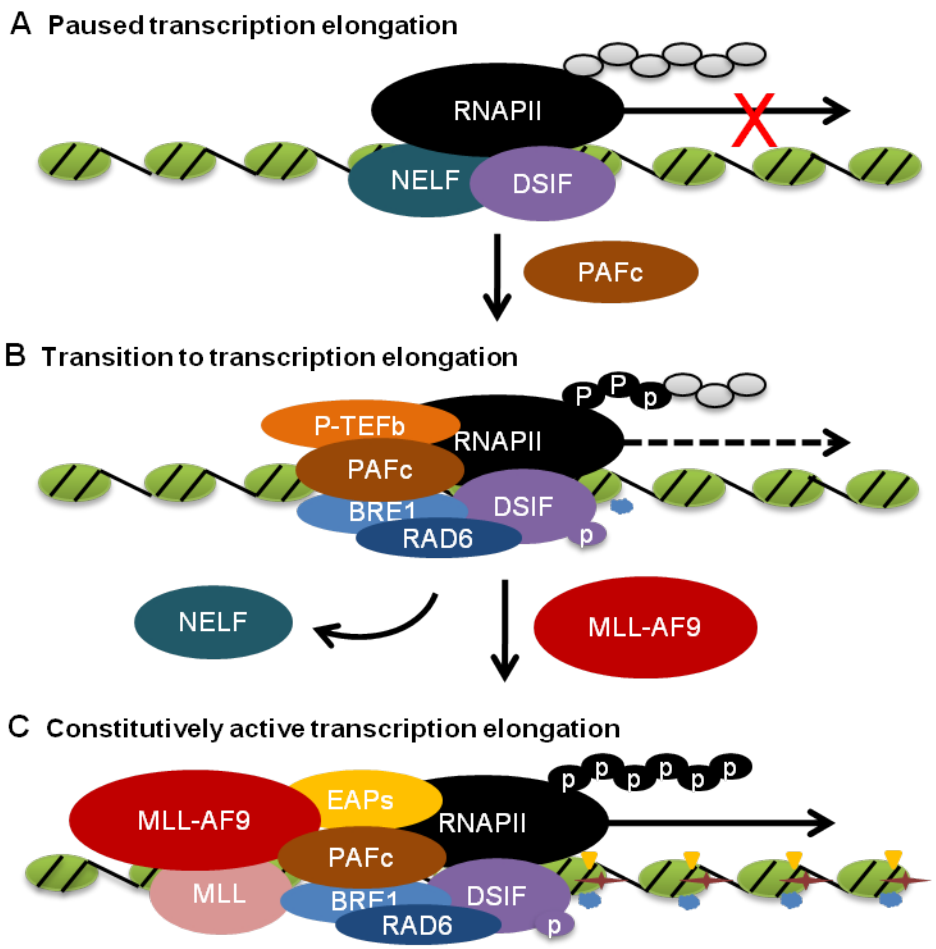

Figure 1.30 Schematic of a Potential Mechanism of MLL-Rearranged Leukemogenesis (top) In the absence of PAFc, RNA polymerase II (RNAP II) elongation is inhibited by the negative elongation factor (NELF) in collaboration with the DRB sensitivity-inducing factor DSIF. (middle) DSIF recruits PAFc that directly interacts with the E1/E2 ubiquitin ligase complex BRE1/RAD6, resulting in histone H2B monoubiquitination. Recruitment of positive transcription elongation factor b (P-TEFb) blocks the negative actions of NELF and DSIF by P-TEFb-dependent phosphorylation of RNAP II CTD and DSIF, priming the target promoter for transcription elongation (bottom) The interaction between PAFc and the most common MLL-rearranged oncoproteins (represented by MLL-AF9) recruits the ENL-associated proteins (EAPs) that include multiple common MLL translocation partners, DOT1L and P-TEFb to the target loci, promoting H2B monoubiquitination ( ), H3K4 methylation ( ) and H3K79 methylation ( ), resulting in constitutively activated transcription.

Under normal conditions, *Hoxa9* is expressed in primitive hematopoietic cells, playing a significant role in early hematopoiesis (Lawrence et al., 2005; Pineault et al., 2002). During hematopoietic differentiation, *Hoxa9* expression is rapidly silenced, likely by pausing transcription elongation, an important mechanism regulating *hox* gene expression in *Drosophila* (Brookes and Pombo, 2009; Chopra et al., 2009). In this case, although RNA polymerase II (RNAP II) still localizes at the promoter region, its C-terminal domain (CTD) is unphosphorylated, and transcription elongation is inhibited by the negative elongation factor (NELF) in collaboration with the DRB sensitivity-inducing factor (DSIF) (Figure 1.30A). DSIF recruits PAFc that directly interacts with the E1/E2 ubiquitin ligase complex BRE1/RAD6, resulting in histone H2B monoubiquitination. Meanwhile, the recruitment of the positive transcription elongation factor b (P-TEFb) reverts the negative actions of NELF and DSIF by P-TEFb-dependent phosphorylation of RNAP II CTD and DSIF (Jaehning, 2010b). Thus, in the presence of PAFc, the target gene promoter region can progress to the active elongation stage (Figure 1.30B). It is worth noting that this status is probably a temporary transition stage, dynamically regulated by cell-specific mechanisms, such as the abundance of PAFc, the binding affinity of other transcription elongation machinery components determined by the phosphorylation level of RNAP II CTD, the recruitment of histone methyltransferases, such as wild-type MLL and DOT1L, exerting H3K4 and H3K79 methylation, respectively, and the regulation of their enzymatic activities. For instance, in hematopoietic stem cells and early-stage progenitor cells, PAFc

is expressed at a high level; therefore, this temporary transition status is more likely to progress into a fully active elongation stage, which in turn leads to the *Hox* gene expression. In contrast, in the differentiated cells, PAFc downregulation may revert this transition status back to the inactive transcription stage, silencing the *Hox* gene expression. The dynamics of the multiple regulatory mechanisms is likely to be disrupted by MLL-rearranged oncoproteins, such as MLL-AF9.

As previously mentioned, the most common MLL-rearranged oncoproteins, including MLL-AF9, MLL-ENL and MLL-AF4, are known to interact with the EAP complex or a closely related complex called AEP (Lin et al., 2010; Muntean et al., 2010; Yokoyama et al., 2010). By interacting with PAFc, these MLL-rearranged oncoproteins recruits EAP that includes DOT1L, P-TEFb and multiple common MLL translocation partners to the target loci, promoting H3K79 methylation, resulting in dysregulated constitutively active gene expression (Figure 1.30C). In addition, wild-type MLL has recently been shown to synergize with MLL-AF9, which further increases the H3K4 methylation level and presumably contributes to target gene transcriptional activation (Thiel et al., 2010). Notably, in the study by Chen et al., the authors showed that LSK ($Lin^-Sca1^+C\text{-}kit^+$) stem cells, but not the more differentiated committed granulocyte-monocyte progenitors (GMPs), can be transformed by MLL-AF9 under endogenous regulatory control, suggesting that under physiological conditions, additional linage-specific transcription factor(s) or coactivator(s), other than the MLL-rearranged oncoproteins, are critical for leukemogenesis (Chen et al., 2008). Given the

downregulation of PAFc during hematopoietic differentiation, it is possible that PAFc might partially accounts for the susceptibility of different progenitor populations to MLL fusion protein induced leukemogenesis.

A number of questions remain regarding the mechanism of the PAFc-MLL interaction in MLL-rearranged leukemogenesis. First, apart from the most common *MLL* translocations resulting in MLL fusion proteins with a nuclear translocation partner, MLL fusion proteins with cytoplasmic partners and MLL-PTD have not been extensively studied. Therefore, the leukemogenic mechanisms of MLL-PTD and MLL-rearranged oncoproteins with a cytoplasmic partner, both of which in effect involve duplication of the N-terminus of MLL (up to the breakpoint region) by either intramolecular partial tandem duplication or intermolecular dimerization, are unknown (Dou and Hess, 2008). Given the pivotal role of PAFc in MLL-rearranged leukemogenesis, it will be important to determine if either of these two types of MLL-rearranged oncoproteins involves enhanced physical or functional interaction with PAFc. Second, although our ChIP results suggest that both PAFc and MLL fusion protein bind to the target gene loci, such as *Hoxa9* and *Meis1*, the specificity of this associated binding pattern warrants further investigation. For instance, whole genome ChIP-seq analysis of the binding sites of PAFc and MLL fusion proteins in MLL-rearranged leukemic cells will be important to determine how significant the overlapped binding might be, therefore better addressing whether the MLL-PAFc association only affects selected loci or plays a general role in the majority, if not all, of the downstream targets of MLL fusion proteins. Third, it is yet to be determined how,

and to what extent, PAFc plays differential roles in the cellular activities of MLL-rearranged oncoproteins vs. wild-type MLL. It will be important to determine if such a therapeutic window exists for targeting PAFc, for example, through targeting the MLL-PAFc interaction with small molecule inhibitors, which could be used as a new therapy for MLL-rearranged leukemias. Last but not least, the data presented here primarily focused on the role of PAFc in one specific type of leukemia, MLL-rearranged leukemia. Since PAFc belongs to the basal transcriptional machinery that plays a general role in transcriptional regulation, it will be of therapeutic value to further explore whether PAFc is involved in the function of MLL-unrelated leukemogenic fusion proteins, therefore shedding light on the specificity of the role of PAFc in leukemogenesis.

* The work presented in Chapter 1 was conducted in collaboration with Dr. Andrew Muntean. Both parties contributed to generating these experimental data.

Chapter 2

The Role of CBX8, a Polycomb Group Protein, in MLL Fusion Protein-Induced Leukemogenesis

Introduction

PcG Complexes

PcG proteins were originally identified in *Drosophila* more than 30 years ago as regulators of anterior-posterior body patterning through the repression of homeobox (Hox) genes (Sauvageau and Sauvageau, 2010). They have since been recognized as evolutionarily conserved global epigenetic modifiers that antagonize the function of TrxG proteins. Generally, PcG proteins establish histone modifications that repress transcription, whereas TrxG proteins establish histone modifications that activate transcription (Mills, 2010). A number of studies have established the key regulatory roles of PcG proteins in multiple physiological processes, such as embryonic development, adult somatic cell differentiation, stem cell pluripotency and X chromosome inactivation (Bracken and Helin, 2009; Cao et al., 2011; Kanhere et al., 2010; Margueron and Reinberg, 2011; Mills, 2010; Sauvageau and Sauvageau, 2010; Sparmann and van Lohuizen, 2006; Surface et al., 2010).

The PcG family comprises a number of chromatin-associated complexes that are assembled from a structurally diverse set of proteins. The composition of these

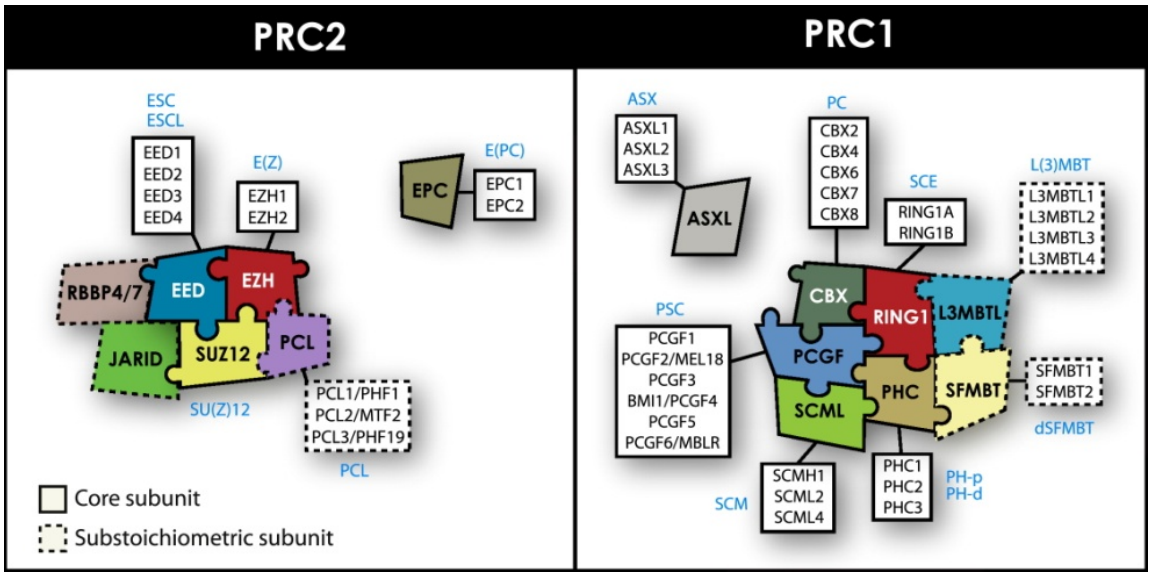

Figure 2.1 Diversity of PRC1 and PRC2 Complexes Formed by Vertebrate PcG Proteins. Subunits of the PRC1 (right panel) and PRC2 (left panel) complexes are indicated. The *Drosophila* homolog of each subunit is indicated in light blue. Multiple combinations of paralog subunits can generate a diversity of PRC1 and PRC2 complexes, which likely have specific and shared functions. Some subunits seem to be present in substoichiometric amounts and interact with the PcG complexes in a cell-context-dependent manner. The core subunits and the substoichiometric subunits are identified. The contacts illustrated in the diagrams are not intended to represent the actual interactions. Involvement of EPC and ASXL subunits with PRC2 or PRC1 complexes is still unclear and requires further investigations. Adapted from (Sauvageau and Sauvageau, 2010).

complexes, termed Polycomb Repressive Complexes (PRCs), is variable and context-dependent, which has been characterized in depth (Sauvageau and Sauvageau, 2010). In mammals, PRCs are mainly classified into two groups. One group is composed of the histone methyltransferase Enhancer of Zeste Homolog (EZH) 1 or EZH2 and its binding partners, Embryonic Ectoderm Development (EED) and Suppressor of Zeste 12 (SUZ12), which form the core of

the PRC2 complex (Figure 2.1, left panel) (Cao et al., 2002; Czermin et al., 2002; Kirmizis et al., 2004). Although not required for complex formation and stability, other proteins, such as PCL proteins, RBBP4/7 and JARID, have been identified as PRC2-associated cofactors that facilitate PRC2 functions (Landeira et al., 2010; Nekrasov et al., 2007; Pasini et al., 2008; Peng et al., 2009). The core of the more heterogeneous PRC1 complex consists of one subunit of the PCGF, RING, CBX, PHC, and SCML paralog groups (Figure 2.1, right panel) (Levine et al., 2002; Valk-Lingbeek et al., 2004). Several less well-characterized components have also been reported to interact with the PRC1 core complex, including L3MBTL, SFMBT, and ASXL1 (Grimm et al., 2009; Ohtsubo et al., 2008; Peterson et al., 2004; Sanchez et al., 2007; Scheuermann et al., 2010).

PRC-Mediated Transcriptional Silencing

A wealth of genetic and biochemical studies have indicated that PRC complexes act as key engines for transcriptional silencing (Francis and Kingston, 2001; Levine et al., 2004; Muller and Verrijzer, 2009; Schuettengruber et al., 2007; Schwartz and Pirrotta, 2007; Simon and Kingston, 2009). However, the precise molecular mechanisms of PRC-mediated gene silencing are a challenging problem to solve due to the difficulty of reconstituting the native regulatory network *in vitro* and the combinatorial diversity of PRC1 complexes (Figure 2.1, right panel) (Kerppola, 2009). There has been evidence showing that PRC2 is involved in the recruitment of PRC1 to the promoter regions of their common targets for executing transcriptional repression (Kuzmichev et al., 2002; Tolhuis et al., 2006). Therefore, one prevailing hypothesis of PRC-mediated gene

silencing is that the histone methyltransferase EZH1/2 of the PRC2 complex catalyzes the trimethylation of lysine 27 of histone H3 (H3K27me3). This typical epigenetic silencing mark can be recognized by chromobox homolog (CBX) proteins in PRC1 complexes, through which PRC1 is recruited to gene loci, which in turn enacts chromatin condensation, blocks the transcriptional elongation of RNA polymerase and finally leads to epigenetic silencing of target genes (Bracken and Helin, 2009; Cao et al., 2011; Simon and Kingston, 2009). The silencing effect is considered at least partially due to the monoubiquitination activity specific for the lysine 119 of H2A (H2AK119ub) by the enzymatic activity of the two core PRC1 components, RING1B and BMI1 (Figure 2.2) (Cao et al., 2011; Wang et al., 2004).

However, it has also been demonstrated that PRC1 and PRC2 can silence genes either synergistically or independently of each other (Richly et al., 2011). In fact, PRC1 recruitment to many sites occurs in the absence of PRC2 (Boyer et al., 2006; Kerppola, 2009; Ku et al., 2008; Schoeftner et al., 2006). For example, Suz12-deficient embryonic stem (ES) cells lack detectable H3K27me3. However, during differentiation of these cells, Cbx8 and Bmi1 can still be recruited the majority of their target loci in WT ES cells (Pasini et al., 2007), suggesting that PRC1 localization can be regulated in a PRC2-independent manner. Indeed, a recent study has reported that the transcription factor REST regulates PRC1 occupancy through interacting with CBX proteins, affecting the PRC1-mediated transcriptional silencing of genes with distal RE1 elements in ES cells (Ren and Kerppola, 2011). In addition, the PRC1 components CBX4 and CBX7, as well as

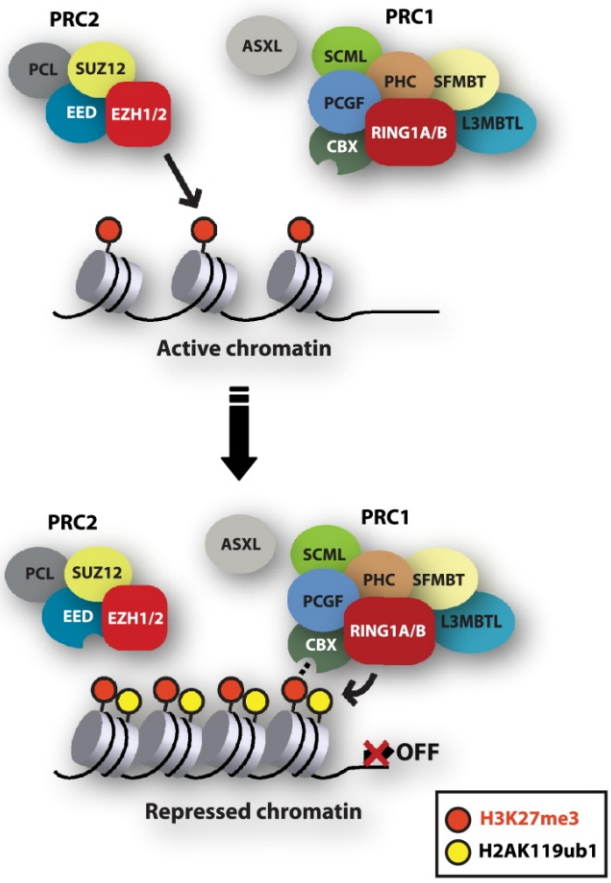

Figure 2.2 Coordinated Epigenetic Silencing Activity of PcG Complexes. Following recruitment of the PRC2 complex to chromatin, the histone methyltransferase EZH1/2 catalyzes the trimethylation of the lysine 27 of histone H3 (H3K27me3). Subsequent recruitment of the PRC1 complex occurs in part through affinity binding of the chromodomain of the CBX subunit to the H3K27me3 covalent mark. The PRC1 RING1 E3 ligase then monoubiquitylates the lysine 119 of histone H2A (H2AK119ub1), which was proposed to consolidate transcriptional repression by preventing access to chromatin remodelers, inhibiting RNA polymerase II-dependent transcriptional elongation and facilitating chromatin compaction (Francis et al., 2004; Zhou et al., 2008). PRC1 has also been reported to be targeted to chromatin independently of PRC2 (Boyer et al., 2006; Ku et al., 2008; Schoeftner et al., 2006). The ASXL subunit has recently been found to be involved in a H2A deubiquitinase complex required for PcG-mediated repression, but its precise role remains unclear. Adapted from (Sauvageau and Sauvageau, 2010).

the PRC2 component EZH2, have been reported to interact with DNA methyltransferases (DNMTs), suggesting that other than their direct enzymatic activities that induce transcriptional repression, PRC proteins may also contribute to gene silencing through recruiting DNMT to catalyze DNA methylation (Kim et al., 2008; Mohammad et al., 2009; Vire et al., 2006).

PcG and Cancer

The multifaceted regulatory functions of PcG proteins in key physiological processes during normal development strongly indicate that they are important players in oncogenesis. Indeed, both PRC1 and PRC2 components have been found to be overexpressed in a variety of tumors. On the one hand, expression changes associated with oncogenic transformation have been found for at least two core PRC1 proteins, BMI1 and RING1B, whose expression levels are elevated in a large series of tumors including gastrointestinal tumors, pituitary and parathyroid adenomas, and lymphomas, compared to the expression in normal cell counterparts (Sanchez-Beato et al., 2006). Especially, BMI1 activity is crucial for the maintenance of both normal and cancer stem cell because loss of BMI1 leads to progressive deletion of these cell population (Lessard and Sauvageau, 2003). On the other hand, the PRC2 proteins are also overexpressed in multiple human cancers (Bracken and Helin, 2009; Sparmann and van Lohuizen, 2006). For instance, increased expression of EZH2 directly correlates to the invasive potential of multiple types of carcinomas, including bladder cancer, prostate cancer and breast cancer (Bachmann et al., 2006; Collett et al., 2006; Richly et al., 2011; Weikert et al., 2005). Moreover, EZH2

deregulation has been associated with the onset of colorectal cancer and oral squamous carcinomas (Kidani et al., 2009; Mimori et al., 2005).

Other than transcriptional upregulation, missense mutations and chromosomal translocations involving PcG components have been identified in different types of human cancers as well (Sauvageau and Sauvageau, 2010). *EZH2* mutations that alter its methyltransferase activity were found in germinal center diffuse large B cell lymphomas, follicular lymphomas and myeloid disorders (Ernst et al., 2010; Morin et al., 2010; Nikoloski et al., 2010). Moreover, *Eed* mutations in mice facilitate the formation and progression of lymphoid tumors (Richie et al., 2002), and a *Suz12* point mutation has been shown to alter the repopulation capacity of the hematopoietic system (Majewski et al., 2008). Together, these studies emphasize that aberrant PRC2 activity is a frequent abnormality that contributes to oncogenesis. In addition, several PcG members, including the PRC1-associated protein ASXL2, SUZ12 and PCL1, are involved in chromosomal translocations observed in human cancers such as acute leukemias and endometrial stromal sarcomas (Li et al., 2007; Nakahata et al., 2009).

Aside from the transcriptional regulation and genetic mutations that alter the PRC activity, RNA-mediated regulatory mechanisms have also been found to gear PcG proteins towards tumorigenesis. First, the large intervening noncoding RNA (lincRNA) HOTAIR was reported to recruit the PRC2 complex for executing gene silencing (Gupta et al., 2010; Rinn et al., 2007). PRC2 relocalization in cancer cells due to HOTAIR overexpression promotes invasion and metastasis of epithelial tumors (Gupta et al., 2010). Additionally, the lincRNA ANRIL has been

shown to interact with the PRC1 component CBX7, which is required for the recruitment of PRC1 to the *INK4A/ARF* loci to induce transcriptional repression (Yap et al., 2010). These findings suggest that deregulated lincRNA-mediated PRC localization may contribute to the tumorigenic role of PcG proteins. Second, post-transcriptional regulation of PcG proteins by miRNAs has been well-documented as an essential mechanism to modify PRC activities. Accumulated evidence suggest that increased PRC2 activity due to loss of miR-101 or miR-26a promotes oncogenesis (Cao et al., 2011). Suppression of mir-183, mir-200c or mir-213, which leads to BMI1 upregulation, has been reported in several types of tumors (Sauvageau and Sauvageau, 2010). Furthermore, a recent study proposed a coordinate regulation of PRC1 and PRC2 activities mediated by miRNAs, which may play a significant role on cancer progression (Cao et al., 2011). Taken together, multiple lines of evidence highlight the correlative role of PcG proteins in tumorigenesis. Abnormal PRC activities due to deregulated expression, somatic mutations, chromosomal translocations and aberrant recruitment of PRC1 and PRC2 are associated with cancer development, mainly because of the broad involvement of PRC complexes in major biological processes that are essential for both normal physiology and pathogenesis.

CBX8

Chromobox homolog 8 (CBX8), also known as HPC3 (Human Polycomb 3), belongs to the CBX protein family (including CBX2, 4, 6, 7 and 8) that are homologs of the *Drosophila* Polycomb (Pc) protein (Kerppola, 2009). CBX8 was originally characterized as a transcriptional repressor, interacting with RING1a/b

and associating with BMI1 in PRC1 (Bardos et al., 2000). A previous study has reported that as a PRC1 component, CBX8 represses the *INK4a/ARF* expression in fibroblasts (Dietrich et al., 2007). Further studies showed that several distinct PRC1 complexes colocalize and regulate the *INK4a/ARF* expression, suggesting that the *INK4a/ARF* locus is a general target for PRC1 complexes, rather than a CBX8-specific downstream target (Maertens et al., 2009). Therefore, the exact role of CBX8 in transcriptional regulation remains largely undefined. It has been reported that certain CBX proteins, such as CBX4, can associate with protein complexes other than PRC1, thereby playing a PRC1-independent role in transcriptional regulation (Kerppola, 2009). However, it remains unknown whether CBX8 has a PRC1-independent function as such, and if so, what the biological implication might be.

Interestingly, despite its well-characterized transcription repressor role, CBX8 has also been shown to be present in complexes recruited by MLL fusion proteins, which induces leukemogenesis through transcriptional activation (Monroe et al., 2010; Mueller et al., 2007). More specifically, CBX8 directly interacts with two of the most common MLL fusion partners, AF9 and ENL, both of which are transcription factors involved in gene activation (Garcia-Cuellar et al., 2001; Hemenway et al., 2001; Monroe et al., 2010). However, the functional significance of this seemingly paradoxical association has not yet been defined, therefore raising the question that what the role of CBX8 plays in MLL-mediated leukemogenesis.

HIV Tat interacting protein of 60 kDa

HIV Tat interacting protein of 60 kDa (TIP60) is a founding member of the MYST (Moz, Ybf2/Sas3, Sas2, Tip60) protein family, the largest family of histone acetyltransferases (HATs) that are highly conserved in all eukaryotes (Voss and Thomas, 2009). TIP60 is the catalytic subunit of the evolutionarily conserved NuA4 (nucleosome acetyltransferase of histone H4) complex (Doyon et al., 2004). Previous studies have shown that TIP60, in the context of the stable multi-protein complex, selectively acetylates nucleosomal H4 at lysines 5, 8, 12, and 16, as well as H2A, *in vitro* (Ikura et al., 2000; Sapountzi et al., 2006). Evidence from *Drosophila* indicates that modified histone variants, such as phospho-H2Av, can also be acetylated by TIP60 (Kusch et al., 2004). Apart from these histone substrates, TIP60 also has by far the most known non-histone targets. The majority of these substrates are transcription factors (Sapountzi and Cote, 2011). For example, one of the extensively studied non-histone substrates of TIP60 is the tumor suppressor p53. TIP60 can specifically acetylates lysine 120 (K120) of p53 upon DNA damage, thereby modulating the decision between cell cycle arrest and apoptosis upon p53 activation and by co-activating p53-driven transcription (Berns et al., 2004; Doyon et al., 2004; Legube et al., 2004; Sykes et al., 2006; Tang et al., 2006). Other transcription factors whose activity is regulated by TIP60-mediated acetylation include c-Myc (Patel et al., 2004), RB (Leduc et al., 2006), and androgen receptor (Brady et al., 1999; Gaughan et al., 2001; Gaughan et al., 2002). In addition to transcription factors, it has been shown that the ATM kinase, a key player in the DNA repair pathway, is also subjected to TIP60-mediated acetylation (Sun et al., 2005).

The broad spectrum of its acetylated substrates indicates that TIP60 plays a role in multiple biological processes. First, it is critically involved in DNA repair, mainly through the TIP60-p53 functional interaction, acetylation-mediated ATM activation, and TIP60-related H2Av modification (Avvakumov and Cote, 2007). Second, TIP60 has been well-characterized as a transcriptional co-activator in multiple key signaling pathways, such as c-Myc signaling, Wnt signaling, NF-κB signaling, and androgen receptor signaling (Baek et al., 2002; Frank et al., 2003; Sapountzi et al., 2006; Sierra et al., 2006). Although in the majority of cases, TIP60 has been associated with transcription activation, it has also been reported to induce gene repression in a context-dependent manner. For instance, TIP60 can interact with HDAC to modulate STAT3 activity (Xiao et al., 2003). The multiple roles of TIP60 in DNA repair and transcriptional regulation have linked it to a number of human diseases, including HIV infection and Acquired Immune Deficiency Syndrome (AIDS), Alzheimer's disease, and cancer (Avvakumov and Cote, 2007; Baek et al., 2002; Cao and Sudhof, 2001; Creaven et al., 1999; Kinoshita et al., 2002). A wealth of studies have suggested the involvement of TIP60 in oncogenesis, although in many of these cases, the direct mechanistic evidence is still lacking (Figure 2.3) (Avvakumov and Cote, 2007).

It is worth noting that so far, TIP60 has not been shown to be involved in chromosomal translocation, which is the most common cause of human leukemias. However, it can act as a transcriptional regulator when interacting with TEL, which fuses with AML1 in the majority of childhood leukemias (So and van der Reijden, 2008). An additional study shows that TIP60 directly interacts

with the myeloid transcription factor C/EBPα *in vitro* and associates with C/EBPα at target gene loci in human leukemic cell lines (Bararia et al., 2008). The authors further suggested that TIP60 acts as a transcriptional co-activator of C/EBPα in an acetyltransferase-dependent manner by luciferase reporter assays (Bararia et al., 2008), raising the intriguing question of whether, and if so how, TIP60 might be involved in myeloid leukemogenesis.

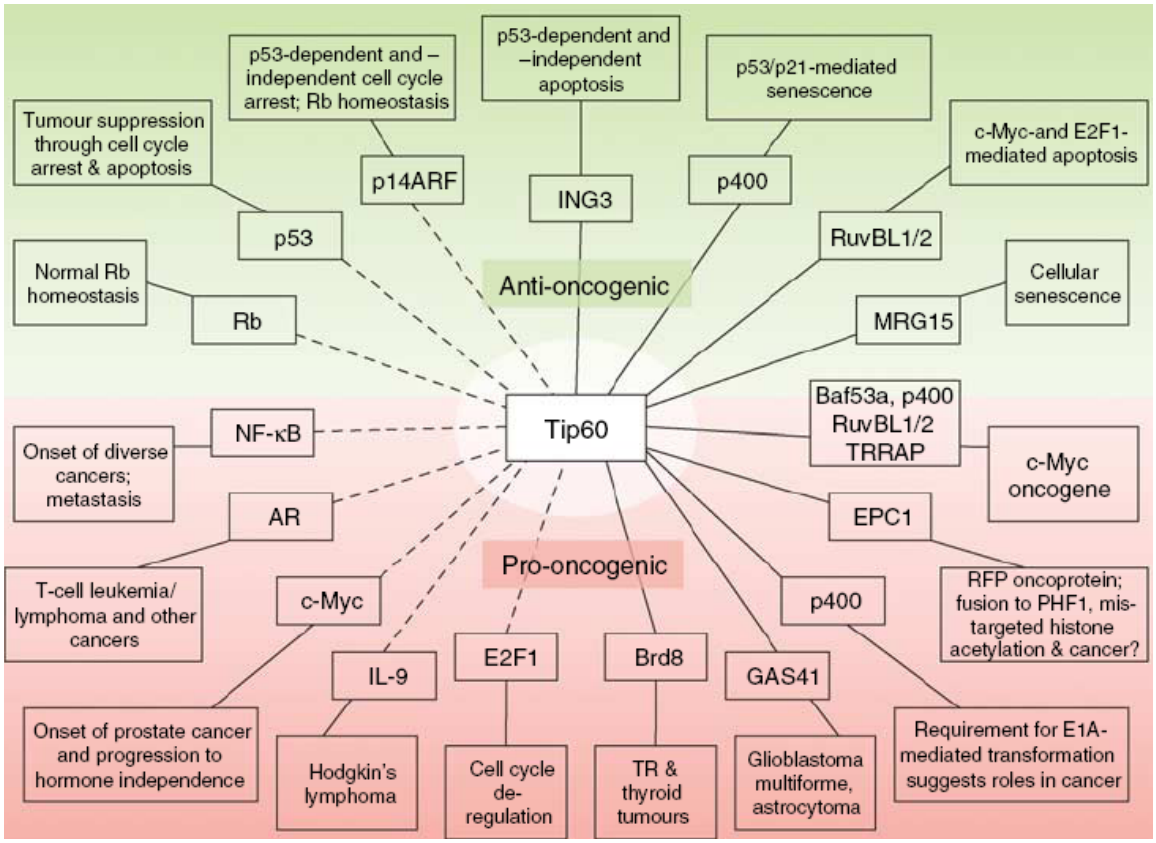

Figure 2.3 Established and Putative Connections of Tip60 to Oncogenesis. Green text boxes denote anti-oncogenic activities, whereas red ones represent potentially pro-oncogenic connections. Solid lines link Tip60 with other NuA4 subunits, whereas dashed lines signify physical or functional interactions with other cellular proteins. Adapted from (Avvakumov and Cote, 2007).

Materials and Methods

Cell Culture and Animal Use

HeLa and 293 cells were cultured in Dulbecco's modified Eagle's medium (DMEM) supplemented with 10% fetal bovine serum (FBS) and non-essential amino acids. MLL-AF9, MLL-ENL and E2A-HLF cells were cultured in Iscove's modified Dulbecco's medium (IMDM) supplemented with 15% fetal calf serum (FCS, Stem Cell Technologies). THP-1, Mono Mac 6 (MM6), and K562 cells were cultured in RPMI-1640 medium supplemented with 10% FBS. The Tripz-RFP-shCBX8 expression was induced by 0.5 μg/ml doxycycline. For conditional knockout of *Cbx8* in mice, two LoxP sites were inserted to flank the exons 2 to 4 of the *Cbx8* gene. *Cbx8* excision was achieved upon 4-OHT treatment. Full details of conditional gene targeting of *Cbx8* and analysis of $Cbx8^{-/-}$ embryos will be provided in a subsequent manuscript (H.K., unpublished). All animal experiments in this study were approved by the University of Michigan Committee on Use and Care of Animals and Unit for Laboratory Animal Medicine (ULAM).

In Vivo Leukemogenesis Assays

Lin- BM was isolated from 6 to 8-week-old mice ($Cbx8^{f/f}$; Cre^{+}) injected with 5-fluorouacil (see Supplemental Information). The harvested Lin- BM cells were retrovirally transduced with MigR1-MLL-AF9 by two rounds of spinoculation in the presence of either 4-OHT (100 nM) or ethanol as a control. The cells were then counted and injected intravenously through the tail vein to cohorts of lethally

irradiated (900 rads) C57BL/6 mice (3.5 x 10^4 cells per injection). Recipient mice were maintained on antibiotics for 2 weeks after transplantation.

Complete Blood Count Analysis

Peripheral blood was harvested in EDTA (ethylenediaminetetraacetic acid)-containing Microtainer tubes (BD Biosciences) and subjected for analysis performed by the ULAM laboratory.

Vector Construction

The pfMLL-AF9 vector and pMSCV-neo constructs encoding MLL-AF9 were previously described (Muntean et al., 2010). The FLAG-CBX8 and HA-DOT1L constructs were generously provided by Dr. Robert Slany (University of Erlangen, Germany). Expression vectors for MLL-AF9 mutants and CxxC-AF9 mutants (T542A and T554A) were generated by restriction enzyme digestion and PCR-based mutagenesis. The pSM2c scrambled, pSM2c shCbx8 (clone ID V2MM_66688), pSM2c shRing1b (clone IDs V2MM_197123 and V2MM_83055), pSM2c shBmi1 (clone ID V2HS_48576) and pSM2c shTip60 (clone ID V2MM_92042) retroviral vectors and the pTRIPZ-shCBX8 lentiviral vector (clone ID V2THS_58819) were purchased from Open Biosystems. An additional shRNA set for Tip60 knockdown based on the pGFP-V-RS retroviral vector system (Catalog Numbers TG512714 and TG30013) was purchased from OriGene.

Immunoprecipitation and Immunoblotting Assays

Cell lysates preparation, immunoprecipitation and immunoblotting were performed as previously described (Muntean et al., 2010). Immunoprecipitation was performed overnight, followed by three times of wash using BC-300 buffer.

Proteins were eluted by boiling in 1X SDS-loading buffer and separated by SDS-PAGE, followed by western blot analysis. Primary antibodies included rabbit anti-FLAG (Sigma), goat anti-Myc (Abcam), rabbit anti-HA (Abcam), rabbit anti-AF9 (Bethyl Laboratories, Inc.), mouse anti-β-actin (Sigma), rabbit anti-CBX8 (Abcam), goat anti-CBX8 (Everest Biotech), mouse anti-MLL N (Millipore), mouse anti-Bmi1 (Millipore), mouse anti-Ring1b (Medical and Biological Laboratories), and goat anti-TIP60 (Santa Cruz). An agarose affinity beads coupled to mouse anti-FLAG M2 monoclonal antibody was purchased from Sigma. An agarose affinity beads coupled to mouse anti-Myc M2 monoclonal antibody was purchased from Clontech. Protein G agarose beads were purchased from Roche.

Virus Production for Bone Marrow Transformation (BMT) Assays

The pMSCV (for FLAG-MLL-AF9 and the mutants), pSM2c (for shScram, shCbx8, shRing1b-1, shRing1b-2, shBmi1 and shTip60) and pGFP-V-RS (for shScram-1 and shTip60-1) constructs were transfected using Fugene 6 reagent (Roche) into Plat-E cells selected in puromycin (1 μg/ml) and blasticidin (10 μg/ml). Media containing the recombinant retrovirus was collected for transduction at 48 and 72 hours post transfection. Lentivirus production was performed by the University of Michigan Vector Core. Medium containing virus was collected 48 h post transfection.

BMT Assays

BMT assays were performed as previously described, with some modifications (Muntean et al., 2010). Briefly, BM was harvested from 6 to 8-week-old mice (*Cbx8* $^{f/f}$; *Cre*$^{+}$, or *Cbx8* $^{f/f}$; *Cre*$^{-}$) injected with 5-fluorouacil. Cells were collected

from the tibia and femur. Lin- BM cells were isolated using the EasySep® Mouse Hematopoietic Progenitor Cell Enrichment Kit (STEMCELL Technologies). The cells were then transduced with recombinant retrovirus containing MLL-AF9 (WT or mutants) by spinoculation and plated in methylcellulose medium (M3234, STEMCELL Technologies), supplemented with IL-3, IL-6, SCF, GM-CSF and 1 mg/ml G418. After three rounds of plating, CFU (with > 50 cells) was scored under the microscope; colonies were stained using 0.1% INT and scanned. Cells harvested at the end of the experiment were cytospun and stained with the Hema 3 Stain Kit (Thermo Fisher Scientific). Images were acquired using a 100x lens under an Olympus BX-51 microscope (Olympus). For secondary transductions, MLL-AF9-transduced cells harvested after the third round of plating were transduced with the indicated shRNA retrovirus by spinoculation and plated as described above, using 2 μg/ml puromycin in methylcellulose medium for selection. For *in vitro Cbx8* excision, cells were treated with 100 nM 4-OHT (Sigma) either during transduction (pre-transformation excision) or after three rounds of plating (post-transformation excision).

Colony Formation Assays

For assessing the total hematopoietic progenitor cell activity, BM was harvested from *Cbx8* $^{f/f}$; *Cre*$^{+}$ mice 6 months after in vivo 4-OHT administration or corn oil control treatment. After red blood cell lysis using ACK lysis buffer (Cambrex), nucleated BM cells were counted and plated in methylcellulose medium (M3534, STEMCELL Technologies). The colony number is counted 7 days after plating.

Quantitative RT-PCR

Reverse transcription and quantitative PCR were performed as previously described (Muntean et al., 2010). FLAG-MLL-AF9 was detected using the following primers for SYBR green detection: FLAG-F-5'-ggactacaaggacgacgatga-3' and MLL-R-5'-acagctgtgcgccatgtt-3'. TaqMan primer probe sets were purchased from Applied Biosystems for mouse *Hoxa9, Cbx8, Ring1b, Bmi1, Tip60, Ink4a/Arf* and *β-actin,* as well as human *HOXA9, CBX8, TIP60* and *β-ACTIN*. Expression levels were analyzed using the comparative ΔΔCt method as described in ABI User Bulletin #2.

Luciferase Reporter Assays

293 cells were transiently transfected with MSCV, MLL-AF9 (WT and mutants), CMV-Renilla, and *Hoxa9*-LUC (or *Myc E box*-LUC) constructs using FuGene 6 (Roche) according to the manufacturer's instructions. The cells then underwent serum starvation in 0.5% FBS in OPTI-MEM media for 48 h. Luciferase reporter assays were performed using a Dual Luciferase assay kit (Promega) according to manufacturer's instructions. Emission was detected using a Monolight 3010 luminometer (BD Biosciences). For the luciferase assay with siRNA knockdown, HeLa cells were transiently transfected with the DNA constructs listed above using Lipofectamine (Invitrogen) and siRNA smart pools for targeting CBX8, RING1b, BMI1 and TIP60 (Dharmacon) using Oligofectamine (Invitrogen) according to the manufacturer's instructions. The firefly luciferase activity readouts are normalized to Renilla luciferase readouts.

Chromatin Immunoprecipitation

ChIP was performed as previously described (Milne et al., 2005b), using primary antibodies for CBX8 (Abcam), Cbx8 (also named as Mpc3, Santa Cruz), RNAP II (Covance), TIP60 (Santa Cruz), AF9 (Bethyl Laboratories, Inc.) and histone H3 (Abcam). Quantitative RT-PCR was performed on the precipitated DNAs using primers and qPCR probes described before (Muntean et al., 2010). Binding was quantitated as follows: $\Delta C_T = C_T(\text{input}) - C_T(\text{Chromatin IP})$, % total = $2^{\Delta CT}$.

Annexin V Staining

For apoptosis analysis, MLL-AF9 leukemic cells from *Cbx8* $^{f/f}$; *Cre*$^{+}$ and *Cbx8* $^{f/f}$; *Cre*$^{-}$ mice were treated with 4-OHT (100 nM) for 72 h, using ethanol as a control treatment. The treated cells were washed and resuspended in Annexin V binding buffer (BD Biosciences). The resuspended cells were stained with Annexin V-FITC (BioLegend) and 1 μg/ml DAPI. Stained cells were then analyzed by flow cytometry.

Cell Cycle Analysis

MLL-AF9 leukemic cells from *Cbx8* $^{f/f}$; *Cre*$^{+}$ and *Cbx8* $^{f/f}$; *Cre*$^{-}$ mice were treated with 4-OHT (100 nM) for 72 h, using ethanol as a control treatment. The treated cells were washed twice in phosphate buffered saline (PBS). The cells were then resuspended in ice-cold PBS and fixed in 70% ethanol for at least 24 h. The fixed cells were washed with standard buffer for flow cytometry, treated with 100 μg/ml RNase and stained with 10 μg/ml PI. Stained cells were then analyzed by flow cytometry.

Competitive Transplantation Assays

Competitive transplantation assays were performed as previously described, with some modifications (Maillard et al., 2009). Briefly, BM was harvested from *Cbx8* $^{f/f}$; *Cre*$^{+}$ mice 6 months after in vivo 4-OHT administration or corn oil control treatment. After red blood cell lysis using ACK lysis buffer (Cambrex), nucleated BM cells were counted and resuspended in ice-cold phosphate-buffered saline (PBS). These cells (CD45.2^{+}) were mixed at specific ratios with 5 x 10^5 CD45.1^{+} competitor BM cells from B6-SJL mice (1:1, 3:1 and 9:1). This mixture was injected intravenously through the tail vein to cohorts of lethally irradiated (900 rads) B6-SJL (B6-CD45.1) mice. Recipient mice were maintained on antibiotics for 2 weeks after transplantation, and their peripheral blood was assessed by flow cytometry.

Flow Cytometry and Cell Sorting

After blocking non-specific binding with unlabeled rat plus mouse IgG (Sigma-Aldrich), cells were stained on ice in PBS plus 4% fetal calf serum (FCS) and sorted on FACSAria (BD Biosciences). Analysis was performed on LSR II, FACSCanto, or FACSAria (BD Biosciences). Files were analyzed in FlowJo (TreeStar).

Statistical Analysis

Statistical significance was determined by Student's *t* test using the Excel software (Microsoft 2007); $p < 0.05$ was considered statistically significant.

Antibodies for Flow Cytometry Analysis

The antibodies used for flow cytometry analysis were obtained from BioLegend and listed in Table 2.1.

Stain	Anti-body	Fluoro-chrome	Stain	Anti-body	Fluoro-chrome
LT-HSC/MPP	CD48	FITC	Myeloid/ Erythroid	CD11b	PE
	CD135	APC		Gr-1	APC
	CD150	PE-Cy7		Ter119	BIO
	cKit	APC-Cy7		SA	Percp-Cy5.5
	Sca-1	Percp-Cy5.5	T Cells	CD8	FITC
	CD11b	PE		CD4	PE
	CD11c	PE		TCRB	APC
	Gr-1	PE	Thymic Progenitors	CD44	FITC
	B220	PE		cKit	APC
	CD19	PE		CD25	PE-Cy7
	Ter119	PE		CD11b	PE
	NK1.1	PE		CD11c	PE
	CD3	PE		Gr-1	PE
	CD8	PE		B220	PE
	CD4	PE		CD19	PE
	TCRB	PE		Ter119	PE
	TCR GD	PE		NK1.1	PE
BM B Cells	B220	FITC		CD3	PE
	CD43	PE		CD8	PE
	AA4.1	APC		TCRB	PE
	IgM	BIO		TCR GD	PE
	CD19	PE-Cy7	Transplant Bleeds	B220	FITC
	SA	Percp-Cy5.5		CD19	APC
Splenic B Cells	CD21/25	FITC		CD3	PE
	CD23	PE		CD45.1	APC-Cy7
	AA4.1	APC		CD45.2	PercP-Cy5.5
	B220	APC-Cy7		CD11b	PE
	CD19	PE-Cy7		GR-1	APC

Table 2.1 Antibodies Used for Flow Cytometry Analysis of Hematopoietic Cells

Results

CBX8 Specifically Interacts with MLL-AF9 at the C-Terminal Domain (CTD)

Previous studies have reported that the MLL fusion partner AF9 directly interacts with CBX8 through the evolutionarily conserved CTD (Figure 2.4A) (Garcia-Cuellar et al., 2001; Hemenway et al., 2001; Monroe et al., 2010). However, whether this interaction is retained in MLL-AF9 fusion protein has not been defined. To address this question, we transiently co-expressed epitope-tagged MLL-AF9 and CBX8 in human embryonic kidney 293 cells, using a FLAG-tagged "empty" vector as a negative control. Specific interaction between CBX8 and MLL-AF9 was detected by immunoprecipitation (IP) experiments. When using AF9-conjugated agarose beads to pull down the full-length fusion protein, we consistently observed that CBX8 coprecipitated with MLL-AF9 (Figure 2.4B). To further characterize this interaction, we performed IP experiments in the presence of Benzonase. Using anti-FLAG antibody to pull down FLAG-tagged MLL-AF9, we detected endogenous CBX8 coprecipitating with the fusion protein, suggesting that CBX8 interacts with MLL-AF9 in a DNA-independent manner (Figures 2.4C). Next, we characterized the critical CBX8 interaction sites on MLL-AF9, by generating 15 point mutants within the CTD through single amino acid substitution. By Co-IP experiments, we identified two point mutants (T542A and T554A) that specifically disrupt the CBX8 interaction (Figures 2.4A and 2.4D). This observation was further supported by reciprocal Co-IP experiments, using anti-FLAG or anti-Myc antibodies to pull down CBX8 or CxxC-AF9, respectively (Figures 2.4E and 2.4F), in which case CxxC-AF9, a previous characterized

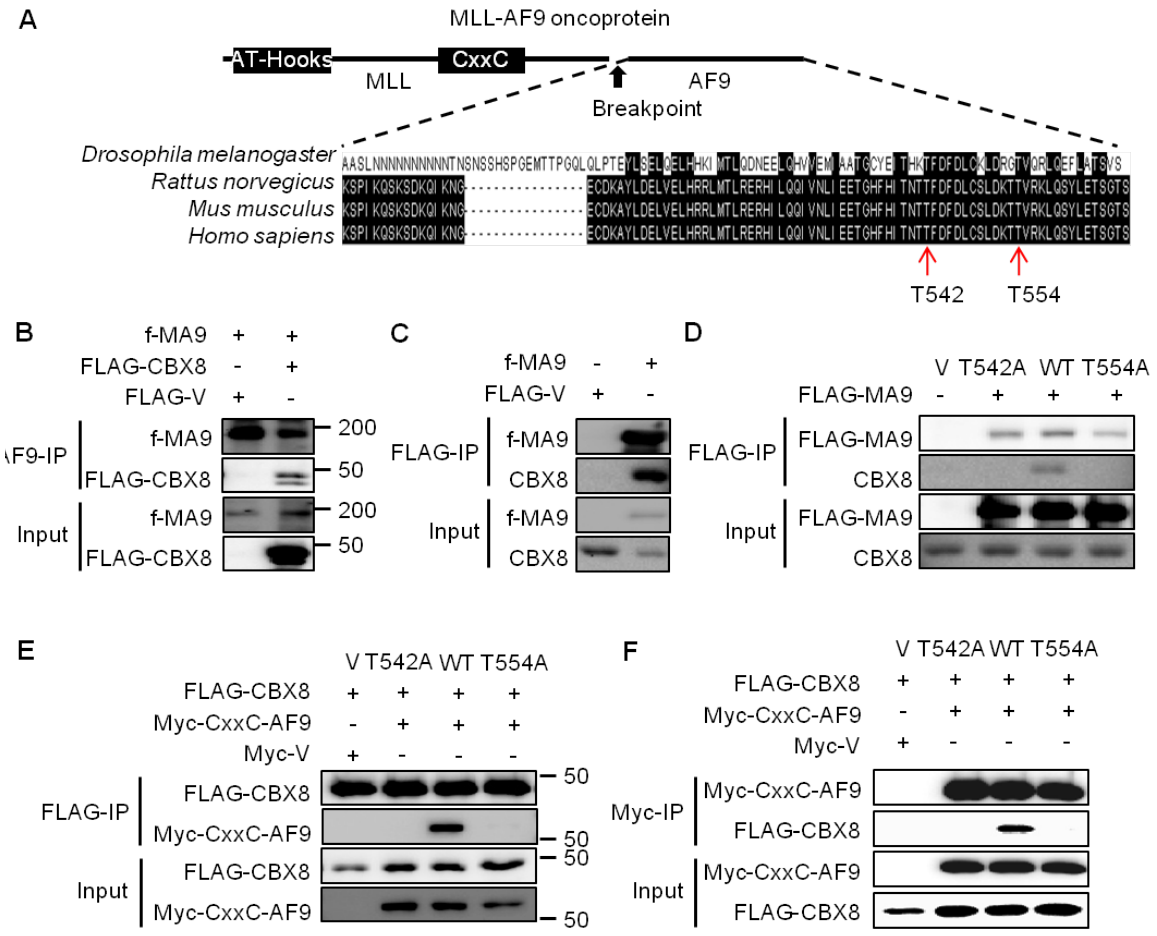

Figure 2.4 CBX8 Specifically Interacts with MLL-AF9 at the C-terminal Domain (CTD) (A) Schematic of full-length MLL-AF9. The amino acid sequence of the evolutionarily conserved CTD of AF9 is aligned with Drosophila, Rattus norvegicus and Mus musculus AF9 homologs. Red arrows indicate the evolutionarily-conserved threonine residues converted to alanine used below. (B) Co-immunoprecipitation of FLAG-tagged CBX8 with fMLL-AF9 (f-MA9). (C) Co-immunoprecipitation of endogenous CBX8 with f-MA9, after Benzonase treatment. (D) Co-immunoprecipitation of endogenous CBX8 with WT FLAG-MA9, but not with the mutants (T542A and T554A). (E) Co-immunoprecipitation of FLAG-CBX8 with WT Myc-CxxC-AF9, but not the mutants. (F) Reciprocal IP of the experiments in (E). WT Myc-CxxC-AF9 or the mutants were coexpressed with FLAG-CBX8, followed by IP with an anti-Myc antibody. Western blot shows that the interaction between Myc-CxxC-AF9 and FLAG- CBX8 is disrupted in the mutants. A fraction (3%) of cell lysate was used for input control.

MLL-AF9 fragment, was used as a surrogate for the full-length fusion protein (Muntean et al., 2010).

Apart from CBX8, AF9 also associates either directly or indirectly with DOT1L, the P-TEFb complex (CDK9 and CYCLINT1) and AF5q31 (Monroe et al., 2010). Therefore, we asked whether the CBX8 interaction is required for interaction with any of these cofactors. To this end, we transiently transfected Myc-tagged CxxC-AF9 (WT or the mutants) in 293 cells and found that the P-TEFb complex (CDK9 and CYCLINT1) and AF5q31 coprecipitated with both the WT CxxC-AF9 fragment and the mutants (Figure 2.5D). Moreover, the interaction between DOT1L and CxxC-AF9 was also retained in the T542A and T554A mutants, as shown by reciprocal IP experiments using anti-FLAG or anti-HA antibodies to pull down CBX8 or DOT1L, respectively (Figures 2.5A and 2.5B). This observation was further confirmed by IP experiments in the context of full-length MLL-AF9 (Figure 2.5C). Together, our results showed that CBX8 specifically interacts with MLL-AF9 at the CTD, and that disrupting the CBX8 interaction does not affect the interaction with either P-TEFb or DOT1L, both of which are required for MLL-AF9-induced leukemogenesis. It is noteworthy that these data did not address the possibility of whether P-TEFb and/or DOT1L might affect the interaction between CBX8 and MLL-AF9.

CBX8 Is Essential for Both Initiation and Maintenance of MLL-AF9 Leukemic Transformation

To assess the importance of the CBX8 interaction in MLL-AF9-induced transformation, we first used bone marrow transformation (BMT) assays to

examine the transformation ability of the MLL-AF9 mutants (T542A and T554A), which lack the CBX8 interaction. Briefly, Lin- hematopoietic cells derived from

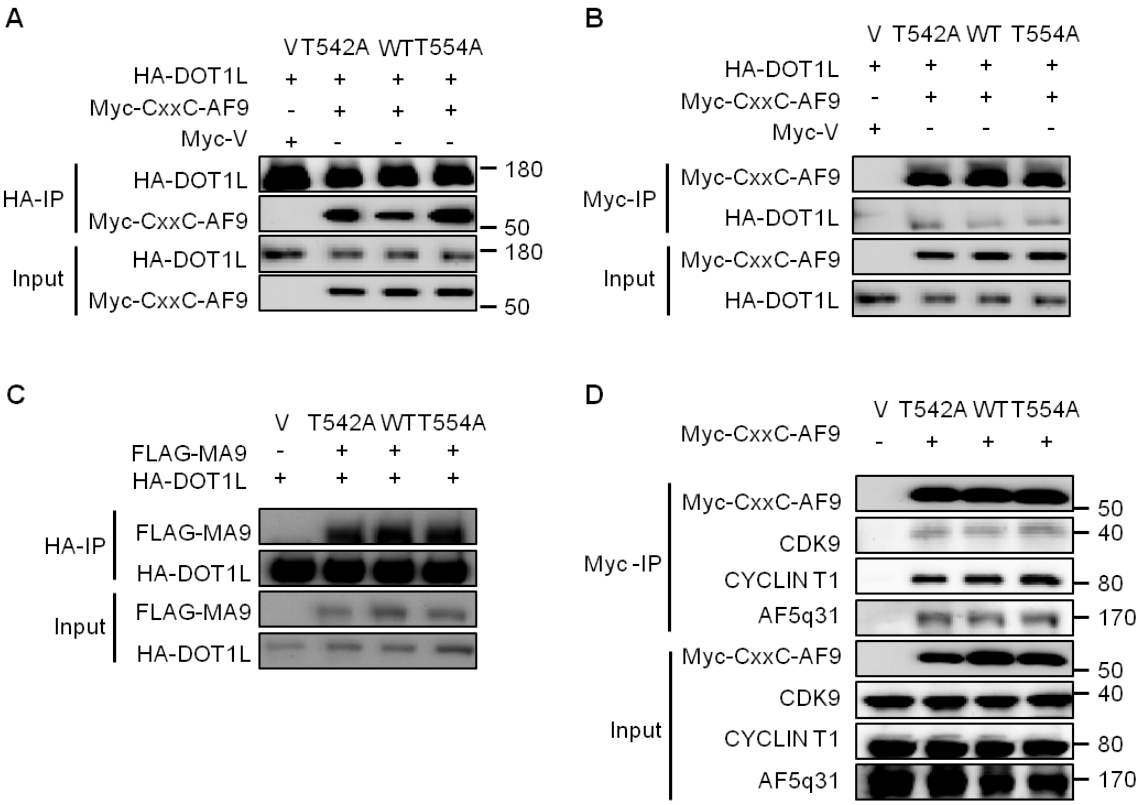

Figure 2.5 Specific Disruption of the CBX8 Interaction Does not Affect the Interaction between DOT1L and MLL-AF9 (A) Co-immunoprecipitation of both WT Myc-CxxC-AF9 and the mutants with HA-DOT1L. (B) WT Myc-CxxC-AF9 or the mutants were coexpressed with HA- DOT1L, followed by IP with an anti-Myc antibody. Western blot shows HA- DOT1L coprecipitating with both WT Myc-CxxC-AF9 and the mutants. (C) WT FLAG-MA9 or the FLAG-MA9 mutants were coexpressed with HA-DOT1L, followed by IP with an anti-HA antibody. Western blot shows HA- DOT1L coprecipitating with both WT FLAG-MA9 and the mutants. (D) Co-immunoprecipitation of endogenous CDK9, CYCLIN T1 and AF5q31 with both WT Myc-CxxC-AF9 and the mutants. All of the Co-IP experiments included an epitope-tagged empty vector (FLAG-V or Myc-V) as a control and were performed in 293 cells. A fraction (3%) of cell lysate was used for input control.

primary murine bone marrow (BM) were retrovirally transduced with either WT MLL-AF9 or the mutants, followed by three consecutive rounds of plating (Figure 2.6A). Despite the comparable expression of the fusion transcripts, as confirmed by real-time quantitative polymerase chain reaction (RT-PCR), the T542A and T554A mutations completely abolished myeloid transformation, whereas the WT control potently transformed primary hematopoietic cells, forming a large number of colonies (Figures 2.6B and 2.6C). The tertiary colonies formed by WT MLL-AF9-transduced cells displayed a dense, compact morphology, indicative of immortalization. Wright Giemsa staining shows that these colonies are composed of myeloblasts (Figure 2.6D). In contrast, the MLL-AF9 mutant-transduced cells failed to form colonies in the second round of selection, and the residual living cells were composed primarily of monocytes and macrophages (Figure 2.6D).

To further confirm that Cbx8 is required for MLL-AF9-induced transformation, we transduced the MLL-AF9-transformed BM cells with either the control shRNA or a shRNA directed against Cbx8 after the third round plating, followed by puromycin selection (Figure 2.7A). *Cbx8* expression, as measured by RT-qPCR, was effectively downregulated (Figure 2.7B), whereas the MLL-AF9 expression level was not significantly affected ($p>0.05$, Figure 2.7C). As expected, knockdown of Cbx8 significantly reduced the colony formation ability of MLL-AF9-transduced cells, compared to the control ($p<0.01$, Figures 2.7D and 2.7E). Together, these results suggest that the CBX8/MLL-AF9 interaction is required for MLL-AF9-mediated immortalization.

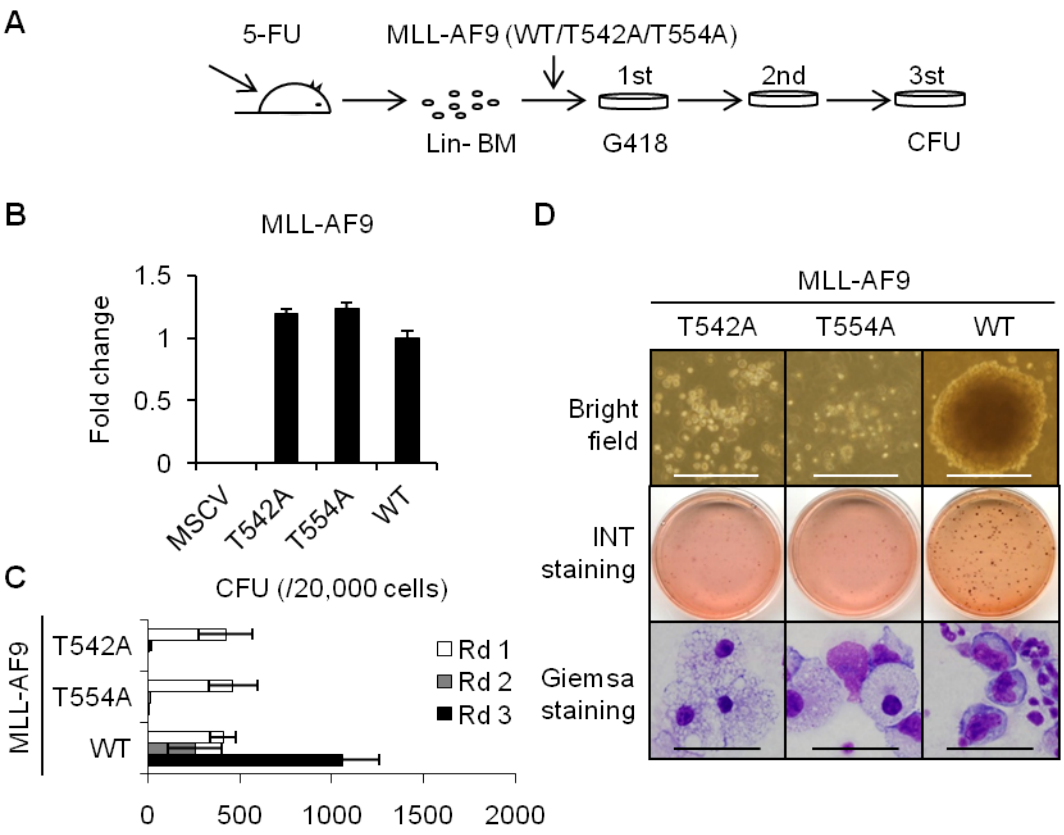

Figure 2.6 CBX8/MLL-AF9 Interaction Is Essential for MLL-AF9 Leukemic Transformation (A) Experimental scheme of the BMT assays evaluating the leukemic transformation ability of WT MLL-AF9 and MLL-AF9 mutants (T542A and T554A). (B) RT-qPCR analysis of the expression levels of WT MLL-AF9 and the mutants in Lin- BM after retroviral transduction. (C) Colony-forming units (CFU) per 20,000 plated cells in each round of plating in methylcellulose. Error bars represent ± standard deviation (SD) from three independent experiments. (D) Morphology of representative colonies from primary BM cells transduced with indicated constructs. The first row shows the representative colony morphology in methylcellulose. Scale bar, 500 μm. The second row shows the p-iodonitro tetrazolium violet (INT)-stained colonies after two rounds of plating. Dense red colonies are visible from WT MLL-AF9. The third row shows the Wright-Giemsa-stained cells isolated after two rounds of plating. Scale bar, 50 μm.

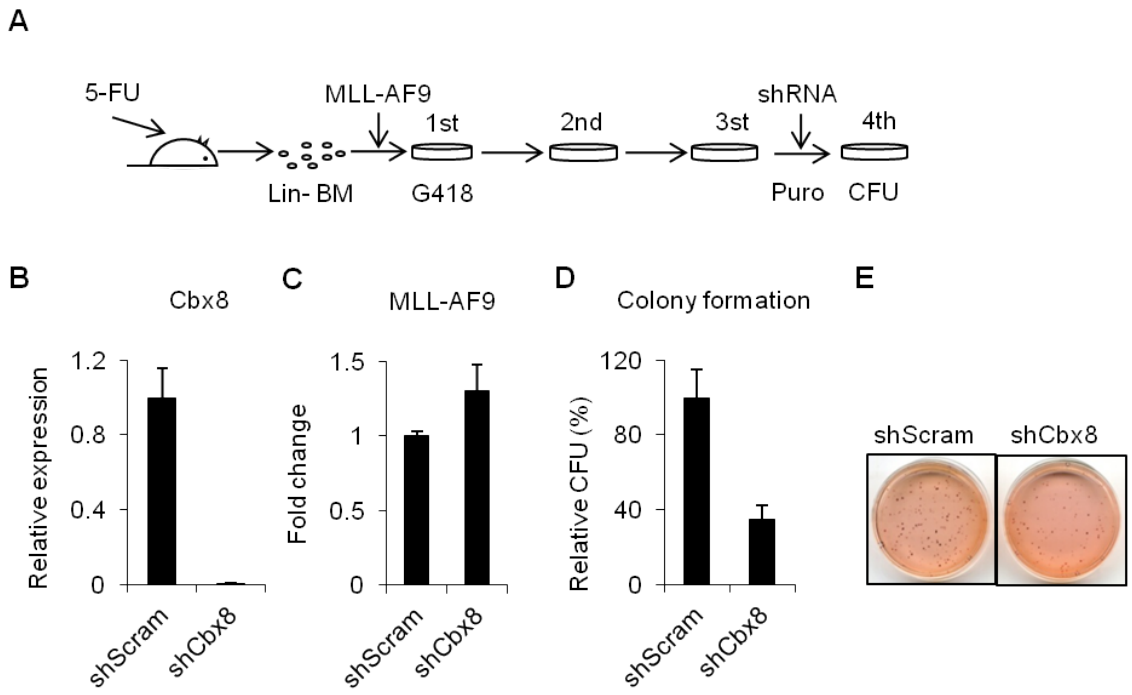

Figure 2.7 Cbx8 Knockdown by shRNA Impairs MLL-AF9 Leukemic Transformation (A) Experimental scheme of the BMT assays with shRNA-mediated Cbx8 knockdown. Experiments were performed as described in Figure 2.6, except for an additional retroviral transduction of shCbx8 or the control construct, followed by one round of plating with puromycin selection, after three rounds of plating. CFU was scored after the fourth plating. (B) RT-PCR analysis of Cbx8 expression in MLL-AF9-transformed primary BM transduced with shCbx8 compared to the control, confirming the efficiency of CBX8 knockdown. (C) RT-PCR analysis of MLL-AF9 expression in MLL-AF9-transformed primary BM transduced with shCbx8, compared to the control. (D) Relative CFU of MLL-AF9-transformed primary BM transduced with shCbx8, compared to the control. Error bars represent ± SD from three independent experiments. (E) Representative INT-stained colonies in methylcellulose after the fourth round of plating.

We then used a conditional *Cbx8* knockout mouse model (generated by Dr. Koseki) to further assess the role of Cbx8 in initiation and maintenance of transformation by MLL-fusion proteins in vitro and in vivo (Figure 2.8A). *Cbx8*$^{f/f}$ mice were bred with Rosa26-*Cre-ERT2* mice to generate *Cbx8* conditional knockout mice. Treatment with 4-hydroxyltamoxifen (4-OHT) induced efficient *Cbx8* excision in primary BM cells from *Cbx8* $^{f/f}$; *Cre*$^{+}$ mice (Figure 2.8B).

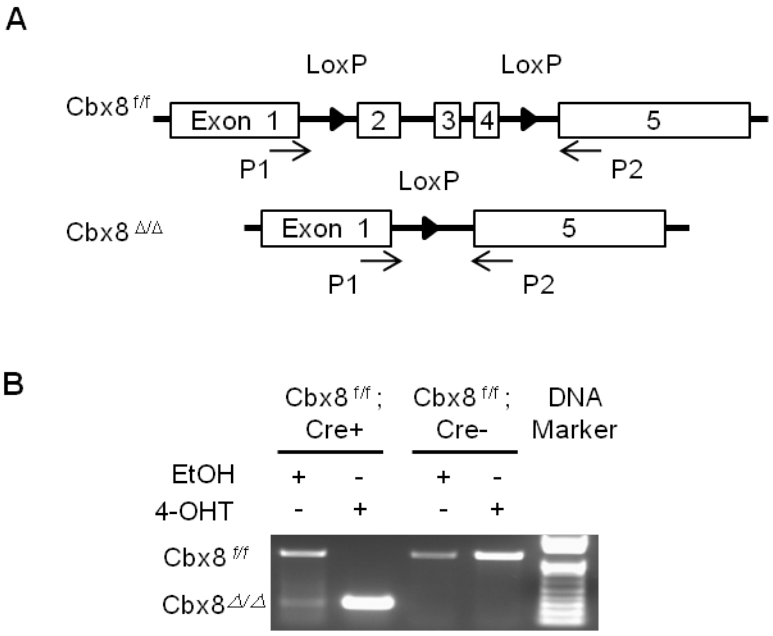

Figure 2.8 Strategy of Conditional Knockdown of Cbx8 in Mice (A) Schematic showing the floxed *Cbx8* and the primers used for detecting the floxed and the excised *Cbx8*. (B) Genotype analysis showing the efficiency of *Cbx8* excision induced by 4-OHT treatment in primary BM from *Cbx8* $^{f/f}$; *Cre*$^{+}$ mice, with ethanol treatment as a control (EtOH).

To assess the role of Cbx8 in initiation and maintenance of MLL-AF9 leukemic transformation, we induced *Cbx8* excision by 4-OHT treatment, simultaneously with MLL-AF9 transduction or after selecting MLL-AF9-transformed cells by three

consecutive rounds of plating, respectively, with BM from *Cbx8*$^{f/f}$; *Cre*$^{-}$ mice serving as a control (Figure 2.9).

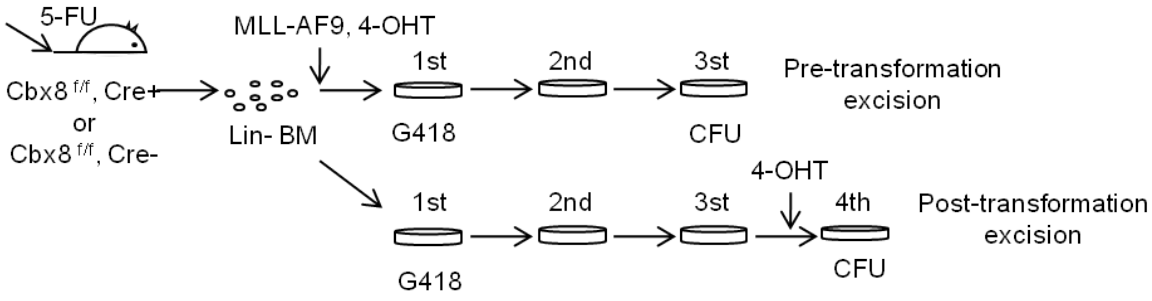

Figure 2.9 Experimental Scheme for the BMT Assays with *Cbx8* Excision in Primary BM from *Cbx8* $^{f/f}$; *Cre*$^{+}$ and *Cbx8* $^{f/f}$; *Cre*$^{-}$ Mice. The first experimental procedure was performed as described in Figure 2.6A, except 4-OHT or ethanol was added during MLL-AF9 retroviral transduction. The second experiment was performed as described in Figure 2.7A, except using 4-OHT treatment instead of shCbx8 transduction.

The expression level of MLL-AF9 was not significantly altered by 4-OHT treatment in either of these experimental settings (Figures 2.10A and 2.10B). Strikingly, loss of *Cbx8* completely abolished colony formation by MLL-AF9-transduced cells under both conditions (Figures 2.10C-2.10E). In contrast to the colonies formed by *Cbx8*$^{f/f}$; *Cre*$^{+}$ cells with the control treatment and the *Cbx8*$^{f/f}$; *Cre*$^{-}$ control cells with or without 4-OHT treatment, which showed dense morphology and were composed predominantly of myeloblasts (Figure 2.10G), Cbx8-depleted cells failed to form colonies and were composed of monocytes and macrophages (Figure 2.10F). Together, our results strongly indicate that

Cbx8 is essential for both initiation and maintenance of MLL-AF9 leukemic transformation.

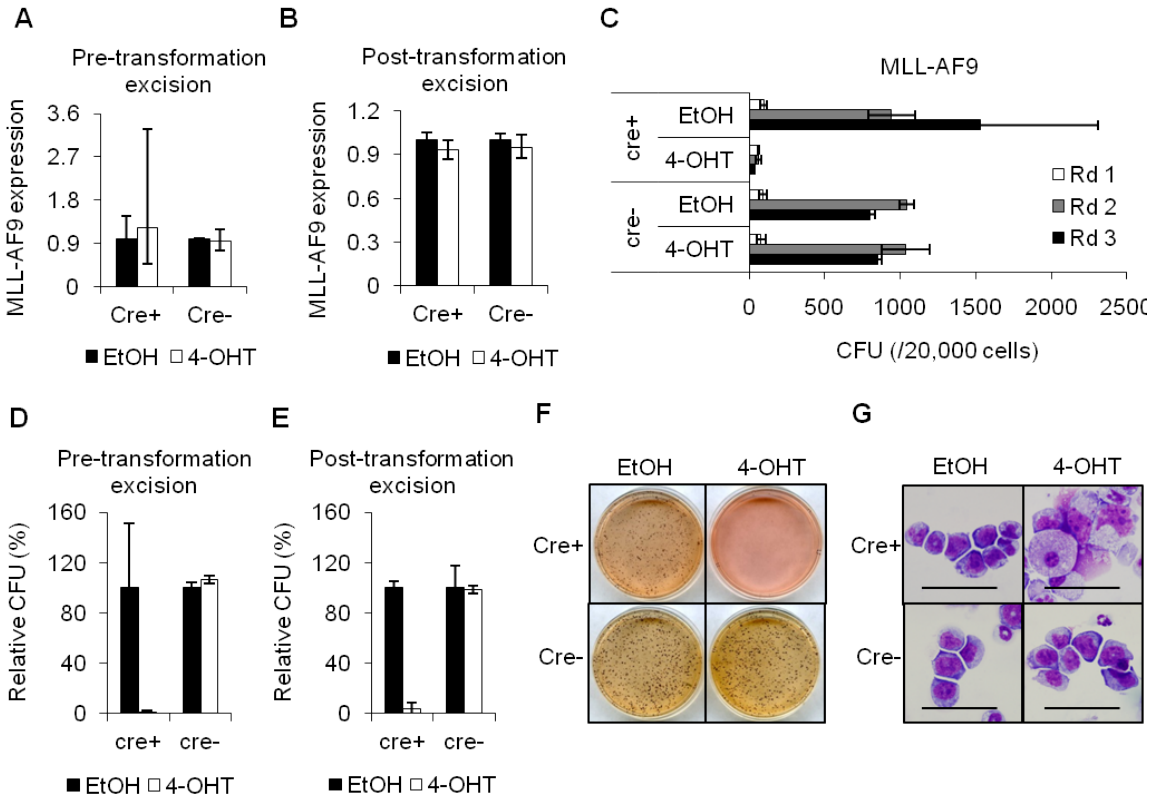

Figure 2.10 Cbx8 Is Required for Both Initiation and Maintenance of MLL-AF9 Leukemic Transformation (A and B) RT-PCR analysis of MLL-AF9 expression in Lin- BM after retroviral transduction, in the two experiment settings shown in Figure 2.9. Error bars represent ± SD from two independent experiments. Each experiment was performed in duplicate. (C) CFU per 20,000 plated cells in each round of plating in methylcellulose. Error bars represent ± SD from two independent experiments. Each experiment was performed in duplicate. (D and E) Relative CFU of MLL-AF9-transduced cells in the two experimental settings. Error bars represent ± SD from two independent experiments. (F) Representative INT-stained colonies in methylcellulose. (G) Wright-Giemsa-stained cells isolated after transformation selection. Scale bar, 50 μm.

Given our findings with the BMT assay, an in vitro surrogate for assessing myeloid transformation ability (Cheung et al., 2007; Lavau et al., 1997; Smith et al., 2011), we then tested the role of Cbx8 in MLL-AF9 leukemogenesis in vivo. The MigR1-MLL-AF9 construct, which expresses both MLL-AF9 and GFP, was used to retrovirally transduce Lin- BM cells derived from the *Cbx8*$^{f/f}$; *Cre*$^{+}$ mice, in the presence or absence of 4-OHT. These cells were then transplanted into syngeneic mice for accessing their leukemogenic potential. Complete *Cbx8* excision in the donor cells was achieved by 4-OHT treatment, as confirmed by genotyping the peripheral blood of the recipient mice three weeks post transplant (Figure 2.11A). Consistent with our in vitro findings, mice receiving Cbx8-deficient, MLL-AF9-transduced cells failed to develop leukemia, whereas mice receiving WT MLL-AF9-transduced BM all died from leukemia, as evidenced by marked splenomegaly and extensive infiltration of peripheral blood, spleen and liver (Figures 2.11B-2.11D). As expected, flow cytometry analysis showed that BM from the leukemic mice was replaced by GFP-positive, MLL-AF9-transformed cells (>99%). In contrast, BM from the mice receiving Cbx8-depleted donor cells was negative for GFP expression (Figure 2.11E). These results strongly demonstrate that CBX8 is required for MLL-AF9-induced leukemogenesis. Notable, a previous study has shown that CBX8 also interacts with another MLL fusion partner, ENL, which is also a component of the EAP (or the related AEP) complex (Garcia-Cuellar et al., 2001). Therefore, it is likely that CBX8 is not only required for MLL-AF9 leukemogenesis but also involved in leukemic transformation by other MLL fusion proteins that interact with the EAP (or the

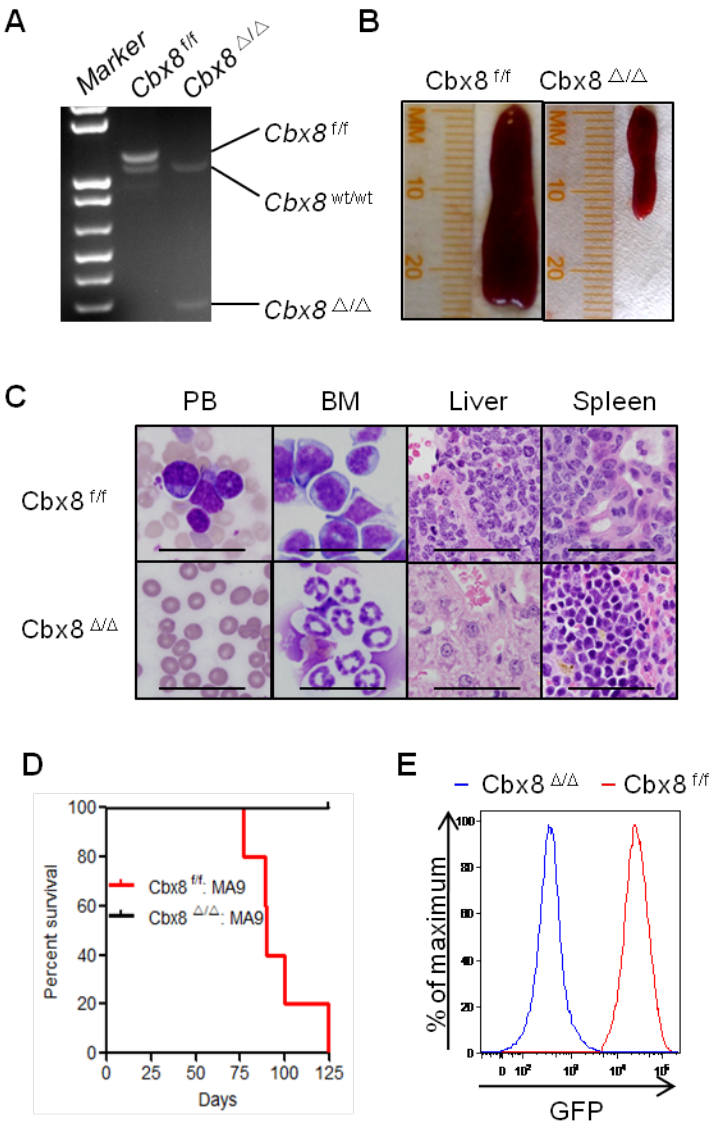

Figure 2.11 Cbx8 Is Required for MLL-AF9-Induced Leukemogenesis in Vivo. (A) Genotype analysis of peripheral blood from recipient mice transplanted with *Cbx8* $^{f/f}$ or Cbx8 $^{\Delta/\Delta}$ donor BM three weeks post transplant. (B) Representative pictures of spleens harvested from recipient mice transplanted with *Cbx8* $^{f/f}$ or Cbx8 $^{\Delta/\Delta}$ donor BM. (C) Wright-Giemsa staining of peripheral blood (PB) smear and BM and histology of liver and spleen from the transplanted mice. (D) Kaplan-Meier survival analysis of mice transplanted with Cbx8 $^{\Delta/\Delta}$ (n=5) or *Cbx8* $^{f/f}$ (n=5) donor BM. (E) GFP expression of BM from the transplanted mice, assessed by flow cytometry.

related AEP and the Dotcom) complex, such as MLL-ENL. Indeed, similar to MLL-AF9, Cbx8 is essential for initiation and maintenance of leukemic transformation induced by MLL-ENL, as shown by BMT assays (Figures 2.12A-2.12D). This finding suggests that the dependence on CBX8 of leukemic transformation is not restricted to MLL-AF9 but may apply to other MLL fusion proteins as well.

CBX8 Is Crucial for Proliferation and Survival of MLL-AF9-transformed Leukemic Cells and for MLL-AF9-Induced Transcriptional Activation

To explore the underlying mechanisms of Cbx8-dependent oncogenic transformation, we first investigated whether the Cbx8 dependence is specific for certain MLL-rearranged transformation or for leukemic transformation in general. Using the conditional *Cbx8* knockout mice, we assessed the impact of Cbx8 deletion on leukemic transformation by E2A-HLF, a leukemogenic fusion protein that transforms through *Hox*-independent pathways (Ayton and Cleary, 2003). Despite the complete depletion of the Cbx8 protein achieved 4-OHT treatment, neither the initiation nor the maintenance of E2A-HLF-induced leukemic transformation was affected, suggesting the specificity of Cbx8-dependent transformation (Figures 2.12E-2.12H and 2.13). Together, these findings suggest that Cbx8 plays a specific role in leukemic transformation by certain MLL fusion proteins, such as MLL-AF9.

We then examined whether Cbx8 is important in regulating the proliferation of MLL-AF9 leukemic cells and found that the Cbx8 shRNA, but not the scrambled control, decreased the growth rate of MLL-AF9 leukemic cells (Figure 2.14A).

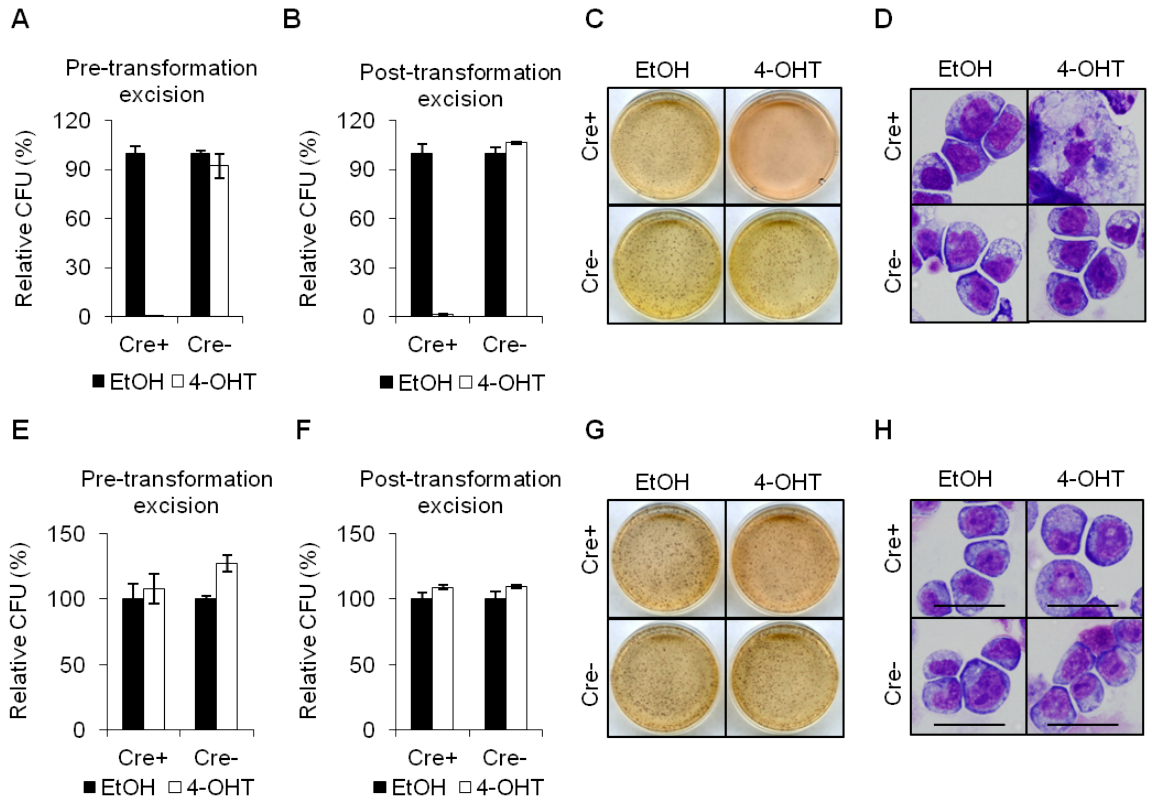

Figure 2.12 Cbx8 Is Required for the Leukemic Transformation by MLL-ENL, but not for That by E2A-HLF (A and B) Relative CFU of MLL-ENL-transduced cells in the two experimental settings. Error bars represent ± SD from two independent experiments. Each experiment was performed in duplicate. (C) INT-stained colonies after transformation selection, following MLL-ENL retroviral transduction. (D) Wright-Giemsa-stained cells isolated after transformation selection, following MLL-ENL retroviral transduction. Scale bar, 30 μm. (E and F) Relative CFU of E2A-HLF-transduced cells in the two experimental settings. (G) INT-stained colonies after transformation selection, following E2A-HLF retroviral transduction. (H) Wright-Giemsa-stained cells isolated after transformation selection, following E2A-HLF retroviral transduction. Scale bar, 30 μm.

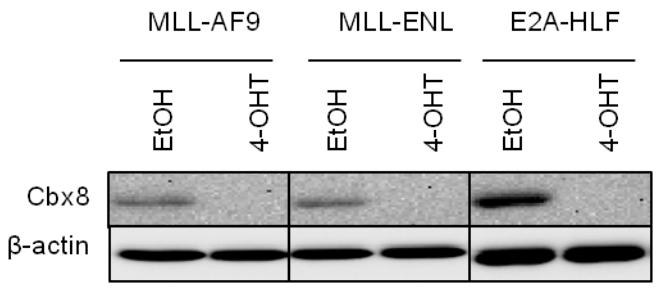

Figure 2.13 Western Blot Showing the Cbx8 Protein Level upon 4-OHT Treatment in Primary BM Transformed by MLL-AF9, MLL-ENL or E2A-HLF β-actin served as a loading control.

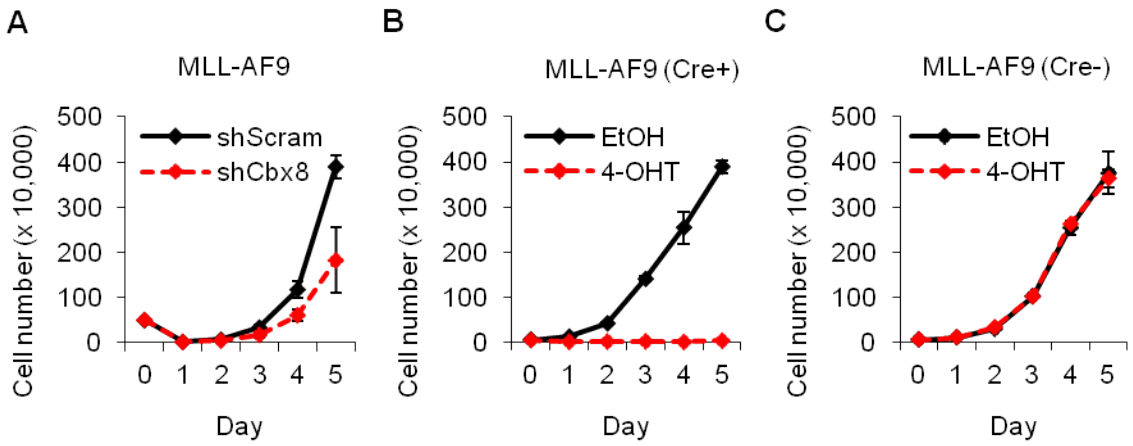

Figure 2.14 CBX8 Is Crucial for Proliferation and Survival of MLL-AF9-transformed Leukemic Cells (A) Growth curve of MLL-AF9 leukemic cells transduced with shCbx8 or control (shScram). Error bars represent ± SD from duplicate experiments. Results from one of three independent experiments are shown. (B and C) Growth curves of MLL-AF9-transformed primary BM from *Cbx8* $^{f/f}$; *Cre*$^{+}$ and *Cbx8* $^{f/f}$; *Cre*$^{-}$ mice, with 4-OHT treatment compared to the control. Error bars represent ± SD from a duplicate experiment. Results from one of two independent experiments are shown.

The phenotype was even more dramatic in primary murine BM cells, where we observed a complete growth arrest in liquid cultured primary BM cells (*Cbx8*$^{f/f}$;

Cre^{+}) with *Cbx8* excision by 4-OHT treatment, whereas no such effect was observed in control cells (*Cbx8*$^{f/f}$; *Cre*$^{-}$) (Figures 2.14B and 2.14C). In agreement with these observations, the apoptotic population of MLL-AF9 leukemic cells increased upon Cbx8 depletion by 4-OHT treatment, but not in the control cells (Figure 2.15). Additionally, we consistently observed a slight decrease of the S-phase cell population upon Cbx8 depletion in MLL-AF9 leukemic cells (Figure 2.16). However, the effect was rather minor, suggesting that the dramatic proliferation defect of MLL-AF9 cells upon Cbx8 depletion is not mainly due to cell cycle arrest.

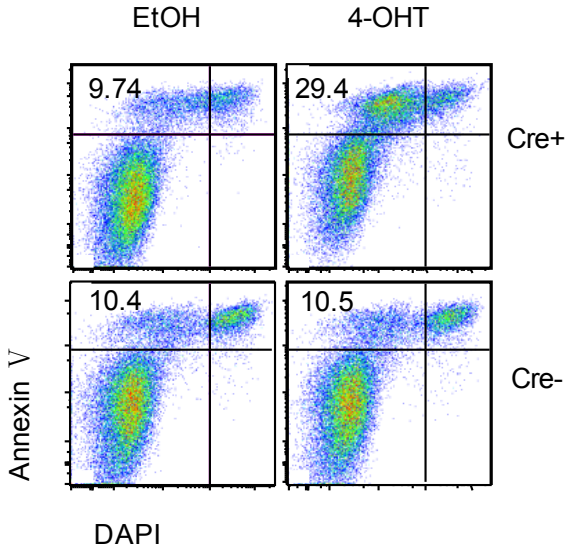

Figure 2.15 Apoptosis Analysis of MLL-AF9 Leukemic Cell in the Presence or Absence of Cbx8 The proportion of annexin V-positive, DAPI-negative cells from MLL-AF9-transformed leukemic cells (*Cbx8* $^{f/f}$; *Cre*$^{+}$ and *Cbx8* $^{f/f}$; *Cre*$^{-}$), after 72-h 4-OHT treatment, using ethanol treatment as a control.

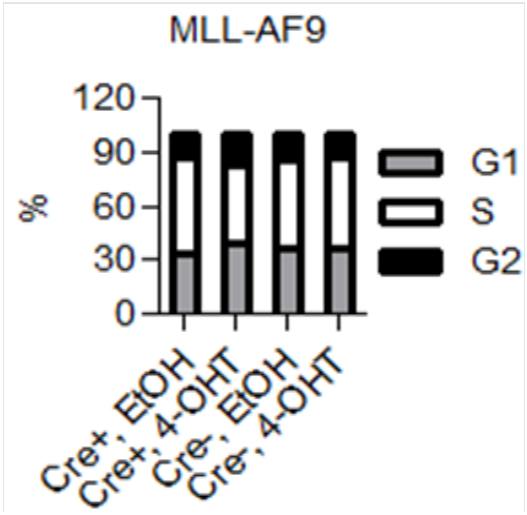

Figure 2.16 Cell Cycle Analysis of MLL-AF9 Leukemic Cell in the Presence or Absence of Cbx8. Cell cycle analysis was performed on MLL-AF9-transformed leukemic cells (*Cbx8* $^{f/f}$; *Cre*$^{+}$ and *Cbx8* $^{f/f}$; *Cre*$^{-}$), after 72-h 4-OHT treatment, using ethanol treatment as a control.

A well-established oncogenic mechanism of MLL-AF9 transformation is the constitutive activation of the *HOX* genes, particularly *HOXA9* along with the HOX cofactor *MEIS1* (Armstrong et al., 2002; Ayton and Cleary, 2003; Kumar et al., 2004), whereas CBX8 was previously shown to be involved in transcriptional repression (Dietrich et al., 2007; Maertens et al., 2009). The seemingly opposite effects of CBX8 and MLL-AF9 on transcriptional regulation raise an intriguing question: what role does CBX8 play in MLL-AF9-induced transcriptional activation? To address this question, we examined *Hoxa9* expression in MLL-AF9-transformed primary BM transduced with the Cbx8 shRNA. Compared to the control, Cbx8 downregulation led to a marked suppression of *Hoxa9* expression (Figure 2.17A). A similar effect was observed in MLL-AF9-transformed *Cbx8*$^{f/f}$; *Cre*$^{+}$ BM, following *Cbx8* excision by 4-OHT treatment, but not in the control cells

(Figures 2.17B and 2.17C). To further confirm that the impact of Cbx8 on *Hoxa9* expression is dependent on the interaction between Cbx8 and MLL-AF9, we compared the *Hoxa9* expression in primary BM cells transduced by WT MLL-AF9 or by the mutants lacking the Cbx8 interaction (T542A and T554A). Notably, MLL-AF9 mutant-transduced cells show significantly reduced *Hoxa9* expression, compared to the cells transduced by WT MLL-AF9 (Figure 2.17D). It is noteworthy that the cells examined in this experiment were harvested after the second round of selection because very few mutant-transformed cells survive the third round of selection. Therefore, few residual non-transformed progenitors may account for the detected *Hoxa9* expression in the mutant-transformed cells, suggesting that the reduction of *Hoxa9* expression in the mutant-transduced cells could be even greater. Nevertheless, these data strongly indicate that Cbx8 serves as a co-activator of MLL-AF9, promoting *Hoxa9* upregulation in MLL-AF9-transformed cells.

To further assess the specificity of the role of Cbx8 in *Hoxa9* transcriptional regulation, we examined the effect of Cbx8 knockdown on *Hoxa9* expression in several human and murine leukemic cell lines. CBX8 inducible knockdown stable cell lines were generated by lentiviral transduction of a TRIPZ-RFP-shCBX8 construct in three human leukemic cell lines. The THP-1 and Mono Mac 6 (MM 6) cells are transformed by MLL-AF9, whereas K562 is a BCR-ABL-transformed cell line that serves as a control. As expected, knocking down of CBX8 induced by doxycycline treatment significantly decreased *Hoxa9* expression in both

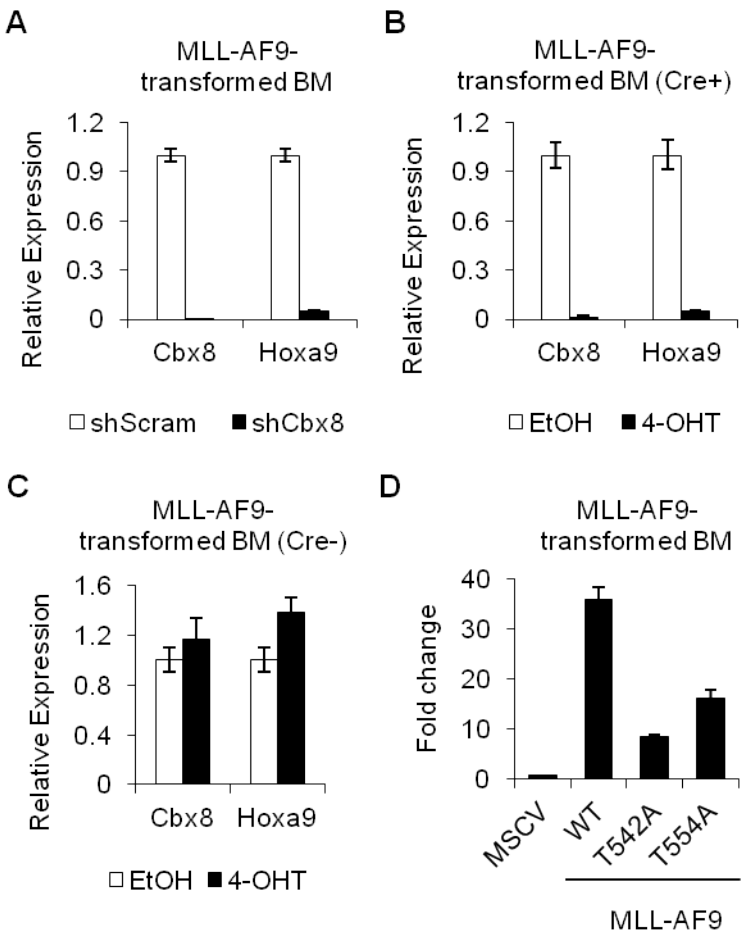

Figure 2.17 Cbx8 Is required for *Hoxa9* Upregulation in MLL-AF9-Transformed Primary BM Cells (A) RT-PCR analysis of the expression of *Cbx8* and *Hoxa9* in MLL-AF9-transformed primary BM, with shCbx8 transduction compared to the control (shScram). (B) RT-qPCR analysis of the expression of *Cbx8* and *Hoxa9* in MLL-AF9-transformed primary BM from *Cbx8* $^{f/f}$; *Cre*$^{+}$ mice, with 4-OHT treatment compared to the control (EtOH). (C) RT-PCR analysis of the expression of *Cbx8* and *Hoxa9* in MLL-AF9-transformed primary BM from *Cbx8* $^{f/f}$; *Cre*$^{-}$ mice, with 4-OHT treatment compared to the control (EtOH). Error bars represent ± SD. (D) RT-PCR analysis of the *Hoxa9* expression in primary BM transduced by WT MLL-AF9 or MLL-AF9 mutants, compared to the vector control.

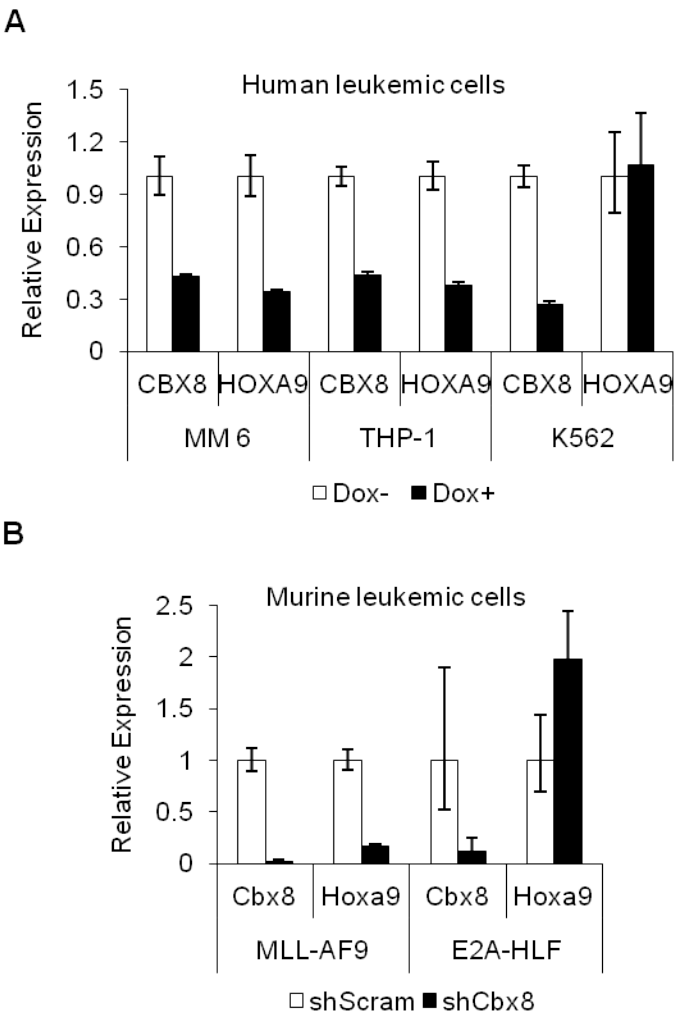

Figure 2.18 Cbx8 Is required for *Hoxa9* Upregulation in Human and Murine MLL-AF9-Transformed Leukemic Cell Lines (A) RT-PCR analysis of the expression of *Cbx8* and *Hoxa9* in two human MLL-AF9 leukemic cell lines (THP-1 and MM 6) and one MLL-independent human leukemic cell line (K562), with shRNA-mediated CBX8 knockdown. These three cell lines were integrated with a TRIPZ-RFP-shCBX8 construct by lentiviral transduction, whose expression can be induced by doxycycline treatment. Error bars represent ± SD. (B) RT-PCR analysis of the expression of *Cbx8* and *Hoxa9* in a MLL-AF9 murine leukemic cell line and an E2A-HLF murine leukemic cell line, with shCbx8 transduction compared to the control (shScram). Error bars represent ± SD.

MLL- AF9-transformed cell lines (MM 6 and THP-1), but not in the control cell line (Figure 2.18A). Consistent with this observation, Cbx8 knockdown by shRNA led to a marked decrease of *Hoxa9* expression in a murine MLL-AF9 cell line, but not in the Hoxa9-independent E2A-HLF cell line (Figure 2.18B). These findings suggest that Cbx8 specifically contributes to MLL-AF9-induced *Hoxa9* transcriptional activation.

In order to mechanistically understand how Cbx8 facilitates MLL-AF9-induced *Hoxa9* upregulation, we investigated the effect of Cbx8 on *Hoxa9* promoter activity in the presence of MLL-AF9. We first performed dual luciferase assays in 293 cells transfected with a MLL-AF9 responsive luciferase construct, under the control of the murine *Hoxa9* promoter (*Hoxa9-LUC*). Our data show that disrupting the CBX8 interaction by the point mutation of T542A or T554A significantly decreased the activation of the *Hoxa9* promoter by MLL-AF9 (T542A: $p<0.01$, T554A: $p<0.01$; Figure 2.19A). Consistent with this result, knocking down the CBX8 expression by siRNAs reduced the MLL-AF9 induced transcriptional activation by around 50% ($p<0.01$, Figures 2.19B and 2.19G). A similar response was observed using another MLL-AF9 responsive luciferase reporter containing the *thymidine* kinase promoter and multimerized *Myc E* box, further supporting the importance of Cbx8 in MLL-AF9-induced transcriptional activation (Figures 2.19C and 2.19D). Notably, neither the point mutations nor CBX8 knockdown significantly affected MLL-AF9 expression, indicating that the reduction in *Hoxa9* promoter activity was not due to a general decrease in the MLL-AF9 level (Figures 2.19E and 2.19F).

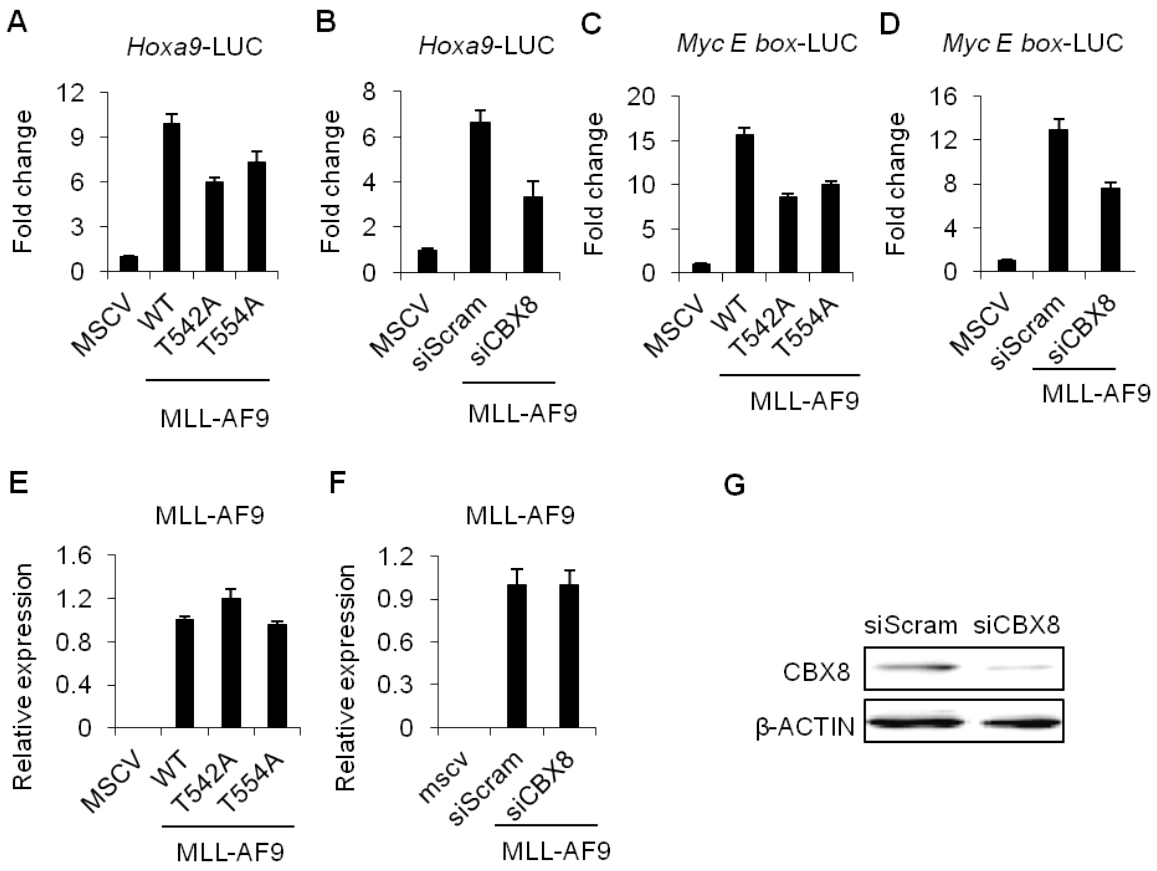

Figure 2.19 CBX8 Is Crucial for MLL-AF9-Induced Transcriptional Activation (A) Luciferase assay with a *Hoxa9* promoter-driven reporter activated by WT or mutant MLL-AF9 (T542A and T554A) in 293 cells. Error bars represent ± SD from three independent experiments. (B) Luciferase assay with the *Hoxa9* promoter-driven reporter activated by MLL-AF9, with CBX8 knockdown (siCBX8) or control treatment (siScram) in HeLa cells. Error bars represent ± SD from three independent experiments. (C) Luciferase assay with a *Myc E box* promoter-driven reporter activated by WT or mutant MLL-AF9 (T542A and T554A) in 293 cells. Error bars represent ± SD from three independent experiments. (D) Luciferase assay with the *Myc E-box* promoter-driven reporter activated by MLL-AF9, with CBX8 knockdown (siCBX8) or control treatment (siScram) in HeLa cells. Error bars represent ± SD from three independent experiments. (E) RT-PCR analysis of the expression of WT MLL-AF9 and the mutants in luciferase reporter assay. (F) RT-PCR analysis of MLL-AF9 expression in luciferase reporter assay, with siCBX8 treatment compared to the control (siScram). (G) Western blot showing CBX8 expression with siCBX8 treatment compared to the control (siScram).

We then carried out chromatin immunoprecipitation (ChIP) in MLL-AF9-transformed murine hematopoietic cells, to examine changes at the *Hoxa9* promoter in response to Cbx8 depletion. In agreement with the suppression of *Hoxa9* activation, a significant decrease of RNA polymerase II (RNAP II) binding to the *Hoxa9* promoter was detected following Cbx8 depletion by 4-OHT treatment, while as expected, Cbx8 binding was essentially ablated (Figures 2.20A and 2.20B). Moreover, the collective binding of MLL-AF9 fusion protein and WT AF9 was not affected by Cbx8 depletion, as shown by ChIP with an anti-AF9 antibody (Figure 2.20C). Because WT AF9 is also a component of the MLL-AF9 complex, and our previous results already showed that the Cbx8 interaction is not required for the assembly between the EAP complex and the MLL-AF9 fusion protein (Figure 2.5), this observation suggest that the recruitment of the MLL-AF9 complex to the *Hoxa9* promoter is not significantly affected by the loss of Cbx8, which is also consistent with previous reports regarding the importance of the retaining MLL portion in MLL fusion complex localization, rather than the fusion partner portion (Ayton et al., 2004; Milne et al., 2010; Muntean et al., 2010; Slany et al., 1998; Yokoyama and Cleary, 2008). Similar findings were observed using the CBX8 inducible knockdown MM6 cell line (Figures 2.20E-2.20J), further supporting that Cbx8 regulates MLL-AF9 target promoter activity, thereby contributing to MLL-AF9-induced transcriptional activation, without affecting the collective localization of MLL-AF9 and WT AF9.

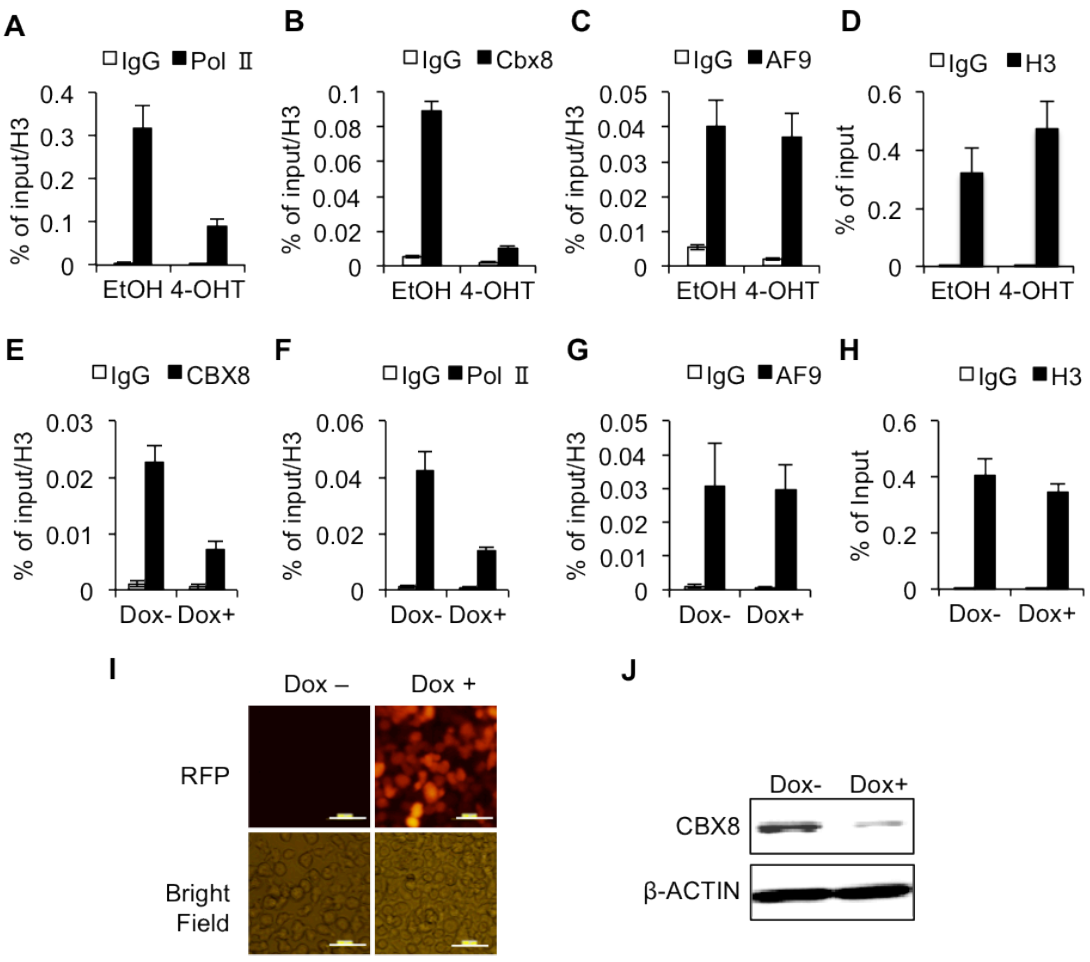

Figure 2.20 Cbx8 Is not Required for the collective localization of MLL-AF9 and WT AF9 at the *Hoxa9* Promoter (A-D) Relative binding of Cbx8, RNAP II and MLL-AF9 together with WT AF9, as well as H3 binding, to the *Hoxa9* promoter in MLL-AF9-transformed cells from *Cbx8* $^{f/f}$; *Cre*$^{+}$ mice, with 4-OHT treatment compared to the control (EtOH). (E-H) Relative binding of CBX8, RNAP II and MLL-AF9 together with WT AF9, as well as H3 binding, to the *HOXA9* promoter in TRIPZ-RFP-shCBX8-containing MM6 cells, with doxycycline treatment compared to the control. Error bars represent ± SD from three independent experiments. (I) RFP expression induced by doxycycline treatment, indicating shRNA induction. Scale bars = 100 μm. (J) Western blot showing the CBX8 protein level in TRIPZ-RFP-shCBX8-containing MM 6 cells after doxycycline treatment, using β-ACTIN as a loading control.

Role of CBX8 in MLL-AF9 Leukemic Transformation and Transcriptional Activation Is Independent of PRC1

To date, the only reported functional characterization of Cbx8 is its role as a transcriptional repressor in PRC1, whereas our data indicate that Cbx8 serves as a transcriptional coactivator in the presence of MLL-AF9. These opposing transcriptional regulatory roles suggest that Cbx8 functions in a PRC1-independent manner in MLL-AF9 leukemic transformation. It has been shown that Ring1b, another PRC1 component, is required for the stability of PRC1 complexes (Leeb and Wutz, 2007; van der Stoop et al., 2008). In addition, previous studies have indicated that Ring1b also interacts with AF9 (Monroe et al., 2010), which we confirmed by IP experiments showing that endogenous RING1b consistently coprecipitates with the MLL-AF9 fragment, CxxC-AF9 (Figure 2.21A). Therefore, to test our hypothesis of the potential PRC1-independent function of Cbx8, we first assessed the impact of Ring1b on MLL-AF9 leukemic transformation by BMT assays. Two individual shRNA molecules specifically targeting *Ring1b* were used to effectively knock down *Ring1b* expression in MLL-AF9-transformed leukemic cells. Reduction in *Ring1b* expression in these experiments did not impair the transformation ability of MLL-AF9 (Figures 2.21B, 2.21C and 2.21F). Knocking down *Ring1b* did not significantly affect the growth rate or *Hoxa9* expression in MLL-AF9 cells either (Figures 2.21D and 2.21E). We also performed dual luciferase assays to examine the impact of knocking down RING1b by siRNA on the MLL-AF9 target

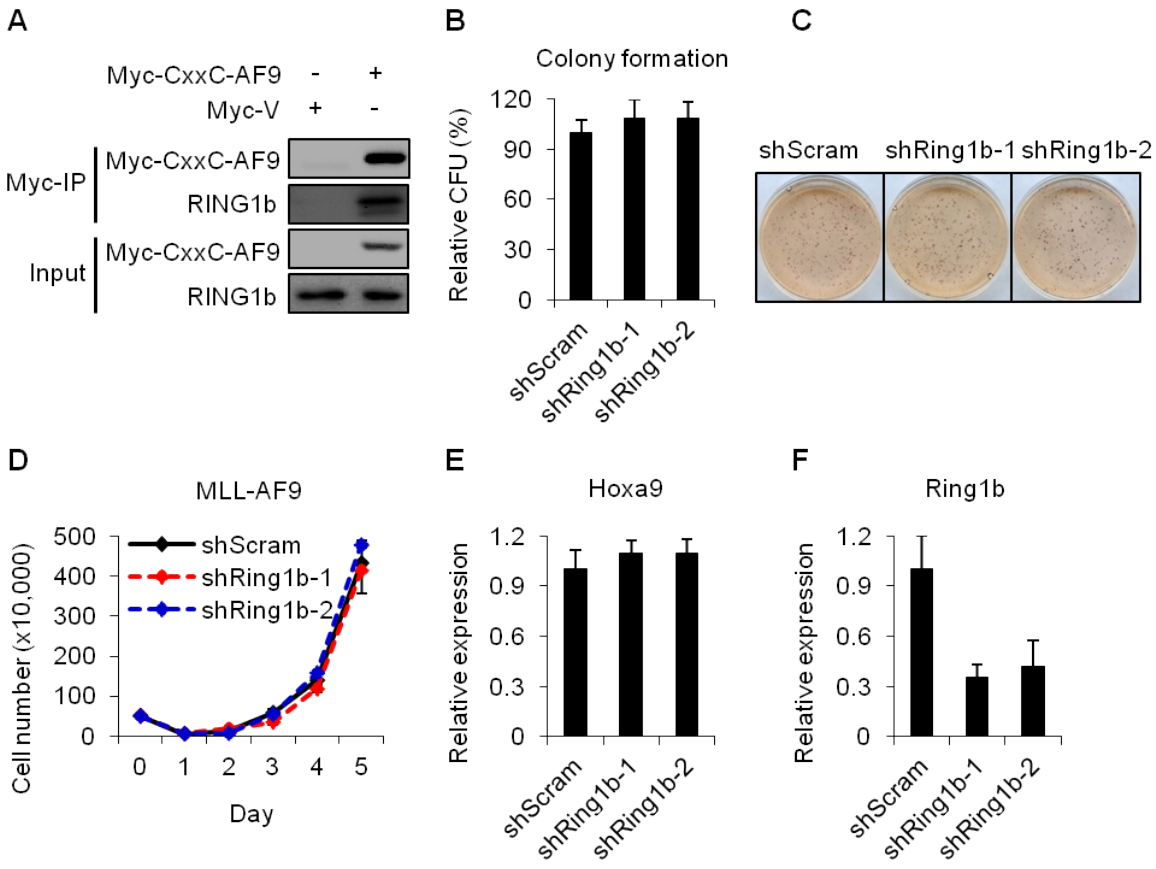

Figure 2.21 Ring1b Knockdown Does not Recapitulate the Effects of Cbx8 Knockdown on MLL-AF9 Leukemic Transformation (A) Co-immunoprecipitation of endogenous RING1b with Myc-CxxC-AF9 in 293 cells. A fraction (3%) of cell lysate was used for input control. (B) Relative CFU of MLL-AF9 leukemic cells with Ring1b knockdown by two individual shRing1b molecules, compared to the control (shScram). Error bars represent ± SD from three independent experiments. (C) Representative INT-stained colonies in methylcellulose. (D) Growth curve of MLL-AF9 leukemic cells with Ring1b knockdown, compared to the control. Error bars represent ± SD from a duplicate experiment. Results from one of three independent experiments are shown. (E) RT-PCR analysis of *Hoxa9* expression in MLL-AF9 leukemic cells with Ring1b knockdown, compared to the control. (F) RT-PCR analysis of *Ring1b* expression in MLL-AF9 leukemic cells, confirming the knockdown efficiency.

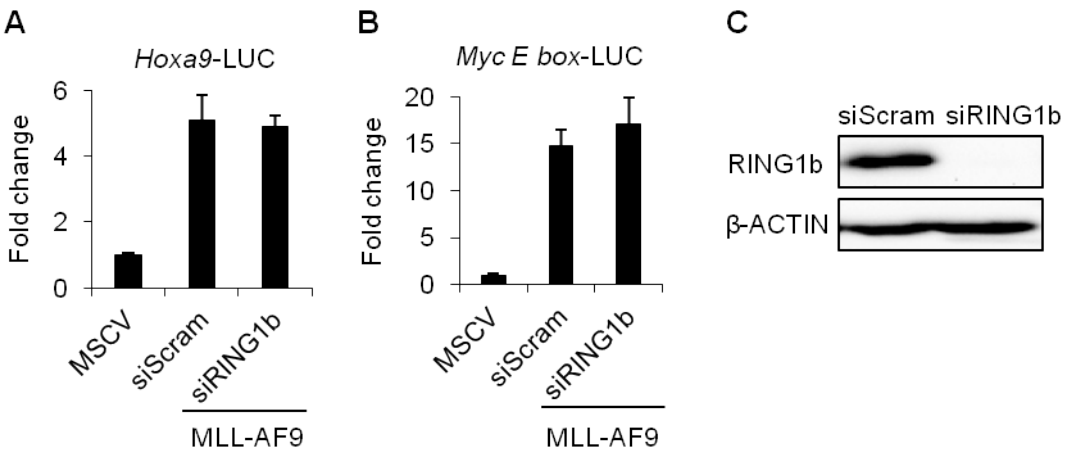

Figure 2.22 Ring1b Knockdown Does not Recapitulate the Effects of Cbx8 Knockdown on MLL-AF9-Induced Transactivation of the Target Promoters (A and B) Experiments were performed as described in Figures 2.19B and 2.19D, except using siRNAs specifically targeting RING1b (siRING1b) in place of siCBX8. Error bars represent ± SD from three independent experiments. (C) Western blot showing RING1b expression with siRING1b treatment, compared to the control (siScram).

promoter activity. Despite the marked reduction of RING1b expression shown by western-blot analysis, MLL-AF9-induced transactivation of the target promoters was not suppressed by RING1b knockdown (Figures 2.22A-2.22C). Similar to our observations with Ring1b, knockdown of Bmi1, another core PRC1 component, did not affect the transformation ability, growth rate or transcriptional activation in MLL-AF9 leukemic cells (Figures 2.23-2.24). Consistent with these observations, Cbx8 depletion in MLL-AF9-transformed BM cells did not affect the global levels of Ring1b and Bmi1, as shown by western-blot analysis (Figure 2.23A). Taken together, these findings suggest that Cbx8 functions as an MLL-AF9 cofactor to promote leukemogenesis in a PRC1-independent manner.

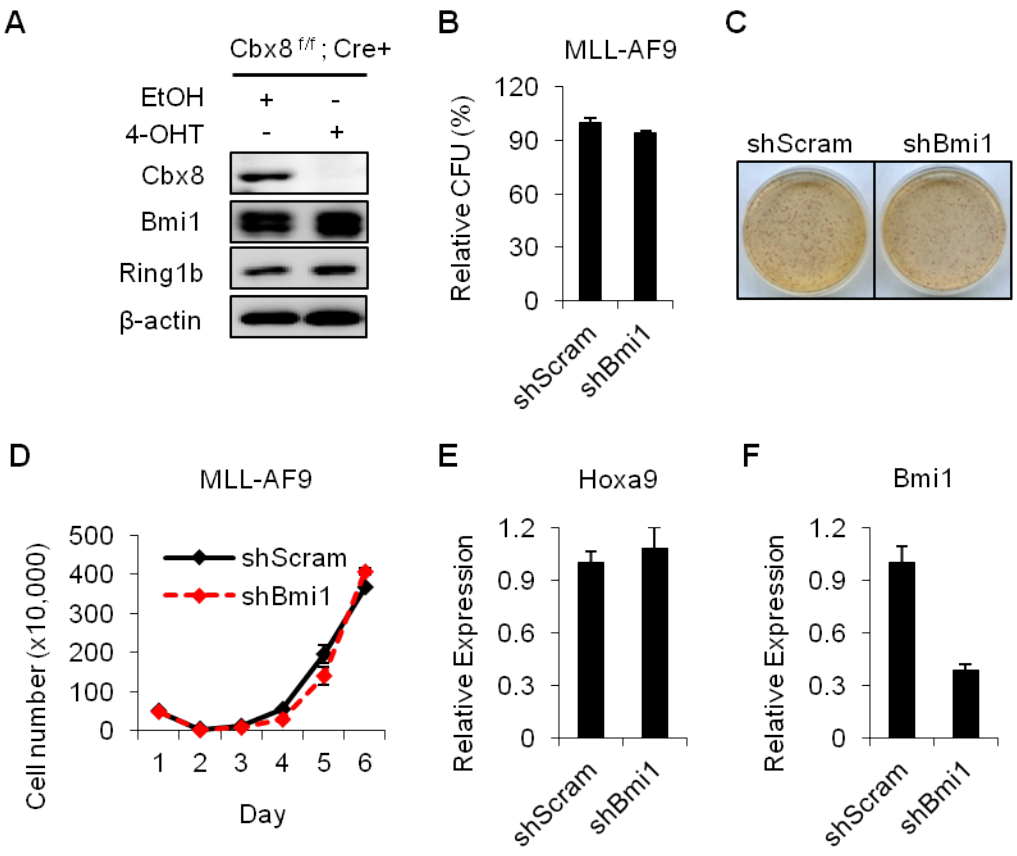

Figure 2.23 Bmi1 Knockdown Does not Recapitulate the Effects of Cbx8 Knockdown in MLL-AF9 Leukemic Transformation (A) Western blots showing the expression of Cbx8, Bmi1 and Ring1b in MLL-AF9-transformed cells from *Cbx8* $^{f/f}$; *Cre*$^{+}$ mice, with 4-OHT treatment compared to the control (EtOH). (B) Relative CFU of MLL-AF9 leukemic cells with Bmi1 knockdown by shBmi1 transduction, compared to the control. Error bars represent ± SD from three independent experiments. (C) Representative INT-stained colonies in methylcellulose. (D) Growth curve of MLL-AF9 leukemic cells with Bmi1 knockdown, compared to the control. Error bars represent ± SD from a duplicate experiment. Results from one of three independent experiments are shown. (E) RT-PCR analysis of *Hoxa9* expression in MLL-AF9 leukemic cells with Bmi1 knockdown, compared to the control. (F) RT-PCR analysis of *Bmi1* expression in MLL-AF9 leukemic cells, confirming the knockdown efficiency.

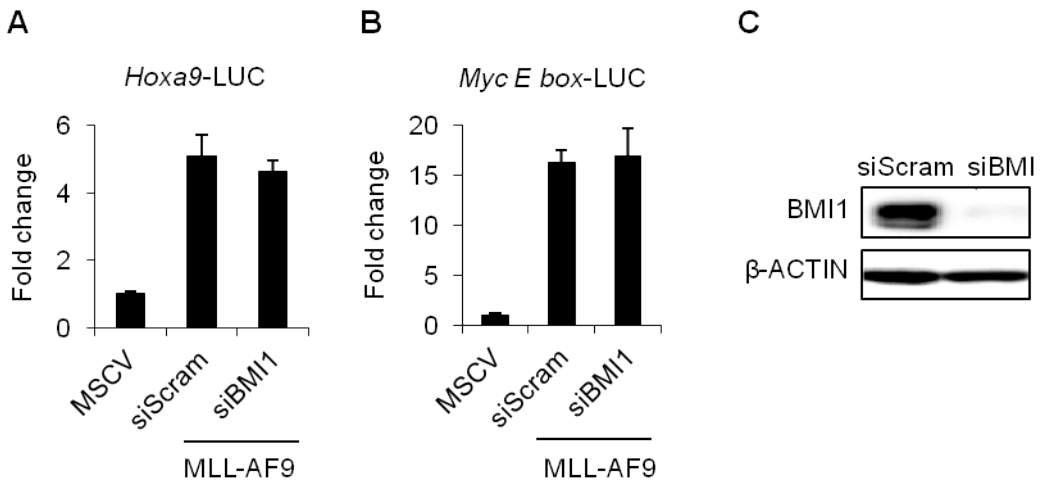

Figure 2.24 Bmi1 Knockdown Does not Recapitulate the Effects of Cbx8 Knockdown on MLL-AF9-Induced Transactivation of the Target Promoters (A and B) Experiments were performed as described in Figures 2.19B and 2.19D, except using siRNAs specifically targeting Bmi1 (siBmi1) instead of siRING1b. Error bars represent ± SD from three independent experiments. (C) Western blot showing BMI1 expression with siBMI1 treatment, compared to the control (siScram), using β-ACTIN as a loading control.

CBX8 Regulation of TIP60 Localization Contributes to MLL-AF9 Leukemic Transformation

The characterization of the PRC1 independence of Cbx8 functions in MLL-AF9 leukemic transformation prompted us to explore the possible involvement of other Cbx8 interacting proteins that may explain the role of Cbx8 in transcriptional activation. A previous study has reported that CBX8 directly interacts with the histone acetyltransferase (HAT) TIP60 by high-throughput yeast two-hybrid screens and mass spectroscopy analysis (Stelzl et al., 2005). However, this observation has not yet been verified in any mammalian cell

system; therefore, the functional implication of this interaction remains an open question. To first confirm this interaction, we transiently expressed FLAG-tagged CBX8 in 293 cells. Specific interaction between CBX8 and TIP60 was detected by IP experiments: using anti-FLAG antibody to pull down CBX8, we observed that CBX8 consistently coprecipitated with endogenous TIP60 in the presence of Benzonase, indicating CBX8 interacts with TIP60 in a DNA-independent manner (Figures 2.25A and 2.25A). This finding implied an intriguing possibility that CBX8 promotes MLL-AF9 leukemic transformation, at least partially through its interaction with the transcriptional coactivator TIP60. To test this hypothesis, we first assessed the impact of Tip60 on MLL-AF9 leukemic transformation by BMT assays. Using shRNA molecules specifically targeting *Tip60*, we observed a reduction in the colony formation ability of MLL-AF9 leukemic cells (Figures 2.25B, 2.25C and 2.25F). Moreover, Tip60 downregulation by shRNA led to a decrease in the growth rate and *Hoxa9* expression of MLL-AF9-transformed cells (Figures 2.25D and 2.25E). Similar results were obtained using a different shRNA pool, further supporting that Tip60 positively contributes to MLL-AF9 leukemic transformation (Figures 2.26B-2.26F).

To further characterize the role of Tip60 in MLL-AF9-induced transcriptional activation, we performed dual luciferase assays to examine the impact of TIP60 downregulation by siRNA on the MLL-AF9 target promoter activity. A significant reduction of TIP60 expression was confirmed by western-blot analysis (Figure 2.27D). As expected, the MLL-AF9-induced transcriptional activation of the target promoters was significantly suppressed by TIP60 knockdown (Figures 2.27A-

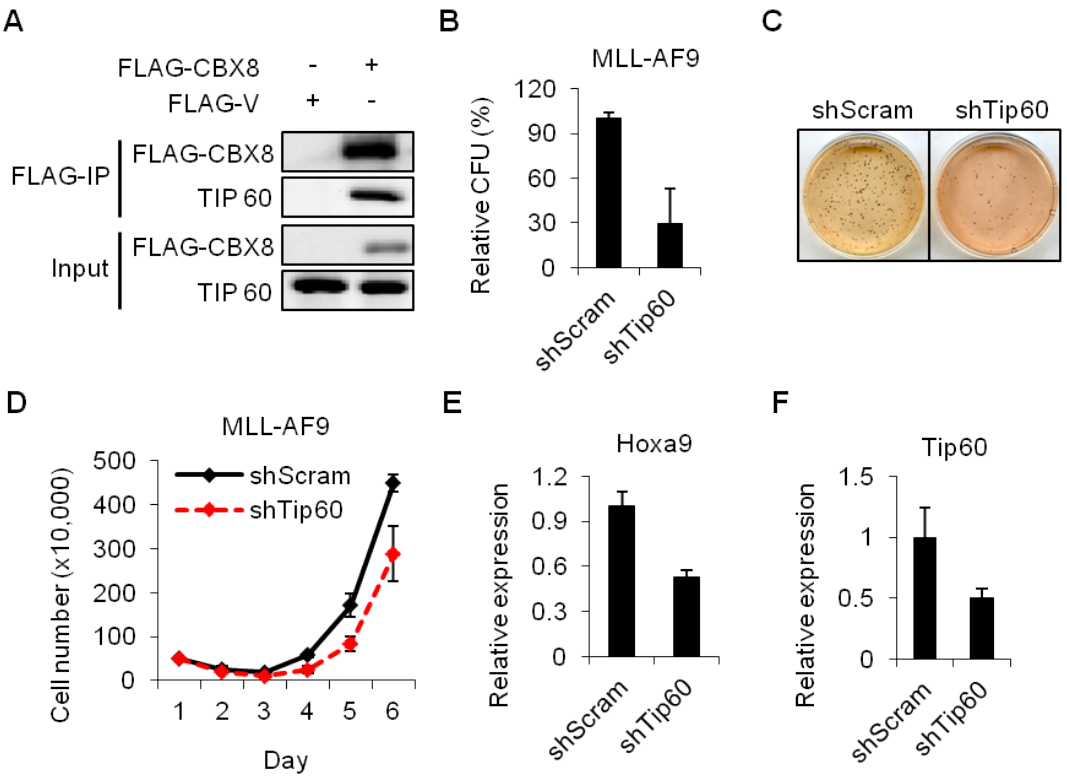

Figure 2.25 CBX8 Interacts with TIP60, Whose Downregulation Phenocopies the Effects of Cbx8 Knockdown on MLL-AF9 Leukemic Transformation (A) Co-immunoprecipitation of endogenous TIP60 with FLAG-CBX8 in 293 cells, after Benzonase treatment. A fraction (3%) of cell lysate was used for input control. (B) Relative CFU of MLL-AF9 leukemic cells with Tip60 knockdown by shRNA, compared to the control (shScram). Error bars represent ± SD from three independent experiments. (C) Representative INT-stained colonies in methylcellulose. (D) Growth curve of MLL-AF9 leukemic cells with Tip60 knockdown, compared to the control. Error bars represent ± SD from a duplicate experiment. Results from one of three independent experiments are shown. (E) RT-PCR analysis of *Hoxa9* expression in MLL-AF9 leukemic cells with Tip60 knockdown, compared to the control. (F) RT-PCR analysis of *Tip60* expression in MLL-AF9 leukemic cells, showing the knockdown efficiency.

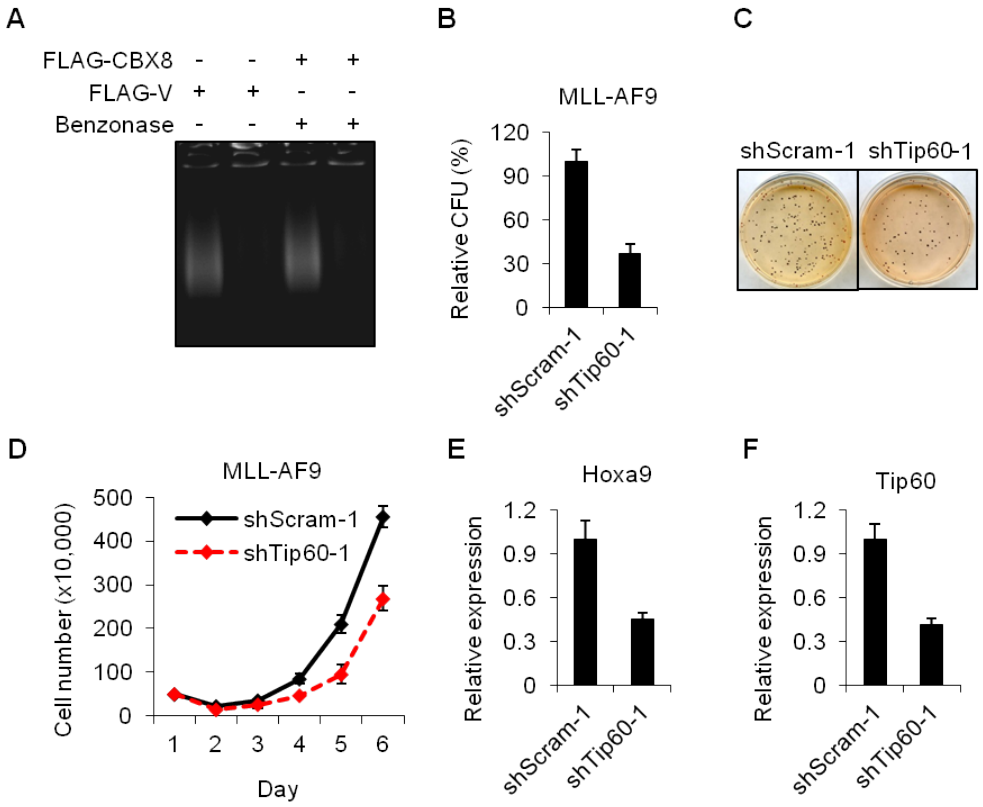

Figure 2.26 Tip60 Knockdown Phenocopies the Effects of Cbx8 Knockdown in MLL-AF9 Leukemic Transformation (A) Lysates from the experiment shown in Figure 2.25A were treated with Benzonase. Ethidium bromide staining of an agarose gel shows complete DNA digestion after Benzonase treatment. (B-F) Experiments were performed as described in Figures 2.25B-2.25F, using a separate shRNA set specifically targeting Tip60 (shTip60-1) compared to the control (shScram-1).

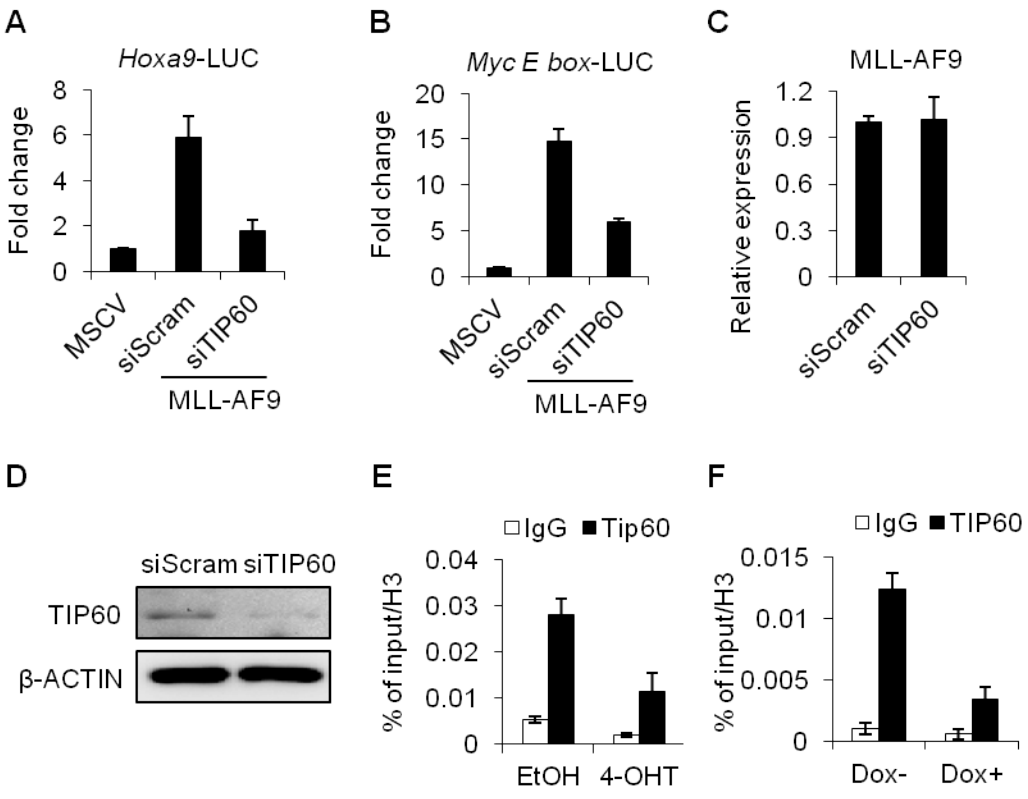

Figure 2.27 Cbx8 Affects Tip60 Binding, Whose Downregulation Phenocopies the Effects of Cbx8 Knockdown on MLL-AF9-Induced Transactivation of the Target Promoters (A and B) Experiments were performed as described in Figures 2.16B and 2.16D, except using siRNAs specifically targeting TIP60 (siTIP60) instead of siCBX8. Error bars represent ± SD from three independent experiments. (C) RT-qPCR analysis of MLL-AF9 expression in luciferase reporter assays, with siCBX8 treatment compared to the control (siScram). (D) Western blot analysis showing the TIP60 protein level in luciferase reporter assays with siTIP60 treatment, compared to the control (siScram), using β-ACTIN as a loading control. (E) Relative binding of Tip60 to the *Hoxa9* promoter in MLL-AF9-transformed cells from *Cbx8* $^{f/f}$; *Cre*$^{+}$ mice, with *Cbx8* excision induced by 4-OHT treatment compared to the control (EtOH). (F) Relative binding of TIP60 to the *HOXA9* promoter in TRIPZ-RFP-shCBX8-containing MM 6 cells, with CBX8 knockdown induced by doxycycline treatment compared to the control. Error bars represent ± SD from three independent experiments.

2.27C). Collectively, these data demonstrate that knocking down Tip60 phenocopies the effect of Cbx8 knockdown in MLL-AF9 leukemic cells, suggesting a functional significance of the CBX8/TIP60 interaction in MLL-AF9 leukemic transformation. To confirm the observed role of Tip60 is indeed associated to the CBX8/TIP60 interaction, we performed ChIP assays in MLL-AF9-transformed leukemic cells, following Cbx8 depletion by 4-OHT treatment. As expected, Cbx8 depletion resulted in decreased Tip60 binding at the *Hoxa9* promoter (Figure 2.27E). Similar findings were seen using MLL-AF9-transformed cell lines, MM6, engineered for inducible knockdown of CBX8. In these cells, TIP60 binding at the *Hoxa9* promoter was significantly reduced upon CBX8 downregulation induced by doxycycline treatment (Figure 2.27F). Together, our results suggest that CBX8 affects TIP60 binding, which plays a positive role in MLL-AF9 leukemic transformation.

Cbx8 Is not Required for Normal Hematopoiesis

The profound impact of Cbx8 on MLL-AF9 leukemogenesis prompted us to examine the role of Cbx8 in normal hematopoiesis. We examined the effect of Cbx8 depletion during steady-state hematopoiesis in vivo. Constitutive depletion of Cbx8 showed no aberrant phenotype, and deletion of Cbx8 by 4-OHT treatment in adult animals had no detectable effect on any measured peripheral blood population as measured by complete blood count (CBC) analysis (Figure 2.28). Moreover, both the cellularity of major hematopoietic organs (BM, spleen and thymus) and the cell number of mature hematopoietic populations as defined by flow cytometry were similar between Cbx8-deficient

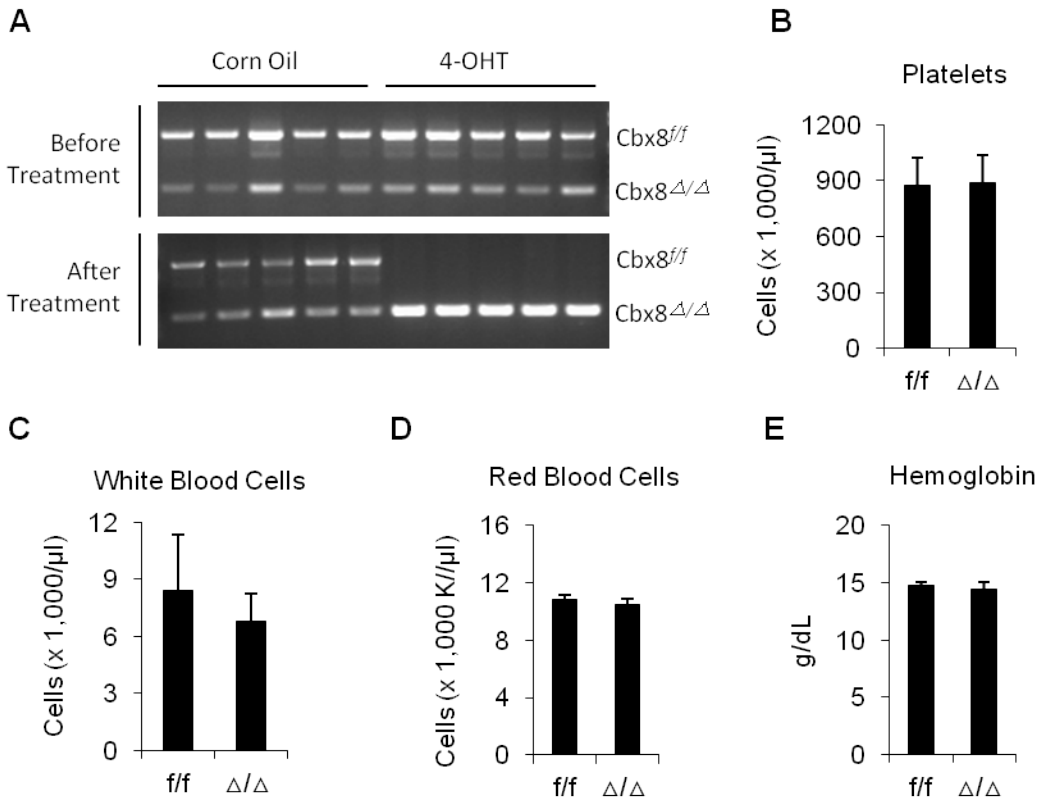

Figure 2.28 Cbx8-Depleted Mice Shows No Abnormality in the CBC Analysis of Peripheral Blood (A) Ethidium bromide-stained agarose gel showing the 4-OHT-induced excision of the floxed *Cbx8*. At the starting and end points of the experiment, peripheral blood from *Cbx8* $^{f/f}$; *Cre*$^{+}$ mice treated with 4-OHT or corn oil as a control was collected, from which genomic DNA was extracted and subjected to PCR analysis. (B-E) Peripheral blood CBC analysis of (B) platelets, (C) white blood cells, (D) red blood cells, and (E) hemoglobin content of *Cbx8* floxed (f/f) and deleted (Δ/Δ) mice.

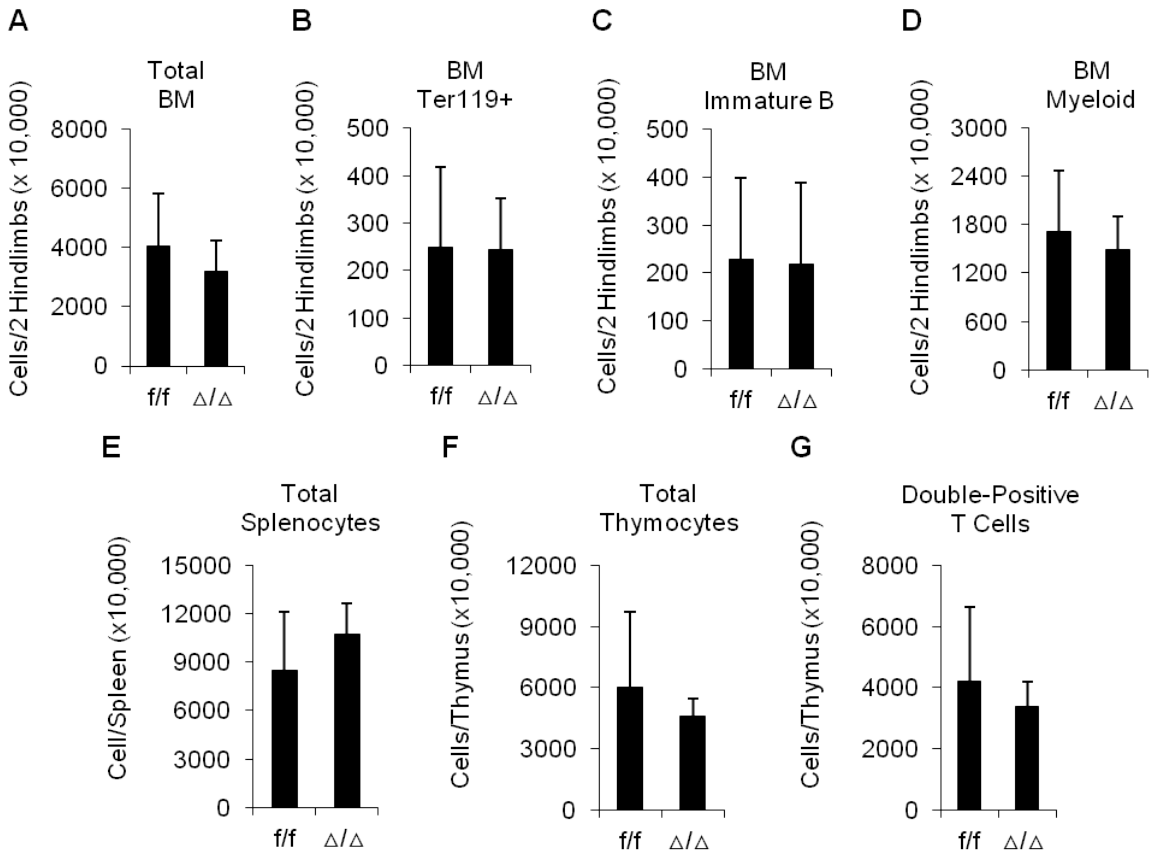

Figure 2.29 Cbx8-Depleted Mice Shows Normality Cellularity of Major Hematopoietic Organs and Mature Hematopoietic Populations (A-D) Absolute quantification of total bone marrow cellularity (A), erythroid cells (Ter119+; B), developing B lymphocytes (AA4.1+CD19+B220+; C), and myeloid cells (CD11b+Gr1+; D) from *Cbx8* $^{f/f}$ and *Cbx8* $^{\Delta/\Delta}$, analyzed by flow cytometry (bars represent mean + SD; n=5 mice/genotype). (C-E) Absolute quantification of total splenocytes (C), thymocytes (D), double-positive T cells (CD4+CD8+; E) analyzed by flow cytometry revealed no significant difference between *Cbx8* floxed (f/f) and deleted (Δ/Δ) mice (bars represent mean + SD; n=5 mice/genotype).

mice and controls (Figure 2.29). To address potential effects of Cbx8 deletion on primitive long-term hematopoietic stem cells (LT-HSCs), we combined flow cytometry for characterization of progenitor populations and competitive BM transplantation assays. These analyses revealed no detectable differences in LT-HSC numbers (Figure 2.30) or hematopoietic reconstitution ability of Cbx8 WT or deficient BM in lethally irradiated recipients (Figure 2.31A). In addition, the total progenitor output from the BM of Cbx8-deficient animals was similar to controls, as measure by colony forming unit assays (Figures 2.31B and 2.31C). Together, these findings indicate that Cbx8 is not required for steady state hematopoiesis, LT-HSC maintenance, or stem and progenitor cell function.

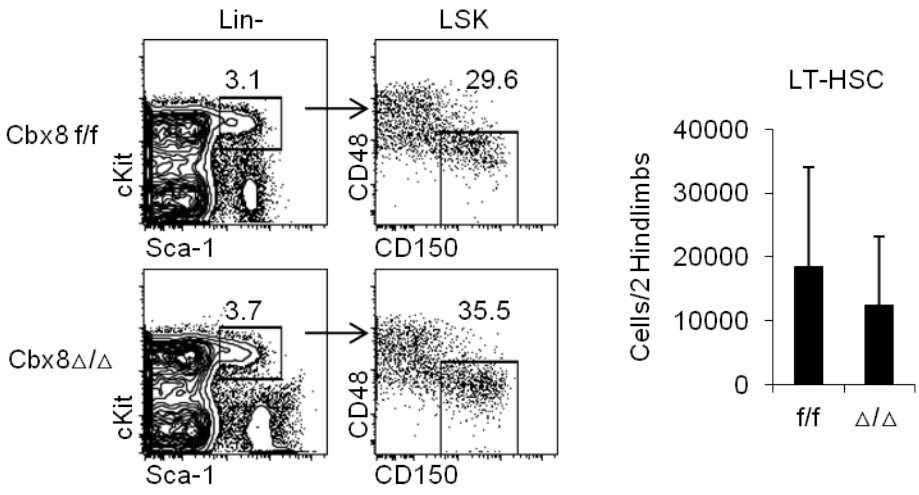

Figure 2.30 Cbx8-Depleted Mice Shows No Abnormality in Maintaining the Primitive Long-Term Hematopoietic Stem Cell (LT-HSC) Population. Flow cytometric analysis of LT-HSCs (CD150+CD48-LSK) from *Cbx8* $^{f/f}$ and *Cbx8* $^{\Delta/\Delta}$ mice (bars represent mean + SD; n=5 mice/genotype).

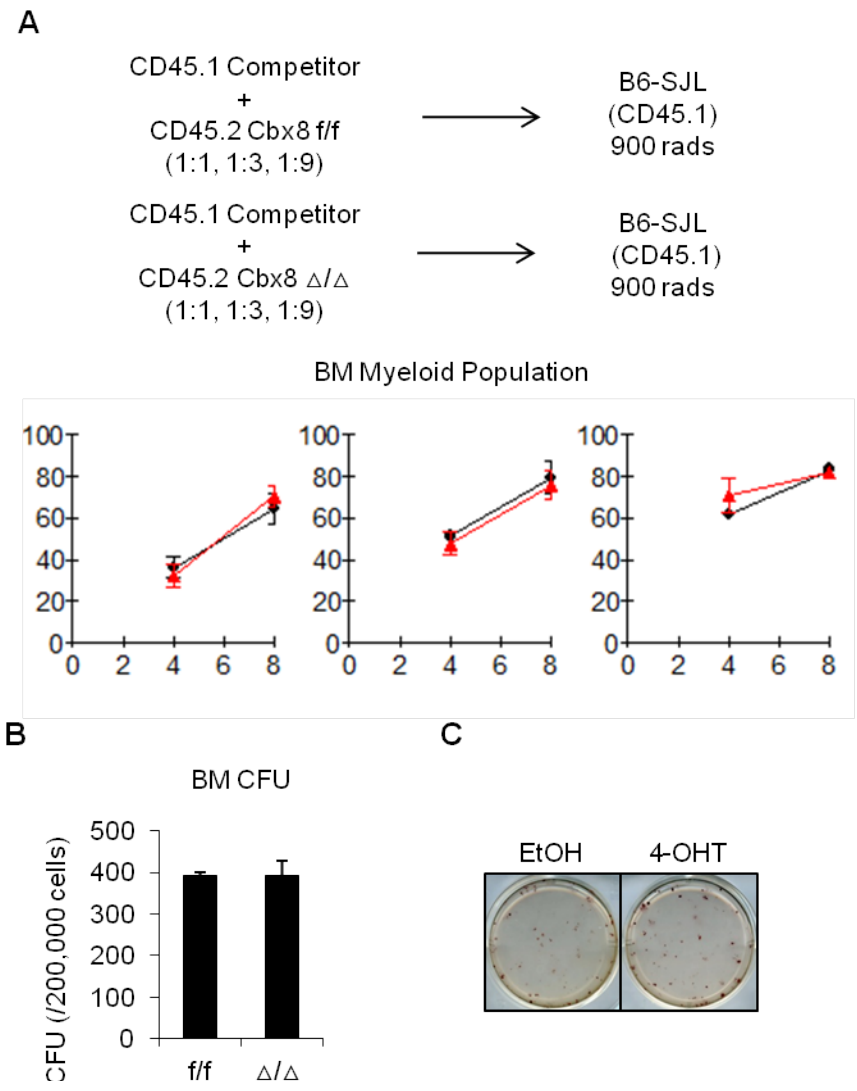

Figure 2.31 Cbx8-Depleted Mice Shows Normal Stem and Progenitor Cell Function
(A) Competitive BM transplantation at competitor: tester ratios of 1:1 (n=10/group), 1:3 (n=5 mice per group), and 1:9 (n=5 mice per group). No difference between *Cbx8* $^{f/f}$ and *Cbx8* $^{\Delta/\Delta}$ mice was observed in tester contribution to myeloid reconstitution at any ratio (data represent mean ± SD). (B) Colony forming assays using BM from *Cbx8* $^{f/f}$ and *Cbx8* $^{\Delta/\Delta}$ mice. The data included 4 independent experiments per genotype (bars represent mean + SD; n=3 plate/experiment). (C) Representative INT-stained CFU in methylcellulose.

DISCUSSION

Working Model of Cbx8-Dependent MLL-AF9 Leukemogenesis

In this study, we investigated the role of CBX8 in MLL-AF9-induced leukemogenesis. We have uncovered a novel mechanism involving the HAT TIP60 that contributes to MLL-AF9 transcriptional activation and transformation but appears dispensable for normal hematopoiesis therefore establishing CBX8 as an essential cofactor required for MLL-AF9-induced transcriptional activation and leukemic transformation (Figure 2.32).

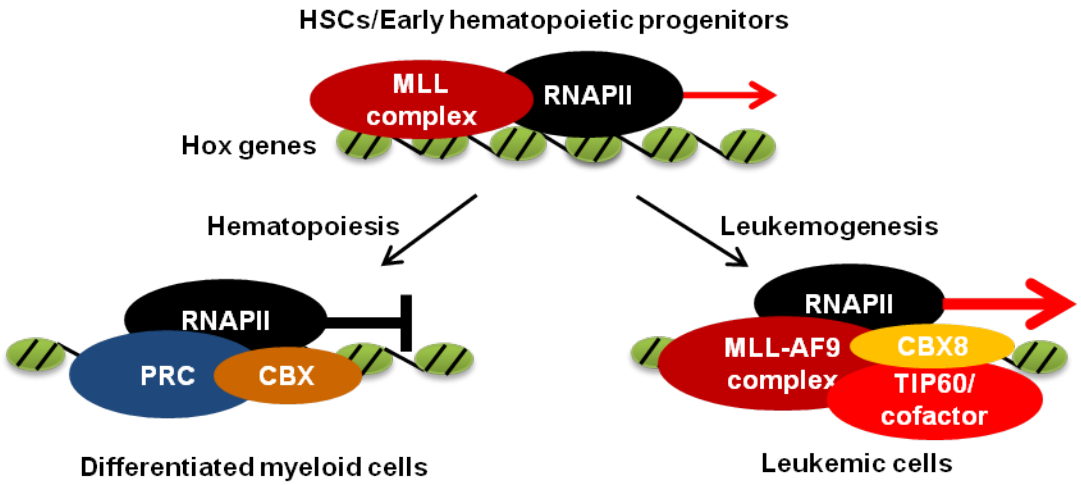

Figure 2.32 Schematic Model Illustrating Role of CBX8 in Promoting MLL-AF9-Induced Leukemogenesis Top: recruitment of WT MLL is required for transcriptional regulation of *Hox* gene expression in HSCs and early progenitor cells. Left: During normal hematopoiesis, *Hox* gene expression decreases due to the transcriptional repression of Polycomb Group proteins. Right: In MLL-AF9 leukemic cells, CBX8 interacts with MLL-AF9 at the target gene loci and functions as a crucial cofactor regulating the localization of TIP60, facilitating target transcriptional activation, thereby promoting leukemogenesis.

Potential Broad Role of CBX8 in MLL-Rearranged Leukemogenesis

CBX8 is one of the five human homologs of the *Drosophila* Pc protein. Although all CBX proteins share highly conserved chromodomains and Pc boxes, their different sizes and the presence of other motifs suggest potentially different functions (Whitcomb et al., 2007). Indeed, previous studies have reported that mice deficient for different PRC1 components show only a partial overlap in phenotype, raising the possibility of PRC1-independent functions of these components that may be context dependent and involve other protein complexes (de Napoles et al., 2004; Katoh-Fukui et al., 1998; Leeb and Wutz, 2007; Suzuki et al., 2002; Voncken et al., 2003). Our study has uncovered such a PRC1-independent function of CBX8 in MLL-AF9-induced transcriptional regulation. Interestingly, contrary to its role as a transcriptional repressor in PRC1, CBX8 serves as a transcriptional coactivator in the MLL-AF9 complex. Furthermore, CBX8 is present in the EAP (or the related AEP and the Dotcom) transcriptional activation complex (Mohan et al., 2010b; Monroe et al., 2010; Yokoyama et al., 2010), and our data show that it is also required for the leukemic transformation induced by MLL-ENL, another EAP-interacting MLL fusion protein, suggesting that the CBX8-dependent leukemogenic mechanism may apply to not only MLL-AF9 but also other MLL fusion proteins whose fusion partners are present in the EAP complex.

The drastic effect of Cbx8 deletion on leukemogenic capacity of MLL-AF9 and MLL-ENL prompted us to ask whether this “Cbx8 addition” is further adopted by the MLL fusion proteins with translocation partners absent in the EAP complex,

such as MLL-GAS7. BMT assays in the Cbx8 conditional knockout system was again used to address this question. Interestingly, an intermediate phenotype was observed in this case. To be more specific, we observed a decrease in the colony numbers with both pre-transformation excision and post-transformation *Cbx8* excision (Figure 2.33). However, there were still compact colonies growing out upon Cbx8 depletion, which was significantly different from the phenotype in the case of MLL-AF9 and MLL-ENL.

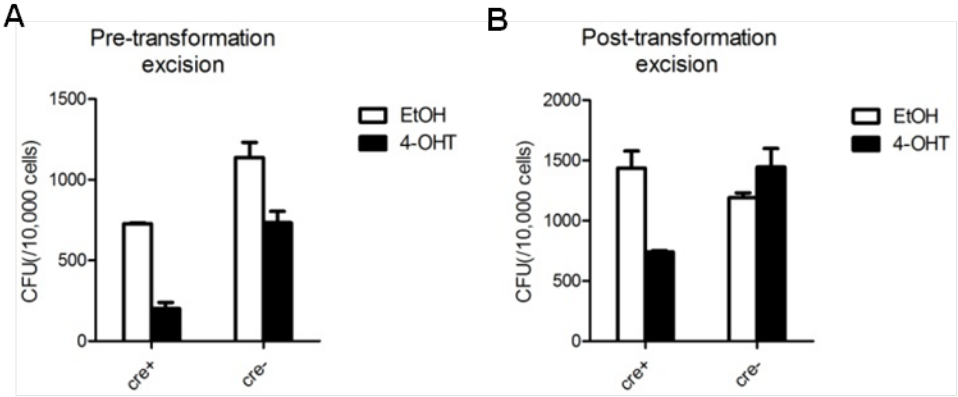

Figure 2.33 Effect of Cbx8 Deletion on Leukemogenic Transformation Induced by MLL-GAS7 (A and B) Relative CFU of MLL-ENL-transduced cells in the two experimental settings. Error bars represent ± SD from two independent experiments. Each experiment was performed in duplicate.

Because it has been known that the *in vivo* leukemogenesis ability of MLL-GAS7 is not as potent as MLL-AF9 in mouse models, it is technically difficult to vigorously elucidate the significance of this intermediate effect *in vivo*. At this point, we do not have a clear mechanistic explanation for this finding. Further

detailed studies are certainly required to fully understand this phenotype. Although it would be premature to draw a definitive conclusion regarding the role of Cbx8 in MLL-GAS7 leukemogenesis based on the current findings, our observation does imply a broader role of CBX8 in MLL-rearranged leukemogenesis, of which the potential differential mechanisms warrant further exploration.

PRC1-Independent CBX8 Addition of MLL-AF9

A significant body of work has suggested the involvement of PRC1 components in regulating hematopoietic function and hematopoietic malignancies (Bracken and Helin, 2009; Martin-Perez et al., 2010; Mills, 2010). Especially, a key component of CBX8-containing PRC1 complex, BMI1, is shown to be important for normal and leukemic hematopoietic stem cells, in part by repressing the INK4a/ARF pathway (Schuringa and Vellenga, 2010). However, consistent with our observations, a recent study showed that Bmi1 is not required for MLL-AF9-induced leukemogenesis (Smith et al., 2011), which, together with our findings, further supports the conclusion that the requirement of CBX8 for MLL-AF9 leukemogenesis is independent of PRC1. Given the finding that CBX8 is involved in the *INK4a/ARF* transcriptional repression by PRC1 in fibroblasts (Dietrich et al., 2007), it is critical to address whether this mechanism is involved in the CBX8 addition of MLL-AF9 leukemic cells shown in our data. We therefore examined the impact of Cbx8 on *INK4a/ARF* expression by RT-PCR in MLL-AF9 leukemic cells. We found neither Cbx8 downregulation/depletion nor Tip60 downregulation

led to *INK4a/ARF* activation (Figure 2.34), confirming that the CBX8-dependent MLL-AF9 transformation is not due to *INK4a/ARF* repression.

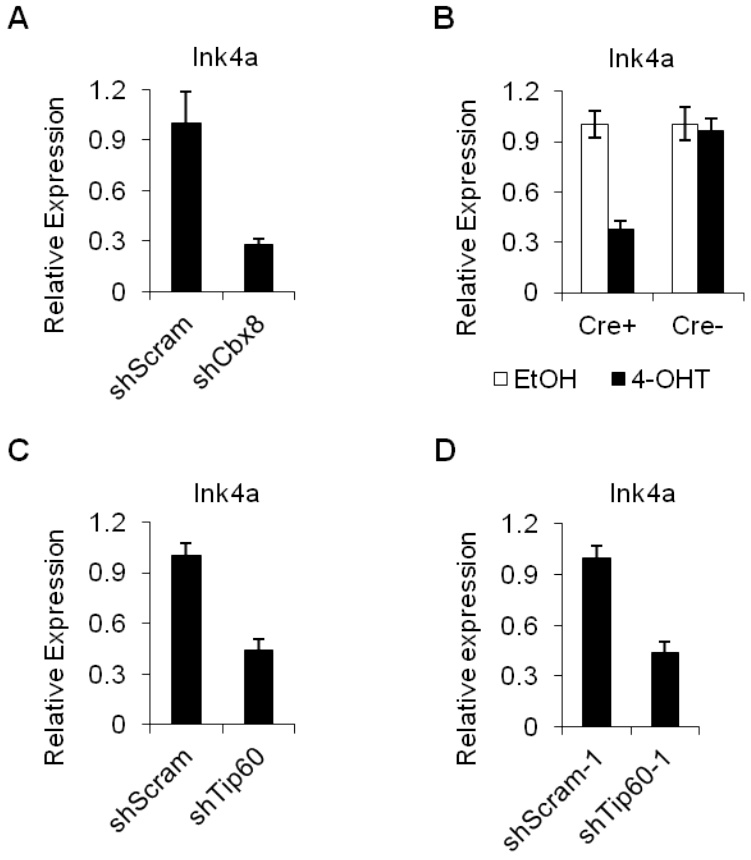

Figure 2.34 *Ink4a/Arf* Expression Is not Activated upon Cbx8 Downregulation or Depletion or upon Tip60 Downregulation (A) RT-PCR analysis of *Ink4a/Arf* expression in MLL-AF9-transformed leukemic cells with shCbx8 transduction compared to the control (shScram). (B) RT-PCR analysis of *Ink4a/Arf* expression in MLL-AF9-transformed leukemic cells from *Cbx8* $^{f/f}$; *Cre*$^{+}$ and *Cbx8* $^{f/f}$; *Cre*$^{-}$ mice, with 4-OHT treatment compared to the control (EtOH). (C and D) RT-PCR analysis of *Ink4a/Arf* expression in MLL-AF9-transformed leukemic cells with Tip60 knockdown by two separate shRNA sets (described in Figures 2.25 and 2.26), compared to the respective control.

TIP60 as the First HAT Associated with the MLL-AF9 Complex

In addition to the MLL fusion partners, CBX8 has previously been shown to directly interact with the HAT TIP60, a core member of the MYST family (Stelzl et al., 2005). Several TrxG complexes are known to recruit HATs during normal development. For example, another core member of the MYST family, MOF (MYST1), has been purified in WT MLL complex, and the HAT CREB-binding protein (CBP) is known to interacts with both MLL and another TrxG protein ASH1 (Bantignies et al., 2000; Dou et al., 2005; Ernst et al., 2001; Petruk et al., 2001). Under normal physiological conditions, HATs function as a coactivator to facilitate TrxG-induced transcriptional activation, antagonizing the transcriptional repressive effect of the PcG complex (Mills, 2010; Pasini et al., 2010). This mechanism contributes to the active *HOXA9* expression in hematopoietic stem cells and early progenitors (Figure 2.32). In addition, another two MYST proteins, MOZ (MYST3) and MORF (MYST4), are directly involved in chromosomal translocations in AML to form chimeric fusion proteins with CBP and/or p300 that lead to leukemogenesis (Katsumoto et al., 2008; So and van der Reijden, 2008). Moreover, MLL is fused to CBP or P300 in a subset of acute leukemias (Wang et al., 2005). Together, multiple lines of evidence have established the critical cooperation between MLL physiological function and HAT activity and the pro-oncogenic role of certain MYST family members in human myeloid leukemias. However, previous studies have not reported HATs as a component of the EAP complex, which is recruited by the most common MLL fusion partners. Therefore, whether HATs contribute to transcriptional activation induced by common MLL-

rearranged oncoproteins remains unknown. Our finding of the CBX8-dependent TIP60 localization at the *HOXA9* promoter indicates that this transcriptional activation mechanism is likely to be adopted by common MLL fusion proteins to activate target gene expression, such as *HOXA9*. Interestingly, a previous RNAi screening study in mouse embryonic stem cells (ESCs) has reported that Tip60 is required for pluripotency, while MLL myeloid leukemia stem cells have been shown to share the transcriptional program with ESCs, rather than adult stem cells (Fazzio et al., 2008; Somervaille et al., 2009). Together, these observations suggest a possible functional association between the TIP60-regulated signaling network and the transcriptional program in MLL-rearranged leukemic cells, therefore further supporting our model that CBX8 is essential for MLL-AF9-induced oncogenic transformation, likely through its interaction with TIP60 at the target gene loci to help establish the transcriptional program required for leukemogenesis (Figure 2.32). Furthermore, this study, together with previous findings, reveals an intriguing mechanistic similarity between WT MLL and oncogenic MLL fusion proteins. Specifically, the synergistic activity between HMT (H3K4me3) and HAT in transcriptional activation by WT MLL is dependent on the C-terminal SET domain, which is absent in MLL fusion proteins as a result of translocations. However, oncogenic MLL fusion proteins regain this classic combination of enzymatic activities by recruiting another HMT that facilitates gene transcription, DOT1L (Bernt et al., 2011; Jo et al., 2011; Nguyen et al., 2011), and an HAT with a high structural similarity of MOF, TIP60 (Figure 2.35), thereby nicely reinforcing the concept of cancer cells hijacking the regulatory

mechanisms of normal physiological functions, which have been proven efficient by their evolutionary conservation, and redirecting them to oncogenesis.

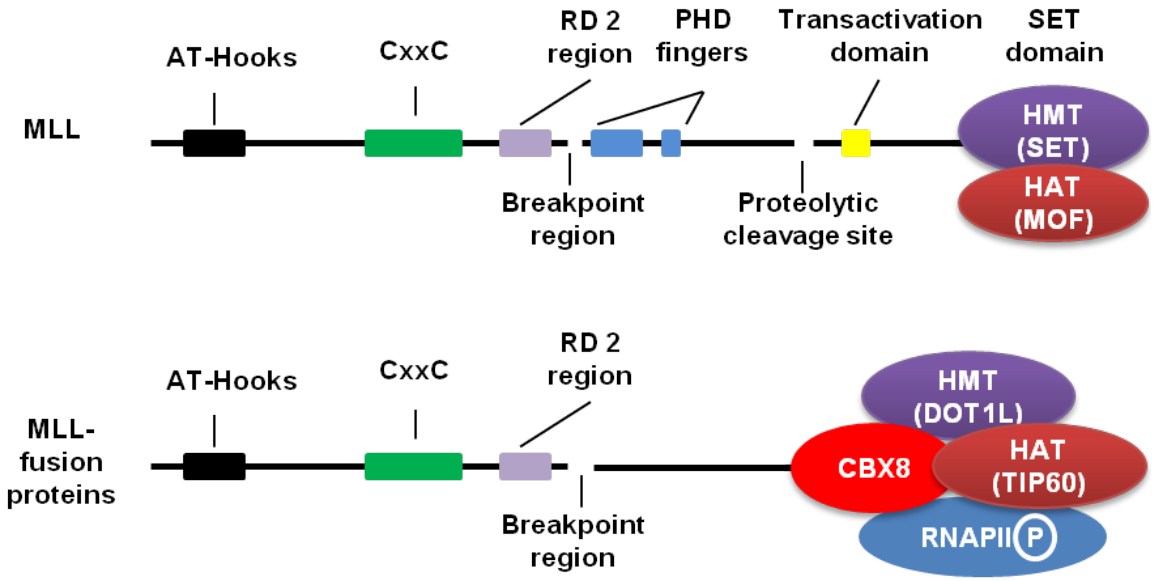

Figure 2.35 Comparison of the Key Enzymatic Components between Wild-Type MLL and Common MLL-Fusion Proteins.

Therapeutic Implications

Our identification of the critical role of the CBX8/MLL-AF9 interaction in leukemogenesis is of particular therapeutic values, in part because of the striking observations that the complete loss of *Cbx8* in mice showed no apparent effect on viability or hematopoiesis, and that *Cbx8*$^{-/-}$ BM cells exhibits no apparent disadvantage in hematopoietic reconstitution, compared to WT cells. These findings suggest an attractive therapeutic window for targeting CBX8 to treat MLL-rearranged leukemias. More specifically, developing small molecule

inhibitors disrupting the CBX8/AF9 interaction may be a particular promising approach. Moreover, the characterization of the CBX8/TIP60 interaction and its contribution in MLL-AF9 leukemogenesis suggests that it may be worthwhile to explore the therapeutic potential of targeting this interaction. Notably, although development and reproduction of Tip60 wild-type and heterozygous mice were normal, homozygous ablation of the Tip60 gene caused embryonic lethality near the blastocyst stage of development in mice (Hu et al., 2009). Given the broad involvement of TIP60 in multiple important biological processes, directly targeting TIP60 may raise the issue of toxicity, in which case careful assessment is certainly required to evaluate the possible side effects. Nonetheless, the essentially null phenotype of Cbx8 knockout mice suggests that this interaction is unlikely to be critical for the major function of TIP60. Therefore, specific disruption of the CBX8/TIP60 interaction might still be an interesting angle for tackling MLL-rearranged leukemias.

Remaining Questions

Several important questions remain to be addressed for both better understanding the biology of MLL-rearranged leukemias and further exploring the clinical application potential of our current findings. First and foremost, it is not yet known which domains or regions in CBX8 are responsible for its role in MLL-AF9-induced leukemogenesis. To address this question, two directions are worth exploring. On the one hand, mapping the critical domains, or amino acids, of CBX8 that are important for CBX8/AF9 and CBX8/TIP60 interactions is of prior importance. A previous study has indicated that Cbx8 binds AF9 within a region

of approximately 130 amino acids that is not conserved in other Polycomb proteins (Hemenway et al., 2001). However, this region is obviously too broad for therapeutic targeting. Generating CBX8 mutants containing small fragment deletions and point mutations in this region may narrow down the interest to a limited region that is suitable for the binding of small molecule inhibitors. Additionally, single amino acid substitution analyses may reveal the key amino acids required for the CBX8/AF9 interaction. Small peptides containing the corresponding sequences may be used to design dominant negative inhibitors. Similar strategies can also be applied to identify the key element of CBX8 for the CBX8/TIP60 interaction. On the other hand, characterizing the role of the CBX8 chromodomain in this particular case is of significant value. Chromodomains are present in many chromatin regulatory proteins and are thought to mediate interaction with methylated histone lysines or RNA molecules (Akhtar et al., 2000; Sapountzi et al., 2006; Utley and Cote, 2003). The chromodomains of Pc proteins are thought to, at least in part, localize the proteins and their respective complexes to appropriately marked sites of the epigenome through reorganization of either H3K9me3 or H3K27me3, both of which indicate transcriptional repression (Kaustov et al., 2011). However, despite the high degree of conservation among the Pc protein chromodomains, previous studies have shown that they display significant differences in histone peptide binding preferences (Bernstein et al., 2006; Kaustov et al., 2011). Specifically, the CBX8 chromodomain has been shown to display essentially no binding preference to either H3K9me3 or H3K27me3, and alternative non-histone sequences are

suggested as potential binding targets for this chromodomain (Bernstein et al., 2006; Kaustov et al., 2011). Therefore, it is intriguing to test whether the CBX8 chromodomain represents a diverged evolutionary direction of Pc chromodomains, which is opposite of their traditional transcription repression role. Most importantly, the structure of the CBX8 chromodomain has been well-characterized, including the potential peptide binding pocket (Kaustov et al., 2011), which has laid a solid foundation for potential small molecule inhibitor development.

Second, based on our findings so far, it is not yet clear what are the exact molecular events responsible for the contribution of TIP60 in MLL-AF9-induced leukemogenesis. On one hand, the specificity of the CBX8-affected TIP60 binding in MLL-AF9 leukemic cells warrants further investigation. For instance, ChIP-seq analysis of the binding pattern of Tip60 in the genome of MLL-AF9 leukemic cells, particularly at MLL-AF9 target loci, in the presence or absence of Cbx8, will be helpful to better understand that, to what extent, Cbx8 may affect the binding of Tip60. This information will be important for further investigation on whether TIP60 may contribute to MLL-AF9 leukemogenesis through both CBX8-dependent and CBX8-independent mechanisms.

On the other hand, it will be useful to identify the critical region of TIP60 required for the CBX8/TIP60 interaction using the mutagenesis approach previously mentioned. Interestingly, TIP60 also contains a chromodomain, and it may have yet unidentified functions other than the traditionally characterized interaction with histone or RNA molecules (Akhtar et al., 2000; Sapountzi et al., 2006; Utley

and Cote, 2003). Apart from the chromodomain, TIP60 contains an MYST domain that is highly conserved among MYST family members. It will also be important to define the role of this particular domain in the CBX8/TIP60 interaction because it may shed light on the possibility of specific targeting this interaction. In addition to defining the functional domains, identifying the downstream events of TIP60 recruitment to the target gene loci is also critical for revealing its exact role in MLL-AF9 leukemogenesis. Several potential mechanisms may account for this role. (1) TIP60 recruitment may facilitate histone acetylation at MLL-AF9 target gene loci, loosing up the chromatin structure, thereby promoting transcriptional activation. (2) Given the broad spectrum of substrates of TIP60-mediated acetylation, it is possible that TIP60 acetylates other components of the MLL-AF9 complex to activate their function, which contributes to the activation of the whole complex and induces leukemogenesis. However, this possible leukemogenic mechanism relies on a prerequisite that at least one of the transcription co-activators in the ML-AF9 complex is regulated by acetylation-dependent activation, whereas none of these co-factors have been previously identified as the substrates of TIP60 acetyltransferase activity. Therefore, much work is still required to directly address this potential mechanism. (3) Proteomic studies of the acetylome in human cells indicate that proteins involved in chromatin biology are frequent targets of acetylation, including histone modifiers and subunits of ATP-dependent chromatin remodelers (Choudhary et al., 2009; Sapountzi and Cote, 2011). In fact, TIP60 itself, together with several TIP60-interacting partners, has been

shown to be acetylated *in vivo* (Choudhary et al., 2009; Kim et al., 2006), raising the possibility of autoacetylation as a potential mechanism of autoregulation. Indeed, a recent report has shown that TIP60 is autoacetylated on lysines, and that this modification autoregulates its histone acetylation activity (Wang and Chen, 2010). It is not yet known whether this autoregulation plays a role in the MLL-AF9 complex. The answer to this question will be helpful for fully deciphering the enzymatic activities required for MLL-AF9-induced transcriptional activation.

Third, it is of both mechanistic and therapeutic values to explore the specificity of TIP60 requirement for MLL-AF9 leukemogenesis. To this end, we knocked down the Tip60 expression by shRNA in E2A-HLF leukemic cells, and observed no significant changes in colony formation capacity of these cells, therefore suggesting at least some extend of specificity of the TIP60 function in the context of MLL-AF9 fusion protein (Figure 2.36). It is worth mentioning that we do not consider these data to be sufficient for arguing the same significance of TIP60 as that of CBX8, in part because of the moderate knockdown efficiency. Nevertheless, further detailed characterization in a Tip60 conditional knockout mouse model is warranted to better address this question in a clean genetic background.

Fourth, our results indicate that there may be at least two CBX8-associated complexes, a CBX8-containing PRC1 and a CBX8-TIP60-containing complex, with opposing functions on transcriptional regulation. The PRC1 complex has been well studied, whereas extensive biochemical analysis is still required to

characterize the composition of the latter in order to fully understand its activity. Furthermore, the kinetics assessment of the dynamics between these two complexes in the presence of MLL fusion proteins may provide valuable information for determining the protein-protein interaction for therapeutic targeting.

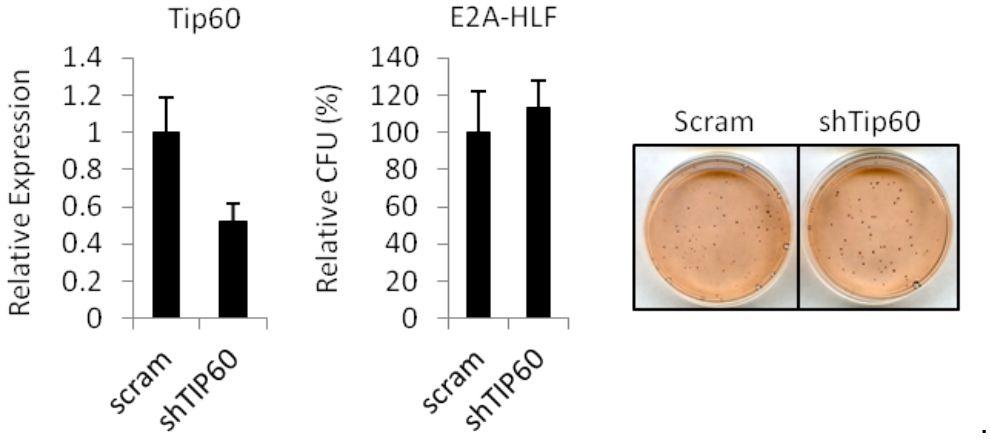

Figure 2.36 Knockdown of Tip60 Does not Affect the Transformation of E2A-HLF Leukemic Cells (Left) RT-qPCR showing the Tip60 knockdown efficiency in E2A-HLF leukemic cell line with shTip60 transduction compared to the control (Scram). Error bars represent ± SD. (Middle) Relative CFU of E2A-HLF leukemic cells transduced with shTip60, compared to the control (Scram). Error bars represent ± SD. (Right) INT-stained colonies form shTip60-transduced E2A-HLF cells, compared to the control (Scram).

Last but not least, our data demonstrate that CBX8 is necessary for MLL-AF9 leukemogenesis, despite that it does not seem to affect the localization of MLL-AF9 to its target gene loci or to be required for the recruitment of the EAP complex. This result suggests that additional key activity for MLL-AF9-induced

transcriptional activation is yet to be identified. Although our finding regarding TIP60 suggests that acetylation activity may be part of the answer, it does not rule out the possibility that in addition to TIP60, other co-factors may be involved in the dependence of MLL-AF9 leukemogenesis on CBX8 as well. Thus, future unbiased analysis is of importance to compare the global changes in gene expression and protein-protein interactions in the presence or absence of CBX8 to fully decipher the leukemogenic mechanisms of MLL-AF9.

Chapter 3

Concluding Remarks

Chromosome translocations at the MLL locus that generate chimeric MLL fusion proteins are one of the major genetic lesions leading to human acute leukemias. Although aberrant target gene activation is known as the primary drive of MLL-rearranged leukemogenesis, the underlying mechanisms remain poorly understood. Multiple lines of evidence have indicated that both the N-terminal MLL portion and the C-terminal translocation partners of MLL fusion proteins bear functional significance. The work described in this thesis explored molecular mechanisms that can help decipher this significance and identified novel co-factors of both the N terminus and the C terminus of MLL fusion proteins, which are critical for leukemogenesis. The key findings are summarized as following:

For the N-terminal MLL portion:

- PAFc interacts with the pre-CxxC and RD2 domains of MLL
- Transcriptional activity of MLL and MLL fusion proteins is stimulated by PAFc
- MLL fusion protein mediated transformation is dependent upon interaction with PAFc
- PAFc expression is coordinately downregulated during myeloid differentiation

For the C-terminal translocation partners (AF9/ENL):

- CBX8 is essential for both initiation and maintenance of MLL-AF9 transformation
- CBX8 is crucial for MLL-AF9-induced transcriptional activation
- Role of CBX8 in MLL-AF9 leukemogenesis is Independent of PRC1
- CBX8 regulation of TIP60 localization contributes to MLL-AF9 transformation

These observations were primarily obtained using the common fusion proteins MLL-AF9 and MLL-ENL. Because of the diversity of MLL fusion partners and the elusive leukemogenic mechanisms for many of the less frequent MLL fusion proteins (Martin et al., 2003; So et al., 2003), it is yet to be evaluated that to what extend our findings can apply to these other fusion proteins. Nevertheless, this study has helped reveal a sophisticated oncogenic system orchestrated by MLL fusion proteins: the oncoproteins promote constitutive transcriptional activation by both hijacking the basal transcriptional machinery (*e.g.,* PAFc) and recruiting the co-factor whose functional significance seems rather context-dependent (*e.g.,* CBX8, evidenced by its dispensable role in normal hematopoiesis). Moreover, it well exemplifies how the oncogenic variants (MLL fusion proteins) of a wild-type protein (MLL) rewire the evolutionarily conserved functional collaboration of enzymatic activities (HMT-HAT for transcriptional activation: SET and MOF for MLL vs. DOT1L and TIP60 for MLL-AF9) for oncogenic purposes.

Taken together, our observations implicate two potential directions for therapeutic application. On the one hand, for the co-factors with critical

physiological functions in normal cells, such as PAFc, it is worthwhile to define the specificity of their importance in the context of MLL-rearranged leukemias, therefore exploring the therapeutic window for preferentially eliminating leukemia cells by targeting these factors. On the other hand, for the co-factors whose roles are highly context-dependent, such as CBX8, it is of great value to identify their differential interaction partners in specific pathogenic processes and to characterize the interaction surface and binding kinetics, which in turn lays a critical foundation for designing small molecular inhibitors to specifically target protein-protein interactions. In summary, this work has presented valuable substrates for employing these approaches to further explore novel therapeutic strategies for treating MLL-rearranged leukemias.

References

Akhtar, A., Zink, D., and Becker, P. B. (2000). Chromodomains are protein-RNA interaction modules. Nature *407*, 405-409.

Allen, M. D., Grummitt, C. G., Hilcenko, C., Min, S. Y., Tonkin, L. M., Johnson, C. M., Freund, S. M., Bycroft, M., and Warren, A. J. (2006). Solution structure of the nonmethyl-CpG-binding CXXC domain of the leukaemia-associated MLL histone methyltransferase. EMBO J *25*, 4503-4512.

Ansari, K. I., and Mandal, S. S. (2010). Mixed lineage leukemia: roles in gene expression, hormone signaling and mRNA processing. FEBS J *277*, 1790-1804.

Armstrong, S. A., Staunton, J. E., Silverman, L. B., Pieters, R., den Boer, M. L., Minden, M. D., Sallan, S. E., Lander, E. S., Golub, T. R., and Korsmeyer, S. J. (2002). MLL translocations specify a distinct gene expression profile that distinguishes a unique leukemia. Nat Genet *30*, 41-47.

Avvakumov, N., and Cote, J. (2007). The MYST family of histone acetyltransferases and their intimate links to cancer. Oncogene *26*, 5395-5407.

Ayton, P. M., Chen, E. H., and Cleary, M. L. (2004). Binding to nonmethylated CpG DNA is essential for target recognition, transactivation, and myeloid transformation by an MLL oncoprotein. Mol Cell Biol *24*, 10470-10478.

Ayton, P. M., and Cleary, M. L. (2003). Transformation of myeloid progenitors by MLL oncoproteins is dependent on Hoxa7 and Hoxa9. Genes Dev *17*, 2298-2307.

Bach, C., Mueller, D., Buhl, S., Garcia-Cuellar, M. P., and Slany, R. K. (2009). Alterations of the CxxC domain preclude oncogenic activation of mixed-lineage leukemia 2. Oncogene *28*, 815-823.

Bachmann, I. M., Halvorsen, O. J., Collett, K., Stefansson, I. M., Straume, O., Haukaas, S. A., Salvesen, H. B., Otte, A. P., and Akslen, L. A. (2006). EZH2 expression is associated with high proliferation rate and aggressive tumor subgroups in cutaneous melanoma and cancers of the endometrium, prostate, and breast. J Clin Oncol *24*, 268-273.

Baek, S. H., Ohgi, K. A., Rose, D. W., Koo, E. H., Glass, C. K., and Rosenfeld, M. G. (2002). Exchange of N-CoR corepressor and Tip60 coactivator complexes links gene expression by NF-kappaB and beta-amyloid precursor protein. Cell *110*, 55-67.

Balgobind, B. V., Zwaan, C. M., Pieters, R., and Van den Heuvel-Eibrink, M. M. (2011). The heterogeneity of pediatric MLL-rearranged acute myeloid leukemia. Leukemia *25*, 1239-1248.

Bantignies, F., Goodman, R. H., and Smolik, S. M. (2000). Functional interaction between the coactivator Drosophila CREB-binding protein and ASH1, a member of the trithorax group of chromatin modifiers. Mol Cell Biol *20*, 9317-9330.

Bararia, D., Trivedi, A. K., Zada, A. A., Greif, P. A., Mulaw, M. A., Christopeit, M., Hiddemann, W., Bohlander, S. K., and Behre, G. (2008). Proteomic identification of the MYST domain histone acetyltransferase TIP60 (HTATIP) as a co-activator of the myeloid transcription factor C/EBPalpha. Leukemia *22*, 800-807.

Bardos, J. I., Saurin, A. J., Tissot, C., Duprez, E., and Freemont, P. S. (2000). HPC3 is a new human polycomb orthologue that interacts and associates with RING1 and Bmi1 and has transcriptional repression properties. J Biol Chem *275*, 28785-28792.

Batra, S. K., Metzgar, R. S., and Hollingsworth, M. A. (1991). Isolation and characterization of a complementary DNA (PD-1) differentially expressed by human pancreatic ductal cell tumors. Cell Growth Differ *2*, 385-390.

Berns, K., Hijmans, E. M., Mullenders, J., Brummelkamp, T. R., Velds, A., Heimerikx, M., Kerkhoven, R. M., Madiredjo, M., Nijkamp, W., Weigelt, B.*, et al.* (2004). A large-scale RNAi screen in human cells identifies new components of the p53 pathway. Nature *428*, 431-437.

Bernstein, E., Duncan, E. M., Masui, O., Gil, J., Heard, E., and Allis, C. D. (2006). Mouse polycomb proteins bind differentially to methylated histone H3 and RNA and are enriched in facultative heterochromatin. Mol Cell Biol *26*, 2560-2569.

Bernt, K. M., Zhu, N., Sinha, A. U., Vempati, S., Faber, J., Krivtsov, A. V., Feng, Z., Punt, N., Daigle, A., Bullinger, L.*, et al.* (2011). MLL-Rearranged Leukemia Is Dependent on Aberrant H3K79 Methylation by DOT1L. Cancer Cell *20*, 66-78.

Boyer, L. A., Plath, K., Zeitlinger, J., Brambrink, T., Medeiros, L. A., Lee, T. I., Levine, S. S., Wernig, M., Tajonar, A., Ray, M. K.*, et al.* (2006). Polycomb complexes repress developmental regulators in murine embryonic stem cells. Nature *441*, 349-353.

Bracken, A. P., and Helin, K. (2009). Polycomb group proteins: navigators of lineage pathways led astray in cancer. Nat Rev Cancer *9*, 773-784.

Brady, M. E., Ozanne, D. M., Gaughan, L., Waite, I., Cook, S., Neal, D. E., and Robson, C. N. (1999). Tip60 is a nuclear hormone receptor coactivator. J Biol Chem *274*, 17599-17604.

Brookes, E., and Pombo, A. (2009). Modifications of RNA polymerase II are pivotal in regulating gene expression states. EMBO Rep *10*, 1213-1219.

Cao, Q., Mani, R. S., Ateeq, B., Dhanasekaran, S. M., Asangani, I. A., Prensner, J. R., Kim, J. H., Brenner, J. C., Jing, X., Cao, X.*, et al.* (2011). Coordinated Regulation of Polycomb Group Complexes through microRNAs in Cancer. Cancer Cell *20*, 187-199.

Cao, R., Wang, L., Wang, H., Xia, L., Erdjument-Bromage, H., Tempst, P., Jones, R. S., and Zhang, Y. (2002). Role of histone H3 lysine 27 methylation in Polycomb-group silencing. Science *298*, 1039-1043.

Cao, X., and Sudhof, T. C. (2001). A transcriptionally [correction of transcriptively] active complex of APP with Fe65 and histone acetyltransferase Tip60. Science *293*, 115-120.

Caslini, C., Yang, Z., El-Osta, M., Milne, T. A., Slany, R. K., and Hess, J. L. (2007). Interaction of MLL amino terminal sequences with menin is required for transformation. Cancer Res *67*, 7275-7283.

Celetti, A., Barba, P., Cillo, C., Rotoli, B., Boncinelli, E., and Magli, M. C. (1993). Characteristic patterns of HOX gene expression in different types of human leukemia. Int J Cancer *53*, 237-244.

Chaudhary, K., Deb, S., Moniaux, N., Ponnusamy, M. P., and Batra, S. K. (2007). Human RNA polymerase II-associated factor complex: dysregulation in cancer. Oncogene *26*, 7499-7507.

Chen, W., Kumar, A. R., Hudson, W. A., Li, Q., Wu, B., Staggs, R. A., Lund, E. A., Sam, T. N., and Kersey, J. H. (2008). Malignant transformation initiated by Mll-AF9: gene dosage and critical target cells. Cancer Cell *13*, 432-440.

Chen, Y. X., Yan, J., Keeshan, K., Tubbs, A. T., Wang, H., Silva, A., Brown, E. J., Hess, J. L., Pear, W. S., and Hua, X. (2006). The tumor suppressor menin regulates hematopoiesis and myeloid transformation by influencing Hox gene expression. Proc Natl Acad Sci U S A *103*, 1018-1023.

Cheung, N., Chan, L. C., Thompson, A., Cleary, M. L., and So, C. W. (2007). Protein arginine-methyltransferase-dependent oncogenesis. Nat Cell Biol *9*, 1208-1215.

Chopra, V. S., Hong, J. W., and Levine, M. (2009). Regulation of Hox gene activity by transcriptional elongation in Drosophila. Curr Biol *19*, 688-693.

Choudhary, C., Kumar, C., Gnad, F., Nielsen, M. L., Rehman, M., Walther, T. C., Olsen, J. V., and Mann, M. (2009). Lysine acetylation targets protein complexes and co-regulates major cellular functions. Science *325*, 834-840.

Collett, K., Eide, G. E., Arnes, J., Stefansson, I. M., Eide, J., Braaten, A., Aas, T., Otte, A. P., and Akslen, L. A. (2006). Expression of enhancer of zeste homologue 2 is significantly associated with increased tumor cell proliferation and is a marker of aggressive breast cancer. Clin Cancer Res *12*, 1168-1174.

Creaven, M., Hans, F., Mutskov, V., Col, E., Caron, C., Dimitrov, S., and Khochbin, S. (1999). Control of the histone-acetyltransferase activity of Tip60 by the HIV-1 transactivator protein, Tat. Biochemistry *38*, 8826-8830.

Czermin, B., Melfi, R., McCabe, D., Seitz, V., Imhof, A., and Pirrotta, V. (2002). Drosophila enhancer of Zeste/ESC complexes have a histone H3 methyltransferase activity that marks chromosomal Polycomb sites. Cell *111*, 185-196.

de Napoles, M., Mermoud, J. E., Wakao, R., Tang, Y. A., Endoh, M., Appanah, R., Nesterova, T. B., Silva, J., Otte, A. P., Vidal, M.*, et al.* (2004). Polycomb group proteins Ring1A/B link ubiquitylation of histone H2A to heritable gene silencing and X inactivation. Dev Cell *7*, 663-676.

DelProposto, J., Majmudar, C. Y., Smith, J. L., and Brown, W. C. (2009). Mocr: a novel fusion tag for enhancing solubility that is compatible with structural biology applications. Protein Expr Purif *63*, 40-49.

Dietrich, N., Bracken, A. P., Trinh, E., Schjerling, C. K., Koseki, H., Rappsilber, J., Helin, K., and Hansen, K. H. (2007). Bypass of senescence by the polycomb group protein CBX8 through direct binding to the INK4A-ARF locus. EMBO J *26*, 1637-1648.

Ding, L., Paszkowski-Rogacz, M., Nitzsche, A., Slabicki, M. M., Heninger, A. K., de Vries, I., Kittler, R., Junqueira, M., Shevchenko, A., Schulz, H.*, et al.* (2009). A genome-scale RNAi screen for Oct4 modulators defines a role of the Paf1 complex for embryonic stem cell identity. Cell Stem Cell *4*, 403-415.

Djabali, M., Selleri, L., Parry, P., Bower, M., Young, B. D., and Evans, G. A. (1992). A trithorax-like gene is interrupted by chromosome 11q23 translocations in acute leukaemias. Nat Genet *2*, 113-118.

Donnelly, M. I., Zhou, M., Millard, C. S., Clancy, S., Stols, L., Eschenfeldt, W. H., Collart, F. R., and Joachimiak, A. (2006). An expression vector tailored for large-scale, high-throughput purification of recombinant proteins. Protein Expr Purif *47*, 446-454.

Dou, Y., and Hess, J. L. (2008). Mechanisms of transcriptional regulation by MLL and its disruption in acute leukemia. Int J Hematol *87*, 10-18.

Dou, Y., Milne, T. A., Ruthenburg, A. J., Lee, S., Lee, J. W., Verdine, G. L., Allis, C. D., and Roeder, R. G. (2006). Regulation of MLL1 H3K4 methyltransferase activity by its core components. Nat Struct Mol Biol *13*, 713-719.

Dou, Y., Milne, T. A., Tackett, A. J., Smith, E. R., Fukuda, A., Wysocka, J., Allis, C. D., Chait, B. T., Hess, J. L., and Roeder, R. G. (2005). Physical association and coordinate function of the H3 K4 methyltransferase MLL1 and the H4 K16 acetyltransferase MOF. Cell *121*, 873-885.

Doyon, Y., Selleck, W., Lane, W. S., Tan, S., and Cote, J. (2004). Structural and functional conservation of the NuA4 histone acetyltransferase complex from yeast to humans. Mol Cell Biol *24*, 1884-1896.

Ernst, P., Wang, J., Huang, M., Goodman, R. H., and Korsmeyer, S. J. (2001). MLL and CREB bind cooperatively to the nuclear coactivator CREB-binding protein. Mol Cell Biol *21*, 2249-2258.

Ernst, T., Chase, A. J., Score, J., Hidalgo-Curtis, C. E., Bryant, C., Jones, A. V., Waghorn, K., Zoi, K., Ross, F. M., Reiter, A.*, et al.* (2010). Inactivating mutations of the histone methyltransferase gene EZH2 in myeloid disorders. Nat Genet *42*, 722-726.

Fazzio, T. G., Huff, J. T., and Panning, B. (2008). An RNAi screen of chromatin proteins identifies Tip60-p400 as a regulator of embryonic stem cell identity. Cell *134*, 162-174.

Felix, C. A. (1998). Secondary leukemias induced by topoisomerase-targeted drugs. Biochim Biophys Acta *1400*, 233-255.

Francis, N. J., and Kingston, R. E. (2001). Mechanisms of transcriptional memory. Nat Rev Mol Cell Biol *2*, 409-421.

Francis, N. J., Kingston, R. E., and Woodcock, C. L. (2004). Chromatin compaction by a polycomb group protein complex. Science *306*, 1574-1577.

Frank, S. R., Parisi, T., Taubert, S., Fernandez, P., Fuchs, M., Chan, H. M., Livingston, D. M., and Amati, B. (2003). MYC recruits the TIP60 histone acetyltransferase complex to chromatin. EMBO Rep *4*, 575-580.

Garcia-Cuellar, M. P., Zilles, O., Schreiner, S. A., Birke, M., Winkler, T. H., and Slany, R. K. (2001). The ENL moiety of the childhood leukemia-associated MLL-ENL oncoprotein recruits human Polycomb 3. Oncogene *20*, 411-419.

Gaughan, L., Brady, M. E., Cook, S., Neal, D. E., and Robson, C. N. (2001). Tip60 is a co-activator specific for class I nuclear hormone receptors. J Biol Chem *276*, 46841-46848.

Gaughan, L., Logan, I. R., Cook, S., Neal, D. E., and Robson, C. N. (2002). Tip60 and histone deacetylase 1 regulate androgen receptor activity through changes to the acetylation status of the receptor. J Biol Chem *277*, 25904-25913.

Grimm, C., Matos, R., Ly-Hartig, N., Steuerwald, U., Lindner, D., Rybin, V., Muller, J., and Muller, C. W. (2009). Molecular recognition of histone lysine methylation by the Polycomb group repressor dSfmbt. EMBO J *28*, 1965-1977.

Gu, Y., Nakamura, T., Alder, H., Prasad, R., Canaani, O., Cimino, G., Croce, C. M., and Canaani, E. (1992). The t(4;11) chromosome translocation of human acute leukemias fuses the ALL-1 gene, related to Drosophila trithorax, to the AF-4 gene. Cell *71*, 701-708.

Guo, Y., Lubbert, M., and Engelhardt, M. (2003). CD34- hematopoietic stem cells: current concepts and controversies. Stem Cells *21*, 15-20.

Gupta, R. A., Shah, N., Wang, K. C., Kim, J., Horlings, H. M., Wong, D. J., Tsai, M. C., Hung, T., Argani, P., Rinn, J. L.*, et al.* (2010). Long non-coding RNA HOTAIR reprograms chromatin state to promote cancer metastasis. Nature *464*, 1071-1076.

He, H., Hua, X., and Yan, J. (2011). Epigenetic regulations in hematopoietic Hox code. Oncogene *30*, 379-388.

Hemenway, C. S., de Erkenez, A. C., and Gould, G. C. (2001). The polycomb protein MPc3 interacts with AF9, an MLL fusion partner in t(9;11)(p22;q23) acute leukemias. Oncogene *20*, 3798-3805.

Hsieh, J. J., Cheng, E. H., and Korsmeyer, S. J. (2003a). Taspase1: a threonine aspartase required for cleavage of MLL and proper HOX gene expression. Cell *115*, 293-303.

Hsieh, J. J., Ernst, P., Erdjument-Bromage, H., Tempst, P., and Korsmeyer, S. J. (2003b). Proteolytic cleavage of MLL generates a complex of N- and C-terminal

fragments that confers protein stability and subnuclear localization. Mol Cell Biol *23*, 186-194.

Hu, Y., Fisher, J. B., Koprowski, S., McAllister, D., Kim, M. S., and Lough, J. (2009). Homozygous disruption of the Tip60 gene causes early embryonic lethality. Dev Dyn *238*, 2912-2921.

Ikura, T., Ogryzko, V. V., Grigoriev, M., Groisman, R., Wang, J., Horikoshi, M., Scully, R., Qin, J., and Nakatani, Y. (2000). Involvement of the TIP60 histone acetylase complex in DNA repair and apoptosis. Cell *102*, 463-473.

Iwata, T., Mizusawa, N., Taketani, Y., Itakura, M., and Yoshimoto, K. (2007). Parafibromin tumor suppressor enhances cell growth in the cells expressing SV40 large T antigen. Oncogene *26*, 6176-6183.

Jaehning, J. A. (2010a). The Paf1 complex: platform or player in RNA polymerase II transcription? Biochim Biophys Acta *1799*, 379-388.

Jaehning, J. A. (2010b). The Paf1 complex: Platform or player in RNA polymerase II transcription? Biochimica Et Biophysica Acta-Gene Regulatory Mechanisms *1799*, 379-388.

Jo, S. Y., Granowicz, E. M., Maillard, I., Thomas, D., and Hess, J. L. (2011). Requirement for Dot1l in murine postnatal hematopoiesis and leukemogenesis by MLL translocation. Blood *117*, 4759-4768.

Jude, C. D., Climer, L., Xu, D., Artinger, E., Fisher, J. K., and Ernst, P. (2007). Unique and independent roles for MLL in adult hematopoietic stem cells and progenitors. Cell Stem Cell *1*, 324-337.

Kanhere, A., Viiri, K., Araujo, C. C., Rasaiyaah, J., Bouwman, R. D., Whyte, W. A., Pereira, C. F., Brookes, E., Walker, K., Bell, G. W.*, et al.* (2010). Short RNAs are transcribed from repressed polycomb target genes and interact with polycomb repressive complex-2. Mol Cell *38*, 675-688.

Katoh-Fukui, Y., Tsuchiya, R., Shiroishi, T., Nakahara, Y., Hashimoto, N., Noguchi, K., and Higashinakagawa, T. (1998). Male-to-female sex reversal in M33 mutant mice. Nature *393*, 688-692.

Katsumoto, T., Yoshida, N., and Kitabayashi, I. (2008). Roles of the histone acetyltransferase monocytic leukemia zinc finger protein in normal and malignant hematopoiesis. Cancer Sci *99*, 1523-1527.

Kaustov, L., Ouyang, H., Amaya, M., Lemak, A., Nady, N., Duan, S., Wasney, G. A., Li, Z., Vedadi, M., Schapira, M.*, et al.* (2011). Recognition and specificity determinants of the human cbx chromodomains. J Biol Chem *286*, 521-529.

Keller, A., Nesvizhskii, A. I., Kolker, E., and Aebersold, R. (2002). Empirical statistical model to estimate the accuracy of peptide identifications made by MS/MS and database search. Anal Chem *74*, 5383-5392.

Kerppola, T. K. (2009). Polycomb group complexes--many combinations, many functions. Trends Cell Biol *19*, 692-704.

Kidani, K., Osaki, M., Tamura, T., Yamaga, K., Shomori, K., Ryoke, K., and Ito, H. (2009). High expression of EZH2 is associated with tumor proliferation and prognosis in human oral squamous cell carcinomas. Oral Oncol *45*, 39-46.

Kim, J., Guermah, M., McGinty, R. K., Lee, J. S., Tang, Z., Milne, T. A., Shilatifard, A., Muir, T. W., and Roeder, R. G. (2009). RAD6-Mediated

transcription-coupled H2B ubiquitylation directly stimulates H3K4 methylation in human cells. Cell *137*, 459-471.

Kim, J., Guermah, M., and Roeder, R. G. (2010). The Human PAF1 Complex Acts in Chromatin Transcription Elongation Both Independently and Cooperatively with SII/TFIIS. Cell *140*, 491-503.

Kim, J., and Roeder, R. G. (2009). Direct Bre1-Paf1 complex interactions and RING finger-independent Bre1-Rad6 interactions mediate histone H2B ubiquitylation in yeast. J Biol Chem *284*, 20582-20592.

Kim, S. C., Sprung, R., Chen, Y., Xu, Y., Ball, H., Pei, J., Cheng, T., Kho, Y., Xiao, H., Xiao, L.*, et al.* (2006). Substrate and functional diversity of lysine acetylation revealed by a proteomics survey. Mol Cell *23*, 607-618.

Kim, S. H., Park, J., Choi, M. C., Park, J. H., Kim, H. P., Lee, J. H., Oh, D. Y., Im, S. A., Bang, Y. J., and Kim, T. Y. (2008). DNA methyltransferase 3B acts as a co-repressor of the human polycomb protein hPc2 to repress fibroblast growth factor receptor 3 transcription. Int J Biochem Cell Biol *40*, 2462-2471.

Kinoshita, A., Whelan, C. M., Berezovska, O., and Hyman, B. T. (2002). The gamma secretase-generated carboxyl-terminal domain of the amyloid precursor protein induces apoptosis via Tip60 in H4 cells. J Biol Chem *277*, 28530-28536.

Kirmizis, A., Bartley, S. M., Kuzmichev, A., Margueron, R., Reinberg, D., Green, R., and Farnham, P. J. (2004). Silencing of human polycomb target genes is associated with methylation of histone H3 Lys 27. Genes Dev *18*, 1592-1605.

Krivtsov, A. V., and Armstrong, S. A. (2007). MLL translocations, histone modifications and leukaemia stem-cell development. Nat Rev Cancer *7*, 823-833.

Krivtsov, A. V., Feng, Z., Lemieux, M. E., Faber, J., Vempati, S., Sinha, A. U., Xia, X., Jesneck, J., Bracken, A. P., Silverman, L. B.*, et al.* (2008). H3K79 methylation profiles define murine and human MLL-AF4 leukemias. Cancer Cell *14*, 355-368.

Krogan, N. J., Dover, J., Wood, A., Schneider, J., Heidt, J., Boateng, M. A., Dean, K., Ryan, O. W., Golshani, A., Johnston, M.*, et al.* (2003). The Paf1 complex is required for histone H3 methylation by COMPASS and Dot1p: linking transcriptional elongation to histone methylation. Mol Cell *11*, 721-729.

Krumlauf, R. (1994). Hox genes in vertebrate development. Cell *78*, 191-201.

Ku, M., Koche, R. P., Rheinbay, E., Mendenhall, E. M., Endoh, M., Mikkelsen, T. S., Presser, A., Nusbaum, C., Xie, X., Chi, A. S.*, et al.* (2008). Genomewide analysis of PRC1 and PRC2 occupancy identifies two classes of bivalent domains. PLoS Genet *4*, e1000242.

Kumar, A. R., Hudson, W. A., Chen, W., Nishiuchi, R., Yao, Q., and Kersey, J. H. (2004). Hoxa9 influences the phenotype but not the incidence of Mll-AF9 fusion gene leukemia. Blood *103*, 1823-1828.

Kusch, T., Florens, L., Macdonald, W. H., Swanson, S. K., Glaser, R. L., Yates, J. R., 3rd, Abmayr, S. M., Washburn, M. P., and Workman, J. L. (2004). Acetylation by Tip60 is required for selective histone variant exchange at DNA lesions. Science *306*, 2084-2087.

Kuzmichev, A., Nishioka, K., Erdjument-Bromage, H., Tempst, P., and Reinberg, D. (2002). Histone methyltransferase activity associated with a human multiprotein complex containing the Enhancer of Zeste protein. Genes Dev *16*, 2893-2905.

Landeira, D., Sauer, S., Poot, R., Dvorkina, M., Mazzarella, L., Jorgensen, H. F., Pereira, C. F., Leleu, M., Piccolo, F. M., Spivakov, M.*, et al.* (2010). Jarid2 is a PRC2 component in embryonic stem cells required for multi-lineage differentiation and recruitment of PRC1 and RNA Polymerase II to developmental regulators. Nat Cell Biol *12*, 618-624.

Lavau, C., Szilvassy, S. J., Slany, R., and Cleary, M. L. (1997). Immortalization and leukemic transformation of a myelomonocytic precursor by retrovirally transduced HRX-ENL. EMBO J *16*, 4226-4237.

Lawrence, H. J., Christensen, J., Fong, S., Hu, Y. L., Weissman, I., Sauvageau, G., Humphries, R. K., and Largman, C. (2005). Loss of expression of the Hoxa-9 homeobox gene impairs the proliferation and repopulating ability of hematopoietic stem cells. Blood *106*, 3988-3994.

Lawrence, H. J., Sauvageau, G., Humphries, R. K., and Largman, C. (1996). The role of HOX homeobox genes in normal and leukemic hematopoiesis. Stem Cells *14*, 281-291.

Leduc, C., Claverie, P., Eymin, B., Col, E., Khochbin, S., Brambilla, E., and Gazzeri, S. (2006). p14ARF promotes RB accumulation through inhibition of its Tip60-dependent acetylation. Oncogene *25*, 4147-4154.

Leeb, M., and Wutz, A. (2007). Ring1B is crucial for the regulation of developmental control genes and PRC1 proteins but not X inactivation in embryonic cells. J Cell Biol *178*, 219-229.

Legube, G., Linares, L. K., Tyteca, S., Caron, C., Scheffner, M., Chevillard-Briet, M., and Trouche, D. (2004). Role of the histone acetyl transferase Tip60 in the p53 pathway. J Biol Chem *279*, 44825-44833.

Lessard, J., and Sauvageau, G. (2003). Polycomb group genes as epigenetic regulators of normal and leukemic hemopoiesis. Exp Hematol *31*, 567-585.

Levine, S. S., King, I. F., and Kingston, R. E. (2004). Division of labor in polycomb group repression. Trends Biochem Sci *29*, 478-485.

Levine, S. S., Weiss, A., Erdjument-Bromage, H., Shao, Z., Tempst, P., and Kingston, R. E. (2002). The core of the polycomb repressive complex is compositionally and functionally conserved in flies and humans. Mol Cell Biol *22*, 6070-6078.

Li, H., Ma, X., Wang, J., Koontz, J., Nucci, M., and Sklar, J. (2007). Effects of rearrangement and allelic exclusion of JJAZ1/SUZ12 on cell proliferation and survival. Proc Natl Acad Sci U S A *104*, 20001-20006.

Lin, C., Smith, E. R., Takahashi, H., Lai, K. C., Martin-Brown, S., Florens, L., Washburn, M. P., Conaway, J. W., Conaway, R. C., and Shilatifard, A. (2010). AFF4, a component of the ELL/P-TEFb elongation complex and a shared subunit of MLL chimeras, can link transcription elongation to leukemia. Mol Cell *37*, 429-437.

Maertens, G. N., El Messaoudi-Aubert, S., Racek, T., Stock, J. K., Nicholls, J., Rodriguez-Niedenfuhr, M., Gil, J., and Peters, G. (2009). Several distinct polycomb complexes regulate and co-localize on the INK4a tumor suppressor locus. PLoS One *4*, e6380.

Magli, M. C., Largman, C., and Lawrence, H. J. (1997). Effects of HOX homeobox genes in blood cell differentiation. J Cell Physiol *173*, 168-177.

Maillard, I., Chen, Y. X., Friedman, A., Yang, Y., Tubbs, A. T., Shestova, O., Pear, W. S., and Hua, X. (2009). Menin regulates the function of hematopoietic stem cells and lymphoid progenitors. Blood *113*, 1661-1669.

Majewski, I. J., Blewitt, M. E., de Graaf, C. A., McManus, E. J., Bahlo, M., Hilton, A. A., Hyland, C. D., Smyth, G. K., Corbin, J. E., Metcalf, D.*, et al.* (2008). Polycomb repressive complex 2 (PRC2) restricts hematopoietic stem cell activity. PLoS Biol *6*, e93.

Margueron, R., and Reinberg, D. (2011). The Polycomb complex PRC2 and its mark in life. Nature *469*, 343-349.

Martin, M. E., Milne, T. A., Bloyer, S., Galoian, K., Shen, W., Gibbs, D., Brock, H. W., Slany, R., and Hess, J. L. (2003). Dimerization of MLL fusion proteins immortalizes hematopoietic cells. Cancer Cell *4*, 197-207.

Martin-Perez, D., Piris, M. A., and Sanchez-Beato, M. (2010). Polycomb proteins in hematologic malignancies. Blood *116*, 5465-5475.

McMahon, K. A., Hiew, S. Y., Hadjur, S., Veiga-Fernandes, H., Menzel, U., Price, A. J., Kioussis, D., Williams, O., and Brady, H. J. (2007). Mll has a critical role in fetal and adult hematopoietic stem cell self-renewal. Cell Stem Cell *1*, 338-345.

Mills, A. A. (2010). Throwing the cancer switch: reciprocal roles of polycomb and trithorax proteins. Nat Rev Cancer *10*, 669-682.

Milne, T. A., Briggs, S. D., Brock, H. W., Martin, M. E., Gibbs, D., Allis, C. D., and Hess, J. L. (2002). MLL targets SET domain methyltransferase activity to Hox gene promoters. Mol Cell *10*, 1107-1117.

Milne, T. A., Dou, Y., Martin, M. E., Brock, H. W., Roeder, R. G., and Hess, J. L. (2005a). MLL associates specifically with a subset of transcriptionally active target genes. Proceedings of the National Academy of Sciences of the United States of America *102*, 14765-14770.

Milne, T. A., Hughes, C. M., Lloyd, R., Yang, Z., Rozenblatt-Rosen, O., Dou, Y., Schnepp, R. W., Krankel, C., Livolsi, V. A., Gibbs, D.*, et al.* (2005b). Menin and MLL cooperatively regulate expression of cyclin-dependent kinase inhibitors. Proc Natl Acad Sci U S A *102*, 749-754.

Milne, T. A., Kim, J., Wang, G. G., Stadler, S. C., Basrur, V., Whitcomb, S. J., Wang, Z., Ruthenburg, A. J., Elenitoba-Johnson, K. S., Roeder, R. G., and Allis, C. D. (2010). Multiple interactions recruit MLL1 and MLL1 fusion proteins to the HOXA9 locus in leukemogenesis. Mol Cell *38*, 853-863.

Mimori, K., Ogawa, K., Okamoto, M., Sudo, T., Inoue, H., and Mori, M. (2005). Clinical significance of enhancer of zeste homolog 2 expression in colorectal cancer cases. Eur J Surg Oncol *31*, 376-380.

Mohammad, H. P., Cai, Y., McGarvey, K. M., Easwaran, H., Van Neste, L., Ohm, J. E., O'Hagan, H. M., and Baylin, S. B. (2009). Polycomb CBX7 promotes initiation of heritable repression of genes frequently silenced with cancer-specific DNA hypermethylation. Cancer Res *69*, 6322-6330.

Mohan, M., Herz, H. M., Takahashi, Y. H., Lin, C., Lai, K. C., Zhang, Y., Washburn, M. P., Florens, L., and Shilatifard, A. (2010a). Linking H3K79 trimethylation to Wnt signaling through a novel Dot1-containing complex (DotCom). Genes Dev *24*, 574-589.

Mohan, M., Lin, C., Guest, E., and Shilatifard, A. (2010b). Licensed to elongate: a molecular mechanism for MLL-based leukaemogenesis. Nat Rev Cancer *10*, 721-728.

Moniaux, N., Nemos, C., Schmied, B. M., Chauhan, S. C., Deb, S., Morikane, K., Choudhury, A., Vanlith, M., Sutherlin, M., Sikela, J. M.*, et al.* (2006). The human homologue of the RNA polymerase II-associated factor 1 (hPaf1), localized on the 19q13 amplicon, is associated with tumorigenesis. Oncogene *25*, 3247-3257.

Monroe, S. C., Jo, S. Y., Sanders, D. S., Basrur, V., Elenitoba-Johnson, K. S., Slany, R. K., and Hess, J. L. (2010). MLL-AF9 and MLL-ENL alter the dynamic association of transcriptional regulators with genes critical for leukemia. Exp Hematol.

Morin, R. D., Johnson, N. A., Severson, T. M., Mungall, A. J., An, J., Goya, R., Paul, J. E., Boyle, M., Woolcock, B. W., Kuchenbauer, F.*, et al.* (2010). Somatic mutations altering EZH2 (Tyr641) in follicular and diffuse large B-cell lymphomas of germinal-center origin. Nat Genet *42*, 181-185.

Morita, S., Kojima, T., and Kitamura, T. (2000). Plat-E: an efficient and stable system for transient packaging of retroviruses. Gene Ther *7*, 1063-1066.

Mueller, D., Bach, C., Zeisig, D., Garcia-Cuellar, M. P., Monroe, S., Sreekumar, A., Zhou, R., Nesvizhskii, A., Chinnaiyan, A., Hess, J. L., and Slany, R. K. (2007).

A role for the MLL fusion partner ENL in transcriptional elongation and chromatin modification. Blood *110*, 4445-4454.

Muller, J., and Verrijzer, P. (2009). Biochemical mechanisms of gene regulation by polycomb group protein complexes. Curr Opin Genet Dev *19*, 150-158.

Muntean, A. G., Giannola, D., Udager, A. M., and Hess, J. L. (2008). The PHD fingers of MLL block MLL fusion protein-mediated transformation. Blood *112*, 4690-4693.

Muntean, A. G., Tan, J., Sitwala, K., Huang, Y., Bronstein, J., Connelly, J. A., Basrur, V., Elenitoba-Johnson, K. S., and Hess, J. L. (2010). The PAF complex synergizes with MLL fusion proteins at HOX loci to promote leukemogenesis. Cancer Cell *17*, 609-621.

Nakahata, S., Saito, Y., Hamasaki, M., Hidaka, T., Arai, Y., Taki, T., Taniwaki, M., and Morishita, K. (2009). Alteration of enhancer of polycomb 1 at 10p11.2 is one of the genetic events leading to development of adult T-cell leukemia/lymphoma. Genes Chromosomes Cancer *48*, 768-776.

Nakamura, T., Mori, T., Tada, S., Krajewski, W., Rozovskaia, T., Wassell, R., Dubois, G., Mazo, A., Croce, C. M., and Canaani, E. (2002). ALL-1 is a histone methyltransferase that assembles a supercomplex of proteins involved in transcriptional regulation. Mol Cell *10*, 1119-1128.

Nekrasov, M., Klymenko, T., Fraterman, S., Papp, B., Oktaba, K., Kocher, T., Cohen, A., Stunnenberg, H. G., Wilm, M., and Muller, J. (2007). Pcl-PRC2 is needed to generate high levels of H3-K27 trimethylation at Polycomb target genes. EMBO J *26*, 4078-4088.

Nesvizhskii, A. I., Keller, A., Kolker, E., and Aebersold, R. (2003). A statistical model for identifying proteins by tandem mass spectrometry. Anal Chem *75*, 4646-4658.

Newey, P. J., Bowl, M. R., and Thakker, R. V. (2009). Parafibromin--functional insights. J Intern Med *266*, 84-98.

Nguyen, A. T., Taranova, O., He, J., and Zhang, Y. (2011). DOT1L, the H3K79 methyltransferase, is required for MLL-AF9-mediated leukemogenesis. Blood *117*, 6912-6922.

Nikoloski, G., Langemeijer, S. M., Kuiper, R. P., Knops, R., Massop, M., Tonnissen, E. R., van der Heijden, A., Scheele, T. N., Vandenberghe, P., de Witte, T.*, et al.* (2010). Somatic mutations of the histone methyltransferase gene EZH2 in myelodysplastic syndromes. Nat Genet *42*, 665-667.

Ohtsubo, M., Yasunaga, S., Ohno, Y., Tsumura, M., Okada, S., Ishikawa, N., Shirao, K., Kikuchi, A., Nishitani, H., Kobayashi, M., and Takihara, Y. (2008). Polycomb-group complex 1 acts as an E3 ubiquitin ligase for Geminin to sustain hematopoietic stem cell activity. Proc Natl Acad Sci U S A *105*, 10396-10401.

Pasini, D., Bracken, A. P., Hansen, J. B., Capillo, M., and Helin, K. (2007). The polycomb group protein Suz12 is required for embryonic stem cell differentiation. Mol Cell Biol *27*, 3769-3779.

Pasini, D., Hansen, K. H., Christensen, J., Agger, K., Cloos, P. A., and Helin, K. (2008). Coordinated regulation of transcriptional repression by the RBP2 H3K4 demethylase and Polycomb-Repressive Complex 2. Genes Dev *22*, 1345-1355.

Pasini, D., Malatesta, M., Jung, H. R., Walfridsson, J., Willer, A., Olsson, L., Skotte, J., Wutz, A., Porse, B., Jensen, O. N., and Helin, K. (2010). Characterization of an antagonistic switch between histone H3 lysine 27 methylation and acetylation in the transcriptional regulation of Polycomb group target genes. Nucleic Acids Res *38*, 4958-4969.

Patel, J. H., Du, Y., Ard, P. G., Phillips, C., Carella, B., Chen, C. J., Rakowski, C., Chatterjee, C., Lieberman, P. M., Lane, W. S.*, et al.* (2004). The c-MYC oncoprotein is a substrate of the acetyltransferases hGCN5/PCAF and TIP60. Mol Cell Biol *24*, 10826-10834.

Peng, J. C., Valouev, A., Swigut, T., Zhang, J., Zhao, Y., Sidow, A., and Wysocka, J. (2009). Jarid2/Jumonji coordinates control of PRC2 enzymatic activity and target gene occupancy in pluripotent cells. Cell *139*, 1290-1302.

Peterson, A. J., Mallin, D. R., Francis, N. J., Ketel, C. S., Stamm, J., Voeller, R. K., Kingston, R. E., and Simon, J. A. (2004). Requirement for sex comb on midleg protein interactions in Drosophila polycomb group repression. Genetics *167*, 1225-1239.

Petruk, S., Sedkov, Y., Smith, S., Tillib, S., Kraevski, V., Nakamura, T., Canaani, E., Croce, C. M., and Mazo, A. (2001). Trithorax and dCBP acting in a complex to maintain expression of a homeotic gene. Science *294*, 1331-1334.

Pineault, N., Helgason, C. D., Lawrence, H. J., and Humphries, R. K. (2002). Differential expression of Hox, Meis1, and Pbx1 genes in primitive cells throughout murine hematopoietic ontogeny. Exp Hematol *30*, 49-57.

Ren, X., and Kerppola, T. K. (2011). REST interacts with Cbx proteins and regulates polycomb repressive complex 1 occupancy at RE1 elements. Mol Cell Biol *31*, 2100-2110.

Richie, E. R., Schumacher, A., Angel, J. M., Holloway, M., Rinchik, E. M., and Magnuson, T. (2002). The Polycomb-group gene eed regulates thymocyte differentiation and suppresses the development of carcinogen-induced T-cell lymphomas. Oncogene *21*, 299-306.

Richly, H., Aloia, L., and Di Croce, L. (2011). Roles of the Polycomb group proteins in stem cells and cancer. Cell Death Dis *2*, e204.

Rinn, J. L., Kertesz, M., Wang, J. K., Squazzo, S. L., Xu, X., Brugmann, S. A., Goodnough, L. H., Helms, J. A., Farnham, P. J., Segal, E., and Chang, H. Y. (2007). Functional demarcation of active and silent chromatin domains in human HOX loci by noncoding RNAs. Cell *129*, 1311-1323.

Rozenblatt-Rosen, O., Hughes, C. M., Nannepaga, S. J., Shanmugam, K. S., Copeland, T. D., Guszczynski, T., Resau, J. H., and Meyerson, M. (2005). The parafibromin tumor suppressor protein is part of a human Paf1 complex. Mol Cell Biol *25*, 612-620.

Ruthenburg, A. J., Wang, W., Graybosch, D. M., Li, H., Allis, C. D., Patel, D. J., and Verdine, G. L. (2006). Histone H3 recognition and presentation by the WDR5 module of the MLL1 complex. Nat Struct Mol Biol *13*, 704-712.

Sanchez, C., Sanchez, I., Demmers, J. A., Rodriguez, P., Strouboulis, J., and Vidal, M. (2007). Proteomics analysis of Ring1B/Rnf2 interactors identifies a

novel complex with the Fbxl10/Jhdm1B histone demethylase and the Bcl6 interacting corepressor. Mol Cell Proteomics *6*, 820-834.

Sanchez-Beato, M., Sanchez, E., Gonzalez-Carrero, J., Morente, M., Diez, A., Sanchez-Verde, L., Martin, M. C., Cigudosa, J. C., Vidal, M., and Piris, M. A. (2006). Variability in the expression of polycomb proteins in different normal and tumoral tissues. A pilot study using tissue microarrays. Mod Pathol *19*, 684-694.

Sapountzi, V., and Cote, J. (2011). MYST-family histone acetyltransferases: beyond chromatin. Cell Mol Life Sci *68*, 1147-1156.

Sapountzi, V., Logan, I. R., and Robson, C. N. (2006). Cellular functions of TIP60. Int J Biochem Cell Biol *38*, 1496-1509.

Sauvageau, M., and Sauvageau, G. (2010). Polycomb group proteins: multi-faceted regulators of somatic stem cells and cancer. Cell Stem Cell *7*, 299-313.

Scheuermann, J. C., de Ayala Alonso, A. G., Oktaba, K., Ly-Hartig, N., McGinty, R. K., Fraterman, S., Wilm, M., Muir, T. W., and Muller, J. (2010). Histone H2A deubiquitinase activity of the Polycomb repressive complex PR-DUB. Nature *465*, 243-247.

Schoeftner, S., Sengupta, A. K., Kubicek, S., Mechtler, K., Spahn, L., Koseki, H., Jenuwein, T., and Wutz, A. (2006). Recruitment of PRC1 function at the initiation of X inactivation independent of PRC2 and silencing. EMBO J *25*, 3110-3122.

Schuettengruber, B., Chourrout, D., Vervoort, M., Leblanc, B., and Cavalli, G. (2007). Genome regulation by polycomb and trithorax proteins. Cell *128*, 735-745.

Schuetz, A., Allali-Hassani, A., Martin, F., Loppnau, P., Vedadi, M., Bochkarev, A., Plotnikov, A. N., Arrowsmith, C. H., and Min, J. (2006). Structural basis for

molecular recognition and presentation of histone H3 by WDR5. EMBO J *25*, 4245-4252.

Schuringa, J. J., and Vellenga, E. (2010). Role of the polycomb group gene BMI1 in normal and leukemic hematopoietic stem and progenitor cells. Curr Opin Hematol *17*, 294-299.

Schwartz, Y. B., and Pirrotta, V. (2007). Polycomb silencing mechanisms and the management of genomic programmes. Nat Rev Genet *8*, 9-22.

Shah, N., and Sukumar, S. (2010). The Hox genes and their roles in oncogenesis. Nat Rev Cancer *10*, 361-371.

Sierra, J., Yoshida, T., Joazeiro, C. A., and Jones, K. A. (2006). The APC tumor suppressor counteracts beta-catenin activation and H3K4 methylation at Wnt target genes. Genes Dev *20*, 586-600.

Simon, J. A., and Kingston, R. E. (2009). Mechanisms of polycomb gene silencing: knowns and unknowns. Nat Rev Mol Cell Biol *10*, 697-708.

Sitwala, K. V., Dandekar, M. N., and Hess, J. L. (2008). HOX proteins and leukemia. Int J Clin Exp Pathol *1*, 461-474.

Slany, R. K. (2009). The molecular biology of mixed lineage leukemia. Haematologica *94*, 984-993.

Slany, R. K., Lavau, C., and Cleary, M. L. (1998). The oncogenic capacity of HRX-ENL requires the transcriptional transactivation activity of ENL and the DNA binding motifs of HRX. Mol Cell Biol *18*, 122-129.

Smith, L. L., Yeung, J., Zeisig, B. B., Popov, N., Huijbers, I., Barnes, J., Wilson, A. J., Taskesen, E., Delwel, R., Gil, J.*, et al.* (2011). Functional Crosstalk between

Bmi1 and MLL/Hoxa9 Axis in Establishment of Normal Hematopoietic and Leukemic Stem Cells. Cell Stem Cell *8*, 649-662.

So, C. W., Lin, M., Ayton, P. M., Chen, E. H., and Cleary, M. L. (2003). Dimerization contributes to oncogenic activation of MLL chimeras in acute leukemias. Cancer Cell *4*, 99-110.

So, C. W., and van der Reijden, B. A. (2008). C/EBPalpha, do not forget your TIP60. Leukemia *22*, 676-677.

Somervaille, T. C., Matheny, C. J., Spencer, G. J., Iwasaki, M., Rinn, J. L., Witten, D. M., Chang, H. Y., Shurtleff, S. A., Downing, J. R., and Cleary, M. L. (2009). Hierarchical maintenance of MLL myeloid leukemia stem cells employs a transcriptional program shared with embryonic rather than adult stem cells. Cell Stem Cell *4*, 129-140.

Southall, S. M., Wong, P. S., Odho, Z., Roe, S. M., and Wilson, J. R. (2009). Structural basis for the requirement of additional factors for MLL1 SET domain activity and recognition of epigenetic marks. Mol Cell *33*, 181-191.

Sparmann, A., and van Lohuizen, M. (2006). Polycomb silencers control cell fate, development and cancer. Nat Rev Cancer *6*, 846-856.

Stass, S., Mirro, J., Melvin, S., Pui, C. H., Murphy, S. B., and Williams, D. (1984). Lineage switch in acute leukemia. Blood *64*, 701-706.

Stelzl, U., Worm, U., Lalowski, M., Haenig, C., Brembeck, F. H., Goehler, H., Stroedicke, M., Zenkner, M., Schoenherr, A., Koeppen, S.*, et al.* (2005). A human protein-protein interaction network: a resource for annotating the proteome. Cell *122*, 957-968.

Strahl, B. D., Ohba, R., Cook, R. G., and Allis, C. D. (1999). Methylation of histone H3 at lysine 4 is highly conserved and correlates with transcriptionally active nuclei in Tetrahymena. Proc Natl Acad Sci U S A *96*, 14967-14972.

Sun, Y., Jiang, X., Chen, S., Fernandes, N., and Price, B. D. (2005). A role for the Tip60 histone acetyltransferase in the acetylation and activation of ATM. Proc Natl Acad Sci U S A *102*, 13182-13187.

Surface, L. E., Thornton, S. R., and Boyer, L. A. (2010). Polycomb group proteins set the stage for early lineage commitment. Cell Stem Cell *7*, 288-298.

Suzuki, M., Mizutani-Koseki, Y., Fujimura, Y., Miyagishima, H., Kaneko, T., Takada, Y., Akasaka, T., Tanzawa, H., Takihara, Y., Nakano, M.*, et al.* (2002). Involvement of the Polycomb-group gene Ring1B in the specification of the anterior-posterior axis in mice. Development *129*, 4171-4183.

Sykes, S. M., Mellert, H. S., Holbert, M. A., Li, K., Marmorstein, R., Lane, W. S., and McMahon, S. B. (2006). Acetylation of the p53 DNA-binding domain regulates apoptosis induction. Mol Cell *24*, 841-851.

Szabo, J., Heath, B., Hill, V. M., Jackson, C. E., Zarbo, R. J., Mallette, L. E., Chew, S. L., Besser, G. M., Thakker, R. V., Huff, V., and et al. (1995). Hereditary hyperparathyroidism-jaw tumor syndrome: the endocrine tumor gene HRPT2 maps to chromosome 1q21-q31. Am J Hum Genet *56*, 944-950.

Takeda, S., Chen, D. Y., Westergard, T. D., Fisher, J. K., Rubens, J. A., Sasagawa, S., Kan, J. T., Korsmeyer, S. J., Cheng, E. H., and Hsieh, J. J. (2006). Proteolysis of MLL family proteins is essential for taspase1-orchestrated cell cycle progression. Genes Dev *20*, 2397-2409.

Tang, Y., Luo, J., Zhang, W., and Gu, W. (2006). Tip60-dependent acetylation of p53 modulates the decision between cell-cycle arrest and apoptosis. Mol Cell *24*, 827-839.

Thiel, A. T., Blessington, P., Zou, T., Feather, D., Wu, X., Yan, J., Zhang, H., Liu, Z., Ernst, P., Koretzky, G. A., and Hua, X. (2010). MLL-AF9-induced leukemogenesis requires coexpression of the wild-type Mll allele. Cancer Cell *17*, 148-159.

Tkachuk, D. C., Kohler, S., and Cleary, M. L. (1992). Involvement of a homolog of Drosophila trithorax by 11q23 chromosomal translocations in acute leukemias. Cell *71*, 691-700.

Tolhuis, B., de Wit, E., Muijrers, I., Teunissen, H., Talhout, W., van Steensel, B., and van Lohuizen, M. (2006). Genome-wide profiling of PRC1 and PRC2 Polycomb chromatin binding in Drosophila melanogaster. Nat Genet *38*, 694-699.

Utley, R. T., and Cote, J. (2003). The MYST family of histone acetyltransferases. Curr Top Microbiol Immunol *274*, 203-236.

Valk-Lingbeek, M. E., Bruggeman, S. W., and van Lohuizen, M. (2004). Stem cells and cancer; the polycomb connection. Cell *118*, 409-418.

van der Stoop, P., Boutsma, E. A., Hulsman, D., Noback, S., Heimerikx, M., Kerkhoven, R. M., Voncken, J. W., Wessels, L. F., and van Lohuizen, M. (2008). Ubiquitin E3 ligase Ring1b/Rnf2 of polycomb repressive complex 1 contributes to stable maintenance of mouse embryonic stem cells. PLoS One *3*, e2235.

Vire, E., Brenner, C., Deplus, R., Blanchon, L., Fraga, M., Didelot, C., Morey, L., Van Eynde, A., Bernard, D., Vanderwinden, J. M.*, et al.* (2006). The Polycomb group protein EZH2 directly controls DNA methylation. Nature *439*, 871-874.

Voncken, J. W., Roelen, B. A., Roefs, M., de Vries, S., Verhoeven, E., Marino, S., Deschamps, J., and van Lohuizen, M. (2003). Rnf2 (Ring1b) deficiency causes gastrulation arrest and cell cycle inhibition. Proc Natl Acad Sci U S A *100*, 2468-2473.

Voss, A. K., and Thomas, T. (2009). MYST family histone acetyltransferases take center stage in stem cells and development. Bioessays *31*, 1050-1061.

Wang, H., Wang, L., Erdjument-Bromage, H., Vidal, M., Tempst, P., Jones, R. S., and Zhang, Y. (2004). Role of histone H2A ubiquitination in Polycomb silencing. Nature *431*, 873-878.

Wang, J., and Chen, J. (2010). SIRT1 regulates autoacetylation and histone acetyltransferase activity of TIP60. J Biol Chem *285*, 11458-11464.

Wang, J., Iwasaki, H., Krivtsov, A., Febbo, P. G., Thorner, A. R., Ernst, P., Anastasiadou, E., Kutok, J. L., Kogan, S. C., Zinkel, S. S.*, et al.* (2005). Conditional MLL-CBP targets GMP and models therapy-related myeloproliferative disease. EMBO J *24*, 368-381.

Weikert, S., Christoph, F., Kollermann, J., Muller, M., Schrader, M., Miller, K., and Krause, H. (2005). Expression levels of the EZH2 polycomb transcriptional repressor correlate with aggressiveness and invasive potential of bladder carcinomas. Int J Mol Med *16*, 349-353.

Whitcomb, S. J., Basu, A., Allis, C. D., and Bernstein, E. (2007). Polycomb Group proteins: an evolutionary perspective. Trends Genet *23*, 494-502.

Woodard, G. E., Lin, L., Zhang, J. H., Agarwal, S. K., Marx, S. J., and Simonds, W. F. (2005). Parafibromin, product of the hyperparathyroidism-jaw tumor syndrome gene HRPT2, regulates cyclin D1/PRAD1 expression. Oncogene *24*, 1272-1276.

Xiao, H., Chung, J., Kao, H. Y., and Yang, Y. C. (2003). Tip60 is a co-repressor for STAT3. J Biol Chem *278*, 11197-11204.

Yap, K. L., Li, S., Munoz-Cabello, A. M., Raguz, S., Zeng, L., Mujtaba, S., Gil, J., Walsh, M. J., and Zhou, M. M. (2010). Molecular interplay of the noncoding RNA ANRIL and methylated histone H3 lysine 27 by polycomb CBX7 in transcriptional silencing of INK4a. Mol Cell *38*, 662-674.

Yokoyama, A., and Cleary, M. L. (2008). Menin critically links MLL proteins with LEDGF on cancer-associated target genes. Cancer Cell *14*, 36-46.

Yokoyama, A., Kitabayashi, I., Ayton, P. M., Cleary, M. L., and Ohki, M. (2002). Leukemia proto-oncoprotein MLL is proteolytically processed into 2 fragments with opposite transcriptional properties. Blood *100*, 3710-3718.

Yokoyama, A., Lin, M., Naresh, A., Kitabayashi, I., and Cleary, M. L. (2010). A higher-order complex containing AF4 and ENL family proteins with P-TEFb facilitates oncogenic and physiologic MLL-dependent transcription. Cancer Cell *17*, 198-212.

Yu, B. D., Hess, J. L., Horning, S. E., Brown, G. A., and Korsmeyer, S. J. (1995). Altered Hox expression and segmental identity in Mll-mutant mice. Nature *378*, 505-508.

Zeisig, B. B., Milne, T., Garcia-Cuellar, M. P., Schreiner, S., Martin, M. E., Fuchs, U., Borkhardt, A., Chanda, S. K., Walker, J., Soden, R.*, et al.* (2004). Hoxa9 and Meis1 are key targets for MLL-ENL-mediated cellular immortalization. Mol Cell Biol *24*, 617-628.

Zhou, W., Zhu, P., Wang, J., Pascual, G., Ohgi, K. A., Lozach, J., Glass, C. K., and Rosenfeld, M. G. (2008). Histone H2A monoubiquitination represses transcription by inhibiting RNA polymerase II transcriptional elongation. Mol Cell *29*, 69-80.

Zhu, B., Mandal, S. S., Pham, A. D., Zheng, Y., Erdjument-Bromage, H., Batra, S. K., Tempst, P., and Reinberg, D. (2005a). The human PAF complex coordinates transcription with events downstream of RNA synthesis. Genes Dev *19*, 1668-1673.

Zhu, B., Zheng, Y., Pham, A. D., Mandal, S. S., Erdjument-Bromage, H., Tempst, P., and Reinberg, D. (2005b). Monoubiquitination of human histone H2B: the factors involved and their roles in HOX gene regulation. Mol Cell *20*, 601-611.

Ziemin-van der Poel, S., McCabe, N. R., Gill, H. J., Espinosa, R., 3rd, Patel, Y., Harden, A., Rubinelli, P., Smith, S. D., LeBeau, M. M., Rowley, J. D., and et al. (1991). Identification of a gene, MLL, that spans the breakpoint in 11q23 translocations associated with human leukemias. Proc Natl Acad Sci U S A *88*, 10735-10739.